RADAR CHARACTERISTICS STUDY FOR THE DEVELOPMENT OF SURROGATE ROADSIDE OBJECTS

A Thesis

Submitted to the Faculty

of

Purdue University

by

Jun Lin

In Partial Fulfillment of the

Requirements for the Degree

of

Master of Science in Electrical and Computer Engineering

December 2018

Purdue University

Indianapolis, Indiana

THE PURDUE UNIVERSITY GRADUATE SCHOOL
STATEMENT OF COMMITTEE APPROVAL

Dr. Stanley Yung-Ping Chien, Chair

Department of Electrical and Computer Engineering

Dr. Lauren Christopher

Department of Electrical and Computer Engineering

Dr. Yaobin Chen

Department of Electrical and Computer Engineering

Approved by:

Dr. Brian King

Head of the Graduate Program

To my parents and brother, who keep encouraging me when I encounter difficulties.

To my Friends, for their company along the way.

ACKNOWLEDGMENTS

The research of this thesis was completed by following the patient guidance of Dr. Stanley Chien. The door to his office is always open whenever I encounter difficulties about my research or writing. His experience and knowledge keep leading me on the right direction. I am forever grateful for his help and support.

I would like to thank Dr. Yaobin Chen. He is a great leader of our Transportation Active Safety Institute (TASI) team. His effects aided the whole process of research to go on successfully.

I would like to thank Dr. Lauren Christopher. All of the fundamental knowledge about signal processing I learned from her help me quickly adapt into this research.

I also would like to thank Dr. Chi-Chih Chen who is a radar field professor at Ohio State University (OSU). His technical inputs help me reduce detours. From him, I learned many useful knowledge about radar. Meanwhile, I would like to give my great thankful to Dr. Qiang Yi for his helpful suggestions throughout my entire research.

Last but not least, I am grateful to Abir Saha, Dan Shen and Wensen Niu for their tremendous help. I enjoy every day working with them.

TABLE OF CONTENTS

Page

LIST OF TABLES viii

LIST OF FIGURES ix

ABBREVIATIONS xv

ABSTRACT xvi

1 INTRODUCTION 1

1.1 Background 1

1.2 Motivation 1

1.3 Structure of the Thesis 2

2 REVIEW OF THEORY 4

2.1 Review of Radar 4

2.2 Frequency Modulated Continuous Wave (FMCW) 4

2.3 Polarization Consideration 5

2.4 Radar Property of Objects 6

2.5 Radar Cross Section (RCS) 7

2.6 Radar Reflectivity 8

2.7 Far Field and Near Field RCS Measurement 9

2.8 Summary 10

3 PREPARATORY WORK OF RADAR MEASUREMENT 11

3.1 Introduction 11

3.2 24GHz Radar 11

3.3 77GHz Radar 12

3.4 Parameters Setting on GUI of SDR-RF 2400AD 13

3.5 Calibration of RCS Measurement 14

3.6 Calibration of Reflectivity Measurement 19

Page

3.7 Summary 22
4 RADAR CHARACTERISTICS OF ROADSIDE OBJECTS 23
4.1 Introduction 23
4.2 Metal Guardrail RCS Measurement 25
4.2.1 W-beam Forward-Looking Measurement 27
4.2.2 W-beam Side-Looking Measurement 30
4.2.3 I-beam Forward-Looking Measurement 44
4.3 Grass RCS Measurement 53
4.3.1 Sample Selection 53
4.3.2 Measurement Method 55
4.3.3 Measurement Result 58
4.3.4 Discussion 63
4.3.5 Summary and RCS Recommendation of Grass 64
4.4 Concrete Divider Reflectivity Measurement 69
4.4.1 Sample Description 69
4.4.2 Concrete Divider Forward-Looking Measurement 71
4.4.3 Concrete Divider Side-Looking Measurement 76
4.4.4 Summary and Reflectivity Recommendation of Concrete Divider 87
4.5 Conclusion 87
5 SURROGATE ROADSIDE OBJECTS 88
5.1 Introduction 88
5.2 Surrogate Metal Guardrail 88
5.2.1 Surrogate W-beam 88
5.2.2 Surrogate I-beam 92
5.3 Surrogate Grass 96
5.3.1 Artificial Turf 96
5.3.2 RCS of two different artificial turfs 97

Page

5.3.3 RCS Comparison between Grass and Artificial Turf 100
5.3.4 Summary 105
5.4 Surrogate Concrete Divider 105
5.4.1 Skin Development 105
5.4.2 Reflectivity Comparison between Real and Surrogate Concrete Divider 106
5.4.3 Summary 111
5.5 Conclusion 111
6 CONCLUSION AND FUTURE WORK 112
6.1 Conclusions 112
6.2 Main Contributions of This Thesis 113
6.3 Future Work 113
REFERENCES 114

LIST OF TABLES

Table Page

3.1 77GHz p-converter specifications 12

4.1 W-beam forward-looking measurement RCS results 28

4.2 Comparison of Vertical and Horizontal 24GHz radar polarization results. . 37

4.3 Comparison of Vertical and Horizontal 77GHz radar polarization results. . 38

4.4 24GHz and 77GHz vertical Radar polarization results comparison. 39

4.5 24GHz and 77GHz horizontal Radar polarization results comparison. . . . 39

4.6 Grass samples 54

4.7 Concrete Divider Samples 71

4.8 Forward-looking measurement results 74

4.9 24GHz Radar Reflectivity of a Curb 81

5.1 Reflectivity of surrogate metal guardrail skin and galvanized steel 89

5.2 Specification of two artificial turfs 97

LIST OF FIGURES

Figure Page

2.1 Radar Vertical Polarization (specific to TASIs antenna). 6

2.2 Radar reflectivity measurement 9

2.3 The maximum dimension of antenna-1 used for 24GHz Radar (left) and antenna-2 for 77GHz Radar (right) 10

3.1 Top view (left) and side view (right) of 24GHz Radar 11

3.2 Two components of 77GHz Radar (left), side view of up/down converter (right) 12

3.3 Parameter setting 13

3.4 Trihedral corner reflector (left) and sphere reflector (right) 15

3.5 Trihedral corner reflector measurement 16

3.6 Sphere reflector measurement 17

3.7 Reflected signal of the trihedral reflector and its background 18

3.8 Reflected Signal of the sphere reflector and its background 19

3.9 Radar reflectivity calibration 20

3.10 Signal response of the metal plate 21

4.1 Old (left) and new (right) metal guardrail 25

4.2 Forward-looking measurement 26

4.3 Side-looking measurement 26

4.4 W-beam forward-looking measurement 27

4.5 W-beam forward-looking measurement RCS result plot 28

4.6 Area of W-beam looked by radar 29

4.7 W-beam at different positions 30

4.8 Vertical polarization (left) and horizontal polarization (right) measurement at 24GHz Radar 31

Figure Page

4.9 Vertical polarization (left) and horizontal polarization (right) measurement at 77GHz Radar . . . 31

4.10 W-beam at 0-degree (left) and 90-degree (right) . . . 32

4.11 Color map of W-beam rotation data . . . 33

4.12 W-beam at around 100-degree . . . 34

4.13 RCS plot of a W-beam at various angles . . . 34

4.14 24GHz radar vertical polarization RCS (left) and horizontal polarization RCS (right) of a W-beam . . . 35

4.15 77GHz radar vertical polarization RCS (left) and horizontal polarization RCS (right) of a W-beam . . . 35

4.16 Old (left) and new (right) W-beams RCS plots . . . 36

4.17 W-beam at 52-degree . . . 36

4.18 Recommended 24GHz Radar RCS in vertical polarization for W-beam . . . 40

4.19 Recommended 24GHz Radar RCS in horizontal polarization for W-beam . . . 41

4.20 Recommended 77GHz Radar RCS in vertical polarization for W-beam . . . 42

4.21 Recommended 77GHz Radar RCS in horizontal polarization for W-beam . . . 43

4.22 I-beam forward-looking top view . . . 44

4.23 Vertical polarization (left) and horizontal polarization (right) measurement at 24GHz Radar . . . 45

4.24 Vertical polarization (left) and horizontal polarization (right) measurement at 77GHz Radar . . . 45

4.25 I-beam at 0-degree (left) and 90-degree (right) . . . 46

4.26 Color map of I-beam rotation data . . . 47

4.27 RCS plot of an I-beam at various angles . . . 47

4.28 24GHz radar vertical polarization RCS result (left) and horizontal polarization RCS result (right). . . . 48

4.29 77GHz radar vertical polarization RCS result (left) and horizontal polarization RCS result (right). . . . 48

4.30 I-beam at 50-degree . . . 49

4.31 Recommended 24GHz Radar RCS in vertical polarization for I-beam . . . 51

Figure Page

4.32 Recommended 24GHz Radar RCS in horizontal polarization for I-beam . . 51

4.33 Recommended 77GHz Radar RCS in vertical polarization for I-beam . . . 52

4.34 Recommended 77GHz Radar RCS in horizontal polarization for I-beam . . 53

4.35 Grass 1 (left), Grass 2 (middle), Grass 3 (left) 54

4.36 24GHz Vertical (left) and horizontal (right) polarization set up 55

4.37 77GHz Vertical (left) and horizontal (right) polarization set up 55

4.38 Grass measurement top view (left) and side view (right) 56

4.39 Color map of grass raw data (left) and RCS result (right) 58

4.40 24GHz Radar vertical polarization measurements from 35-degree to 10-degree for 3 grass samples 59

4.41 24GHz Radar horizontal polarization measurements from 35-degree to 10-degree for 3 grass samples 60

4.42 77GHz Radar vertical polarization measurements from 35-degree to 10-degree for 3 grass samples 61

4.43 77GHz Radar horizontal polarization measurements from 35-degree to 10-degree for 3 grass samples 62

4.44 Recommended 24GHz vertical polarization RCS for surrogate grass 65

4.45 Recommended 24GHz horizontal polarization RCS for surrogate grass . . . 66

4.46 Recommended 77GHz vertical polarization RCS for surrogate grass 67

4.47 Recommended 77GHz horizontal polarization RCS for surrogate grass . . . 68

4.48 Concrete Divider 1 69

4.49 Concrete Divider 2 70

4.50 Concrete Divider 3 70

4.51 Concrete Divider 4 70

4.52 Concrete Divider 5 70

4.53 Concrete Divider 6 71

4.54 Measurement-1 of the Forward-looking measurement setup 72

4.55 The measurement result of Measurement-1 73

4.56 Measurement-2 setup (right) and result (right) 73

Figure Page

4.57 Measurement-3 setup (right) and result (right) 74
4.58 Concrete divider forward-looking measurement analyzation 75
4.59 Concrete divider side-looking measurement 76
4.60 Reflectivity calibration using an aluminum plate 77
4.61 Concrete divider measurement using 24GHz (left) and 77GHz (right) Radar 77
4.62 Concrete divider measurement result (left) and aluminum plate measurement result (right) 78
4.63 24 GHz radar reflectivity of concrete divider 2 78
4.64 Summary of the 24 GHz reflectivity of all concrete divider samples. 79
4.65 Summary of the 77 GHz reflectivity of all concrete divider samples. 79
4.66 Curb reflectivity measurement 81
4.67 Surface of Concrete Divider 5 82
4.68 Spray water on concrete divider surface-1 83
4.69 Spray water on concrete divider surface-2 83
4.70 Spray water on concrete divider surface-3 83
4.71 Groups of concrete divider samples 84
4.72 Gravels visible on the surface of concrete divider sample 2 85
4.73 The rough surface of Concrete Divider 4 85
4.74 Surface of Concrete Divider 6 86
4.75 Concrete Divider 4 rough surface (left) and broken surface (right) 86
5.1 Surrogate metal guardrail skin 89
5.2 Surrogate vertical (left) and horizontal (right) polarization measurement at 24GHz Radar 90
5.3 Surrogate vertical (left) and horizontal (right) polarization measurement at 77GHz Radar 90
5.4 Real W-beam RCS result (left) and surrogate W-beam RCS result (right) under vertical polarization at 24GHz Radar 90
5.5 Real W-beam RCS result (left) and surrogate W-beam RCS result (right) under horizontal polarization at 24GHz Radar 91

Figure Page

5.6 Real W-beam RCS result (left) and surrogate W-beam RCS result (right) under vertical polarization at 77GHz Radar 91

5.7 Real W-beam RCS result (left) and surrogate W-beam RCS result (right) under horizontal polarization at 77GHz Radar 92

5.8 Surrogate vertical (left) and horizontal (right) polarization measurement at 24GHz Radar 93

5.9 Surrogate vertical (left) and horizontal (right) polarization measurement at 77GHz Radar 93

5.10 Real I-beam RCS result (left) and surrogate I-beam RCS result (right) under vertical polarization at 24GHz Radar 94

5.11 Real I-beam RCS result (left) and surrogate I-beam RCS result (right) under horizontal polarization at 24GHz Radar 94

5.12 Real I-beam RCS result (left) and surrogate I-beam RCS result (right) under vertical polarization at 77GHz Radar 95

5.13 Real I-beam RCS result (left) and surrogate I-beam RCS result (right) under horizontal polarization at 77GHz Radar 95

5.14 Front side and back side of the Artificial turf 96

5.15 Artificial turf top close view (left) and side close view (right) 96

5.16 Two artificial turfs put on together (Long blade turf up, short blade turf down) 97

5.17 Measurement results of three experiments 98

5.18 Artificial turf measurement alone different sides 99

5.19 RCS plots of measurement alone different sides 100

5.20 Turf on clay (left top), on sand (right top), on asphalt (left bottom), on concrete (right bottom) 101

5.21 The measurement result of Turf on clay (black) on sand (blue) on asphalt (pink) on concrete (cyan) at different pitch angle under 24 GHz vertical polarization 102

5.22 The measurement result of Turf on Asphalt (black) at different pitch angle under 77 GHz horizontal polarization 104

5.23 Final surrogate concrete divider 106

5.24 Measurement data of real concrete divider and surrogate concrete divider at 24GHz Radar 106

Figure Page

5.25 Measurement data of real concrete divider and surrogate concrete divider at 77GHz Radar 107

5.26 Concrete divider surrogate is placed between real concrete dividers . . . 107

5.27 Moving measurement setup 108

5.28 Measurement result at 0-degee 109

5.29 Measurement result at 5-degee 110

5.30 Measurement result at 10-degee 110

5.31 Measurement result at 15-degee 110

5.32 Measurement result at 20-degee 111

ABBREVIATIONS

AEB	Autonomous Emergency Braking
LDWS	Lane Departure Warning System
LKAS	Lane Keeping Assistant System
RDWS	Roadway Departure Warning System
RCS	Radar Cross Section
SDR	Software-Defined Radar
FMCW	Frequency-Modulated Continuous-Wave
FSK	Frequency Shift Keying
CW	Continuous-Wave

ABSTRACT

Lin, Jun. M.S.E.C.E., Purdue University, December 2018. Radar Characteristics Study for the Development of Surrogate Roadside Objects. Major Professor: Stanley Y.P. Chien.

Driving safety is a very important topic in vehicle development. One of the biggest threat of driving safety is road departure. Many vehicle active safety technologies have been developed to warn and mitigate road departure in recent years. In order to evaluate the performance of road departure warning and mitigation technologies, the standard testing environment need to be developed. The testing environment shall be standardized to provide consistent and repeatable features in various locations worldwide and in various seasons. The testing environment should also be safe to the vehicle under test in case the safety features do not function well. Therefore, soft, durable and reusable surrogates of roadside objects need to be used. Meanwhile, all surrogates should have the same representative characteristics of real roadside objects to different automotive sensors (e.g. radar, LIDAR and camera). This thesis describes the study on identifying the radar characteristics of common roadside objects, metal guardrail, grass, and concrete divider, and the development of the required radar characteristics of surrogate objects. The whole process is divided into two steps. The first step is to find the proper methods to measure the radar properties of those three roadside objects. The measurement result of each roadside object will be used as the requirement for making its surrogate. The second step is to create the material for developing the surrogate of each roadside object. In the experimental results demonstrate that all three surrogates satisfy their radar characteristics requirements.

1. INTRODUCTION

1.1 Background

Safety is one of the most important topics throughout the history of car development. Many people are killed in car accidents each year. According to the Fatality Analysis Reporting System (FARS) [1], there were more than 37,000 fatal crashes each year in the United States before 2009. This number goes down a little bit after 2009 but still is around 30,000 per year. Government, colleges and automotive companies are spending lots of time and money to develop new technologies to keep improving car safety. Autonomous Emergency Braking (AEB) was introduced in 2009 [2]. It automatically stops the vehicle at some emergency situations when the driver does not apply to brake. Since the year 2000, Lane Keep Assist System (LKAS) [3], Lane Departure Warning System (LDWS) [4] are quickly developed. They warn the driver when the car moves out of the lane. These systems require the road to have clear lane marking. However, many roads in suburban of USA do not have clear lane marking or even do not have lane marking at all. Therefore, a new technology, called Road Departure Warning System (RDWS) is being developed [5]. RDWS helps a vehicle to keep running on the road by detecting road edges. While these technologies are being developed, there emerges a need to develop a standard way to test these new technologies.

1.2 Motivation

Test the effectiveness of new vehicle technologies is essential for technology development. Some companies use software simulation to test their new technologies. However, software simulation can only test the system to a certain extent. Since the

simulated environment is not equal to real environment testing, some potential problem may not be revealed. Some companies directly test their vehicle on the real road. Although testing results are reliable, the scenarios may not be repeatable and the test itself creates potential safety hazards. Therefore, creating a controllable testing environment is necessary. Actually, the Euro New Car Assessment Program (Euro NCAP) has worked on car safety performance assessment since 1997 [6]. Since the RDW technology is new, there is not a standard testing environment and methodology defined anywhere in the world yet.

In a standard controllable road-departure testing environment, the testing environment should be representative of the real road and roadside objects. However, some roadside objects, such as grass, change their appearance to vehicle sensors throughout the year. Since the color, density and height of grass commonly change in different seasons and different locations. Testing in different site and time of the year causes the testing results hard to compare. In this case, representative surrogate roadside objects are needed as a standard for RDW testing anywhere in the country. Additionally, the vehicle testing environment should be safe to the vehicle and driver. It means that the vehicle under test (VUT) will not be damaged and the driver will not be injured when a test fails. Therefore, many real roadside objects such as metal guardrail, concrete divider are not suitable for RDW testing. One approach is to create surrogates of these roadside objects and use them on the test track for RDW testing. These surrogates should have the same properties as real roadside objects as seen by commonly used automotive radar, LIDAR, and camera. Surrogates should also be light weight, soft, and durable to prevent the damage of VUT and itself in failed tests.

1.3 Structure of the Thesis

The rest of this thesis are planned as follows:

- Chapter 2 reviews radar theories.

- Chapter 3 introduces the preparatory work of radar measurement.
- Chapter 4 gives the details of measurement methods of roadside objects.
- Chapter 5 focuses on the generation and verification of the surrogate objects.
- Chapter 6 is the conclusion of the whole thesis.

2. REVIEW OF THEORY

2.1 Review of Radar

The basic principle of Radar is simple [7]. Radar generates electromagnetic (EM) waves [8]. EM waves travel forward at the speed of light until they hit an object. Depend on an objects property, part of the waves are absorbed by the object; some of the waves travel through the object, and rest of the waves are reflected back. Based on the difference between the transmitted waves and the reflected waves, Radar can determine the distance between the Radar and the object, the moving speed of the object, the property (such as shape, material) of the object, etc.

There are many different types of Radar [9]. Based on the frequency, there are L-band Radar, S-band Radar, C-band Radar, X-band Radar, etc. Based on the waveform, there are Frequency Shift Key (FSK) Radar, Continuous Wave (CW) Radar, Frequency Modulated Continuous Wave (FMCW) Radar, etc. Based on the applications, there are Tracking Radar, Weather Radar, Automotive Radar, etc.

This research focus on Automotive Radar [10]. Typically, the Automotive Radar usually uses two frequency bands, one is 24GHz and the other is 77GHz. 24GHz Automotive Radar is a Short Range Radar (SRR), it is mostly used for side looking applications. Its measurement range is around 20m [11]. 77GHz Automotive Radar is a Long Range Radar so it is mostly used as forward-looking Radar. Its measurement range could reach 150m [12].

2.2 Frequency Modulated Continuous Wave (FMCW)

As mentioned before, there are many types of Radar waveform, such as CW, FSK, FMCW, etc. CW Radar [13] can easily measure targets moving speed, but cannot

tell the distance between Radar and object. FSK Radar [14] is good at measuring moving objects but does not work well for stationary objects. Typically, Automotive Radar chooses Frequency Modulated Continuous Wave (FMCW) as the waveform. It can measure both moving and stationary objects. Moreover, FMCW Radar has very high range resolution.

For FMCW Radar [15], the frequency of the transmitted signal changes periodically over time. In other words, time is marked by frequency. By knowing the frequency change of received echo signal, the system can calculate the time difference between transmitted and received signals. Equation 2.1 shows the calculation of the distance between the Radar and object according to the time change. Equation 2.2 shows the calculation of the distance between the radar and object according to the frequency change.

$$R = \frac{C * \Delta t}{2} \tag{2.1}$$

Where R is the distance between Radar and object. C is light speed ($3 * 10^8 m/s$). Δt is delay time between transmitting and receiving. Since Δt equals to $\Delta f/(df/dt)$, following formula can also be used to calculate the distance.

$$R = \frac{C * \Delta f}{2 * (df/dt)} \tag{2.2}$$

Where f is a measured frequency difference between transmitting and receiving signals, and df/dt is frequency shift per unit of time.

2.3 Polarization Consideration

It is necessary to consider the polarization of radar wave in Radar measurement since polarization will affect the measurement result [16]. The Radar wave is an Electromagnetic (EM) wave, which consists of an electric field and a magnetic field. Two fields are perpendicular to each other. The direction of polarization of the wave is determined by the electric field. There are two basic polarization directions. One is vertical polarization; the other is horizontal polarization. Based on these two

polarization, any other degrees polarization can be calculated. Therefore, normally Radar measurement only needs to consider these two kinds of polarization.

For vertical radar polarization, the antenna filament is perpendicular to the ground (Fig. 2.1). For horizontal radar polarization, the antenna filament is in parallel with the ground. Different polarization measurements will get the same result when the target object is symmetric about the origin, such as a sphere.

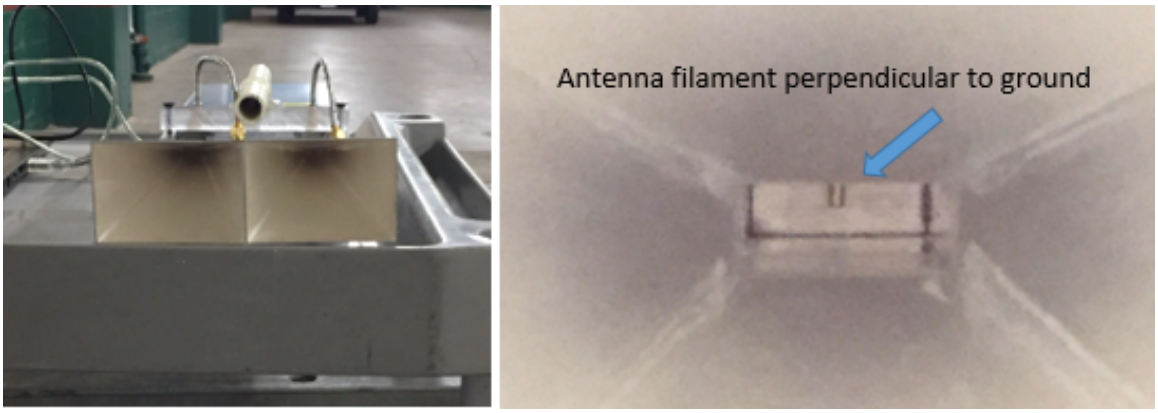

Fig. 2.1. Radar Vertical Polarization (specific to TASIs antenna).

2.4 Radar Property of Objects

In general, an object having higher electrical conductivity will get stronger Radar response than the same shaped object that has lower electrical conductivity. The shape of the object also affects the Radar response. For example, an object with cone shape has higher Radar response than an object that just has a flat surface. Moreover, the Radar response is affected by the smoothness of the objects surface as well. Usually, if the Radar center beam is perpendicular to the surface, then the smoother surface gets higher Radar response than the rough surface since rough surface will let some of the waves reflect to other directions and will not be received by the antenna. However, if the Radar center beam is not perpendicular to the surface,

then the smoother surface gets lower Radar response than the rough surface since most of the waves that shoot on a smooth surface will not reflect back.

2.5 Radar Cross Section (RCS)

Radar Cross Section (RCS) shows the ability of a target to reflect radar energy [17]. The unit of RCS is decibel square meter (dBsm). RCS is related to the Radar frequency and the radar-viewing angle. It is also affected by the shape and material of objects. When the material is the same, the larger sized object will have a higher RCS. When the size is the same, the object made of higher conductive material will have a higher RCS value. In addition, (if an object is not flat and does not have uniform curvature,) measuring the object from different angles will get different RCS values unless the object shows the same shape when viewing from different angles, such as a sphere. The theoretical formula to calculate RCS is:

$$P_r = \frac{P_t G_t G_r \lambda^2 \sigma}{(4\pi)^3 R^4} \tag{2.3}$$

Where P_r (watts) is the power received by Radar, P_t (watts) is transmitted power, G_t (dimensionless) is the gain of transmitting antenna, G_r (dimensionless) is gain of receiving antenna, R (meters) is the distance between Radar and the surface of object that is aimed by Radar, (meters) is Radars wavelength, and (meters squared) is RCS. Based on Equation 2.3, RCS is affected by Radar wavelength. However, most of Automotive Radar use FMCW waveform whose frequency (wavelength) is periodically changed. In this case, center frequency (wavelength) is used to calculate the RCS. For instance, if the frequency of FMCW is changed between 24GHz and 26GHz (2GHz bandwidth), then 25GHz is used to calculate the RCS.

For practical RCS measurement, the formula can be converted to

$$\sigma_{target} = \frac{P_r^{target}}{P_r^{reference}} \sigma_{reference} \tag{2.4}$$

In order to use this formula, one reference object is required, and the ideal RCS of that reference object can be calculated. Then by knowing P_r of the target and P_r of

the reference object, RCS of the target object can be quickly obtained. In addition, if Equation 2.4 is used in dB scaling, then the equation will become as follows:

$$\sigma_{target}(dBsm) = 10 * log_{10}(\frac{P_r^{target}(W)}{P_r^{reference}(W)} * \sigma_{reference}(m^2)) \tag{2.5}$$

$$\sigma_{target}(dBsm) = P_r^{target}(dB) - P_r^{reference}(dB) + \sigma_{reference}(dBsm) \tag{2.6}$$

2.6 Radar Reflectivity

Reflectivity is a material property of the object [18]. To be more precise, reflectivity refers to the electrical conductivity of the object. Since radar signal is electromagnetic (EM) wave, the higher conductive material has higher reflectivity. When resistivity is as low as in metals, the resistivity differences of different metals are too small to be detected by 24GHz and 77GHz automotive radar. Therefore, Radar cannot distinguish between different metals. In other words, when using radar to measure different metals, the power strengths of responses of different metal are not distinguishable. The reflectivity of metal is defined as 0 dB. The power response that gets from the flat and smooth metal plate is usually used as a reference of reflectivity measurement. The Reflectivity measurement will be used when the object has infinite sized flat surface. Ground, wall, etc. can be considered having infinite flat-sized surface practically for reflectivity measurements. Moreover, when doing Radar reflectivity, the Radar center beam should be perpendicular to the surface (Fig. 2.2). The equation for calculating Radar reflectivity is similar to equation 2.6. The main difference is their units. The unit of RCS is dBsm, but the unit of Radar reflectivity is dB. The equation of Radar reflectivity is shown below:

$$\sigma_{target}(dB) = P_r^{target}(dB) - P_r^{reference}(dB) + \sigma_{reference}(dB) \tag{2.7}$$

Where $\sigma_{target}(dB)$ is the Radar reflectivity of the target, $P_r^{target}(dB)$ is the power intensity of the target, $P_r^{reference}(dB)$ is power intensity of reference, and $\sigma_{reference}(dB)$

is Radr reflectivity of reference. Additionally, since the metal plate is used as the reference and the reflectivity of metal plate is 0dB, equation 2.7 can be written as:

$$\sigma_{target}(dB) = P_r^{target}(dB) - P_r^{reference}(dB) \tag{2.8}$$

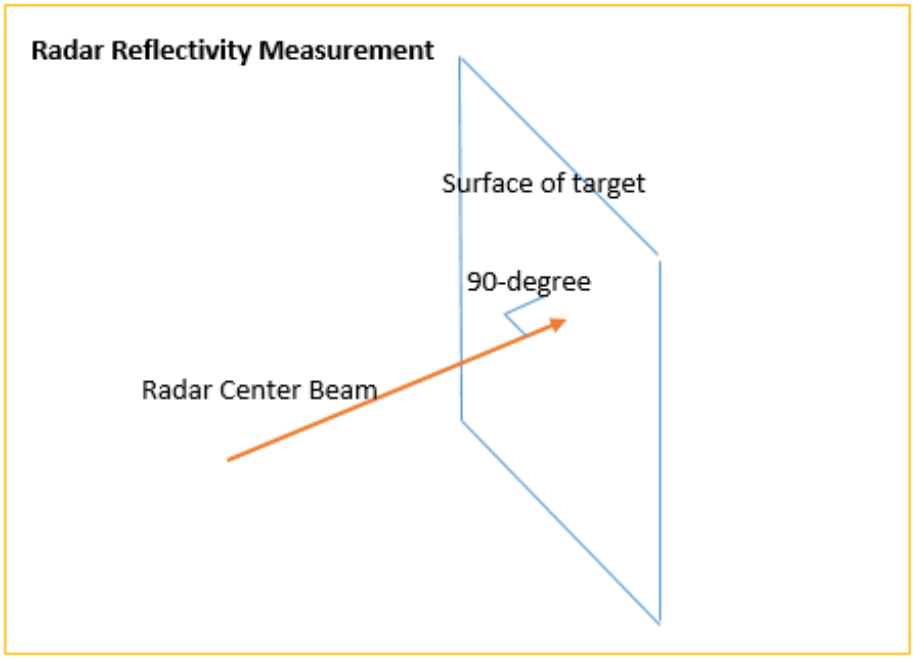

Fig. 2.2. Radar reflectivity measurement

2.7 Far Field and Near Field RCS Measurement

RCS relates to the distance between Radar and target object. Based on the distance, RCS measurement is divided into two types. One is near field measurement; the other one is far-field measurement [19]. The field distribution changes as the distance changes in near field range. In far-field range, the field distribution is almost consistent. Therefore, RCS measurement result changes as distance change in near field range, but the RCS keeps the same as the distance changes in far field range. In this case, far-field RCS measurement is preferred. Just point out that current

technology can predict far field RCS measurement result from near filed RCS measurement result [20]. The boundary distance, R, between near field and far filed can be calculated by using Fraunhofer distance [21]:

$$R = \frac{2 * D^2}{\lambda} \tag{2.9}$$

Where D is the maximum linear dimension of an antenna, and λ is the frequency of Radar. For example, Fig. 2.3 shows that the maximum linear dimension of antenna-1 for a 24GHz Radar is about $3.5cm$, and the maximum linear dimension of antenna-2 for a 77GHz Radar is about $1.5cm$. Based on the Fraunhofer distance, the far field distance is about 0.19m for antenna-1; and about $0.12m$ for antenna-2.

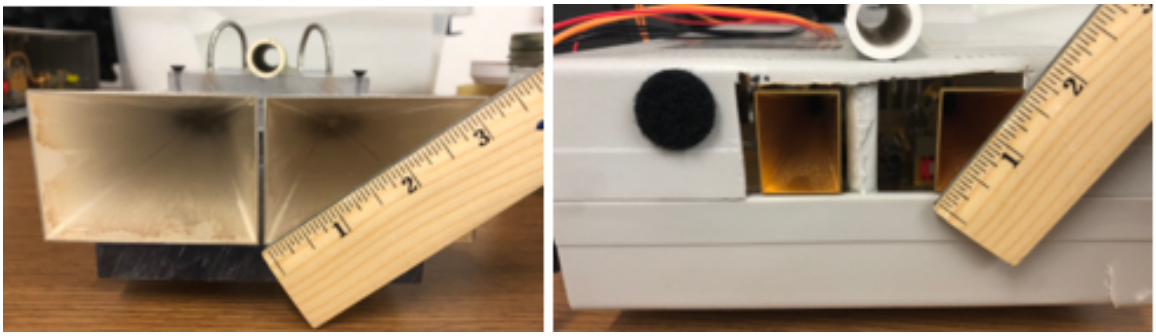

Fig. 2.3. The maximum dimension of antenna-1 used for 24GHz Radar (left) and antenna-2 for 77GHz Radar (right)

2.8 Summary

This research focuses on both 24GHz and 77GHz Automotive Radar. FMCW waveform will be used for these two types of Radar. Radar reflectivity measurement and far filed RCS measurement will be applied for target objects. For RCS measurement, horizontal and vertical polarization are both considered.

3. PREPARATORY WORK OF RADAR MEASUREMENT

3.1 Introduction

This chapter provides the detailed information of 24GHz and 77GHz Radar that were used in measurements and explains how to set up Radar parameters on its software interface. At the end of this chapter, two kinds of calibration will be introduced. One is RCS calibration. The other one is reflectivity calibration.

3.2 24GHz Radar

The 24GHz Radar we used is a Software-Defined Radar (SDR) (shown in Fig. 3.1). The model of this Radar is SDR-RF 2400AD. Low power consumption and high performance are the key advantages of this module. The bandwidth of this radar is 2 GHz. It can support three operating modes: FMCW (Frequency Modulated Continuous Wave), FSK (Frequency-shift keying), and CW (Continuous Wave).

Two high gain antennas (transmitter and receiver) are connected to this radar. The model of these two horn antennas is VT220SGAH20+K2.92K. The antenna gain is 22 dB when Radar is operated at 24-26 GHz. The beam width of these antennas is 18-degrees. The high gain and narrow beam width antenna make the radar focus easily on the target and reduce background influence.

Fig. 3.1. Top view (left) and side view (right) of 24GHz Radar

3.3 77GHz Radar

As shown in Fig. 3.2, 77GHz Radar has two components. One is SDR-RF 2400AD, which is the 24GHz Radar kit. The other one is an up/down converter. Table. 3.1 shows the specifications of this up/down converter. The 24GHz Radar kit generates 24-26 GHz Radar signal and sends the signal to the up/down converter. The up/down converter converts that signal to 76-78 GHz Radar signal.

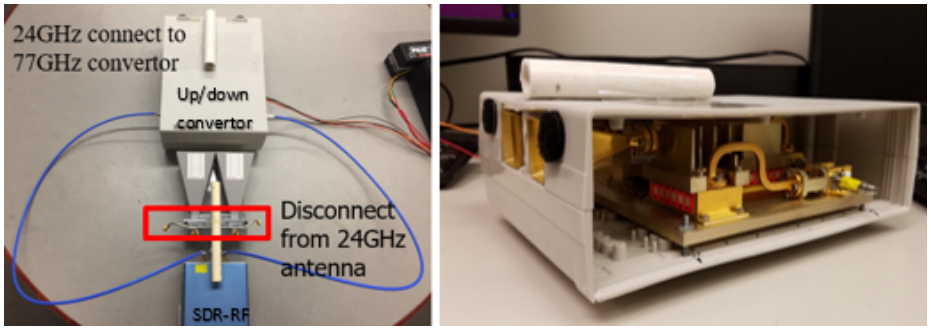

Fig. 3.2. Two components of 77GHz Radar (left), side view of up/down converter (right)

Table 3.1.
77GHz p-converter specifications

	Specifications
RF Frequency	76 to 78 GHz
LO Frequency	52 GHz, Internal
Tx RF Output Power	+20 dBm
IF Frequency	24 to 26 GHz
Rx Conversion Loss	8 dB
Tx IF Input Power	+16 dBm
Low Side Band Rejection	40 dB
DC Bias	+12V (420 mA), +8V (990 mA)

3.4 Parameters Setting on GUI of SDR-RF 2400AD

SDR-RF 2400AD can be configured by the software of a PC that is connected to the SDR-RF 2400AD through a USB interface. The set up uses the Graphical user interface. As shown in Fig. 3.3, FMCW is selected as the operating mode. As mentioned in Chapter 2, FSK can only detect moving objects, and CW cannot measure the distance between Radar and object. FMCW does not have those drawbacks and can provide high detection accuracy. The bandwidth can determine the range resolution. The wider bandwidth, the higher range resolution. The 2GHz bandwidth is selected. It is the maximum bandwidth shows on this interface. In this case, the frequency of Radar wave changes from 24 GHz to 26 GHz within one sweep. Sweep time and Samples per Sweep determine how many data are generated within recording time. In our case, sweep time is set to be 1ms and using 512 for Samples per Sweep. Therefore, Radar generates 512 sample data each millisecond. The upper limit of this setting is 1024 sample data each millisecond. However, too many data will slow down data processing speed, and sometimes cause the device not work to properly. Moreover, 512 sample data each millisecond already provides very high measurement accuracy.

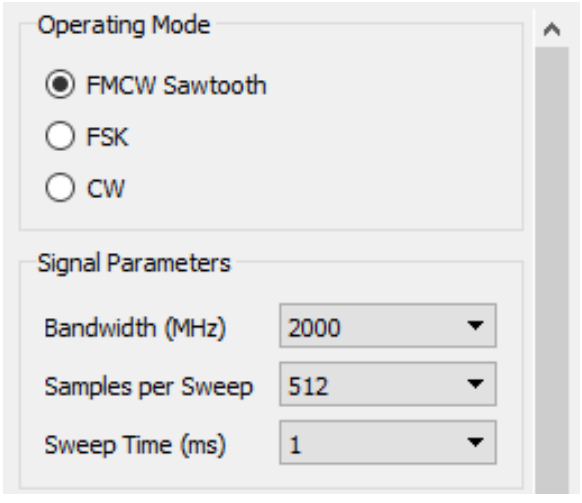

Fig. 3.3. Parameter setting

3.5 Calibration of RCS Measurement

There are two main reasons for doing RCS calibration. First, RCS calibration is used to check if the Radar works correctly or not. It needs to check if the difference between the measured RCS value of a reference object matches its ideal RCS within 1 dBsm or not. Second, RCS calibration is used to get reference data ($P_r^{reference}$ as shown in equation 2.6). The reference data is used to convert raw target data to RCS value (as in equation 2.6). Since the raw target data collected by a Radar always relate to the Radar type, antenna pattern, distance, etc. The same object measured by different Radar will get different raw data. However, after calibration, their RCS value will be the same.

The key point of RCS calibration is to measure some reference objects with known theoretical RCS values. These reference objects are known as reflectors. There are many types of reflectors, such as a trihedral reflector, sphere reflector, cylinder reflector, etc.

In this research, trihedral corner reflector (Fig. 3.4 left image) and sphere reflector (Fig. 3.4 right image) were used to do the calibration. The trihedral corner reflector (model: SAJ-060-S1) is made of aluminum. The outer dimension (the blue line in Fig. 3.1.5-2 left image) is: 6" x 6" x 6" (6" = 15.24 cm); and the inner dimension (the red line in Fig. 3.1.5-2 left image) is: 4.21" x 4.21" x 4.21" (4.21" = 10.7 cm). The theoretical RCS value of trihedral corner reflector (dBsm) is:

$$\sigma = 10 * \log_{10}(\frac{4\pi L^4}{3\lambda^2}) \tag{3.1}$$

Where L is the inner dimension value (meters), and λ is the wavelength (meters). By calculation, the RCS value of this trihedral corner reflector is 5.8 dBsm for 24GHz, and 15.6 dBsm for 77GHz. The sphere reflector (item 710-S) is also made of aluminum. The diameter is 10" (10" = 25.4 cm). The theoretical RCS value of sphere reflector (dBsm) is:

$$\sigma = 10 * \log_{10}(\pi r^2) \tag{3.2}$$

Where r is the radius of the sphere (meters). The RCS value of the sphere does not relate to wavelength. By calculation, the RCS value of this sphere reflector is -12.95 dBsm for any frequency wave.

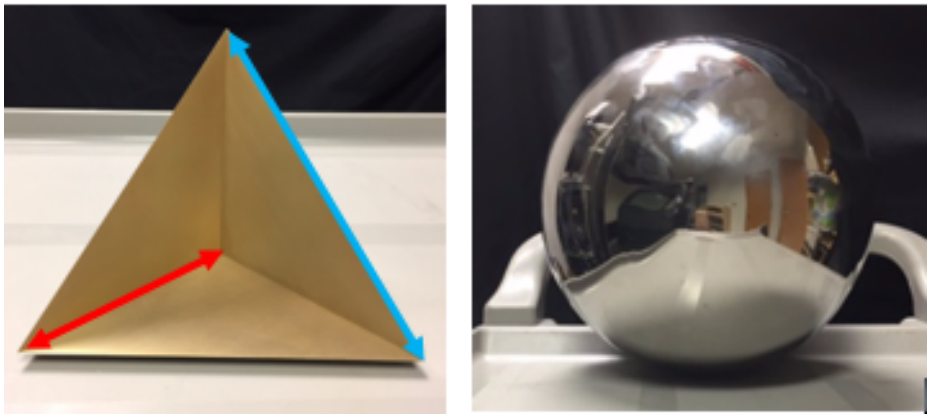

Fig. 3.4. Trihedral corner reflector (left) and sphere reflector (right)

RCS calibration for Radar checking purpose includes five steps (24GHz Radar is selected in following measurement. 77GHz Radar RCS calibration follows exactly the same process).

1. Measure the trihedral corner reflector:

   As shown in Fig. 3.5, the trihedral corner reflector is placed on a tripod. The geometric center of trihedral corner reflector to the ground is about 55cm. There is no special requirement for the height. However, the height should be reasonable. If the height is too low, Radar will receive many noises from the ground. If the height is too high (e.g. Higher than normal people's height), then it is not easy to do the measurement. After fixing the trihedral corner reflector, Radar is placed 3m away from the trihedral corner. The distance between Radar and target object should not be too short. Otherwise, the measurement result will be affected by antenna coupling. However, long distance is also not a good choice, since Radar signal becomes weaker as distance increases. The center of the antenna to the ground should also be the same height as the height of the center of the reflector. Moreover, the antennas central beam should aim to the

geometric center of a trihedral corner reflector. The absorb foams are placed between the middle of the Radar and the trihedral corner reflector to reduce the ground reflection. Use PC software interface to record 2 seconds data. This data is called $P_r^{Trihedral}$. The trihedral corner reflector measurement is done.

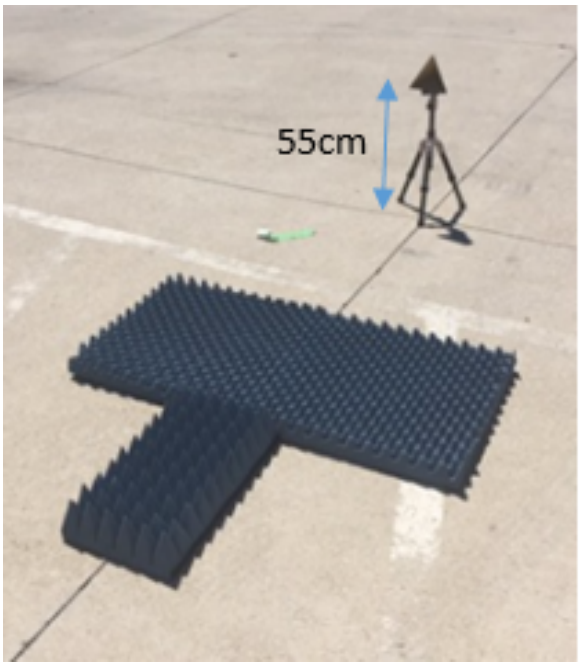

Fig. 3.5. Trihedral corner reflector measurement

2. Measure the background of trihedral corner reflector:

   Slowly remove the trihedral corner reflector from the tripod. Make sure the position of the tripod is not shifted. Record 2s data. This data is called $P_r^{TrihedralBackground}$.

3. Measure the sphere reflector:

   This step is similar to step one. The only difference is that sphere is mounted on a foam cup since the tripod is not able to hold sphere (Fig. 3.6). The center of the sphere to the ground is still about 55cm, and the distance between Radar and sphere maintains at 3 m. Record 2 seconds data. This data is called P_r^{Sphere}.

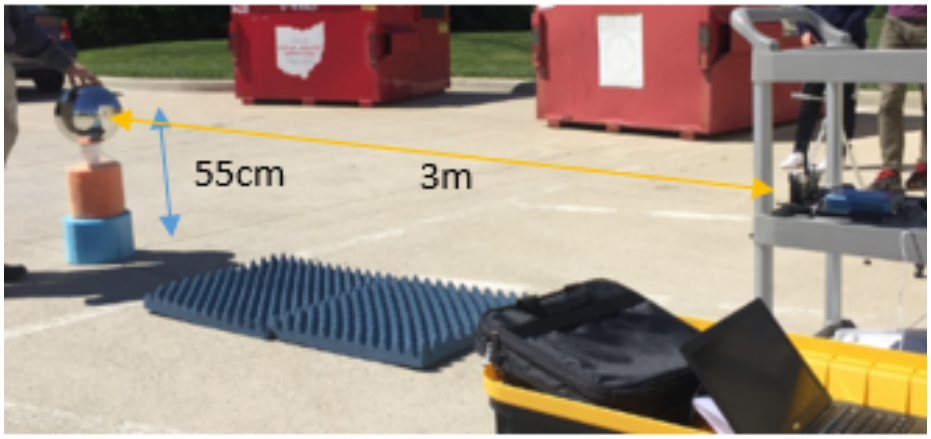

Fig. 3.6. Sphere reflector measurement

4. Measure the background of sphere reflector:

   Similar to step 2, slowly remove the sphere reflector from the tripod. Make sure any of other equipment's position is not shifted. Record 2-seconds data. Give a name to this data: $P_r^{TrihedralBackground}$.

5. Data analysis:

   Fig. 3.7 shows the 2-seconds data plot of the trihedral corner reflector measurement. The x-axis is the time (ns). The y-axis of this figure is the magnitude (dB) of the response signal. Trihedral corner reflectors background measurement is shown in the blue plot. The red plot is the total signal response minus the background measurement response (the background effect has been eliminated so that the pure signal response of trihedral corner reflector can be found). The maximum peak which pointed by the horizontal yellow arrow in this figure is generated by antenna coupling. Antenna coupling happens when two antennas (transmitter and receiver) are placed too close. However, the antenna coupling will not affect measurement result, as long as the target object is not too close to antennas so we can tell which signal is due to antenna coupling and which signal is from the object measured. Normally, it is good enough if the distance between antenna and target is greater than 1m.

The peak response of the red plot pointed by the vertical yellow arrow is the signal response of trihedral corner reflector. The peak responses of both the red plot and blue plot pointed by the horizontal yellow arrow are the antenna coupling effect. In this measurement, $P_r^{Trihedral}$ is 57.9 dB. Fig. 3.8 is the plot of the measurement of the sphere reflector (red line) and its background (blue line). Based on this figure, P_r^{Sphere} is 39.8 dB. Knowing the theoretical RCS value of sphere reflector ($P_r^{ideal_sphere} = -12.95dB$), the measured RCS value of trihedral corner reflector can be calculated using equation 2. 6. In this case, the measured RCS value of trihedral corner reflector is: (57.9dB - 39.8dB) + (-13.0dBsm) = 5.1 dBsm.

The ideal RCS value of this trihedral corner reflector is 5.8 dBsm. Since the difference between the ideal RCS value and measured RCS value is less than 1 dBsm, the Radar is considered working property. The collected data of both trihedral corner reflector and sphere reflector can be used to calibrate other objects.

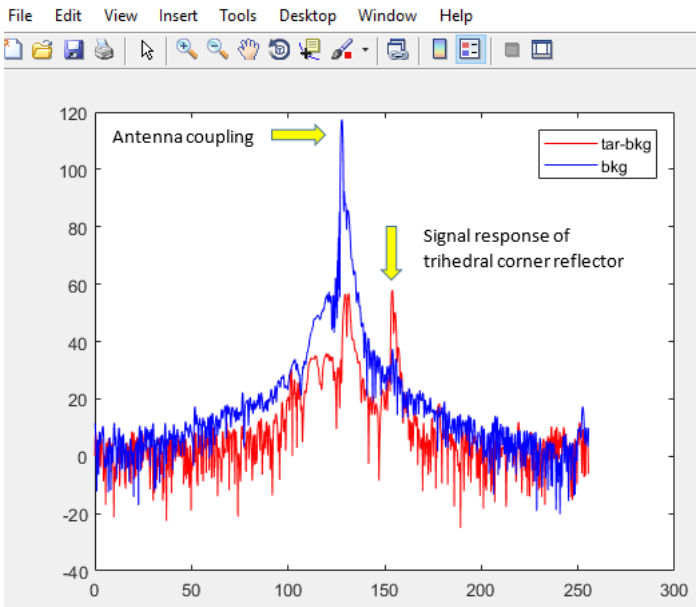

Fig. 3.7. Reflected signal of the trihedral reflector and its background

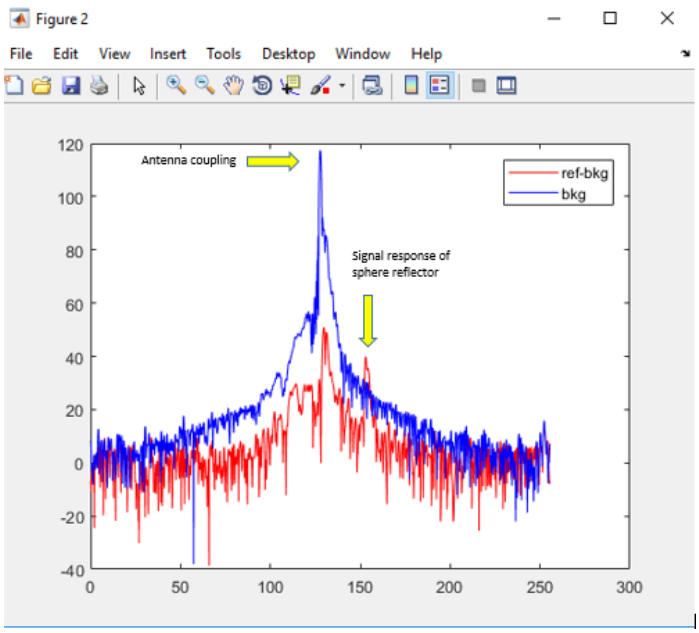

Fig. 3.8. Reflected Signal of the sphere reflector and its background

If RCS calibration is just for getting reference data, then doing step 1, 2 and 5 is enough.

3.6 Calibration of Reflectivity Measurement

Reflectivity Calibration cannot check if Radar works well or not. Therefore, the meaning of calibration here is just that using reference data (received power intensity from reference) to calibrate the raw data of the target (received power intensity from the target). Equation 2.8 in chapter 2 can be used to calculate Radar reflectivity. However, the received power intensity from a reference metal plate should be measured first. This reference data will be used to calculate the reflectivity of the surface of other targets. The Radar reflectivity calibration has five steps (the reflectivity measurement of the 24GHz Radar is described below. The reflectivity measurement of the 77GHz Radar follows exactly the same process.

1. Set the reference object:

   Put a big metal plate on the big flat surface to be measured. For example, to measure the radar reflectivity of the concrete divider, the reference metal plate is placed on the surface of the concrete divider (Fig. 3.9).

Fig. 3.9. Radar reflectivity calibration

2. Set radar height:

   Mount the radar on the tripod. Set the radar to the same height as the height of the center of the metal plate.

3. Adjust the distance between the Radar and the metal plate:

   Adjust the distance between the radar and the reference metal plate in following steps until Radar can only see the metal plate. Put an absorber foam on the right side of the metal plate. Slowly move the absorber from right to left until the Radar peak response dropping down. Mark there as the right boundary of Radar viewing area. Using the same way to find the left boundary, top boundary, bottom boundary. This four boundary will define the Radar view area of Radar viewing area. If the Radar viewing area is only on a metal plate, then the distance is correct. If the distance is too long, the radar viewing area contains the area outside of the metal plate so the data will be incorrect. If the distance is too short, the target signal will be too close to the coupling signal, so it will be difficult or impossible to distinguish these two signals.

4. Adjust the Radar aiming angle:

   Following steps describe how to set the Radar beam perpendicular to the surface of the metal plate. This is essential to ensure that the radar can receive the maximum power response. Firstly, rotate the Radar left and right horizontally to find the maximum power response, and stop the radar at that horizontal aiming angle. Then rotate radar up and down to find the maximum power response and keep the radar vertical aiming angle there. Record radar response data of the metal plate for 2 seconds.

5. Plot the recorded data:

   In the plot (Fig. 3.10), the highest peak is antenna coupling. The second-highest peak is the signal response of the metal plate. In this measurement, the signal response of the metal plate ($P_r^{metal_plate}$) is 93.7 dB. Now, equation 2.8 can be used to calculate other material's Radar reference.

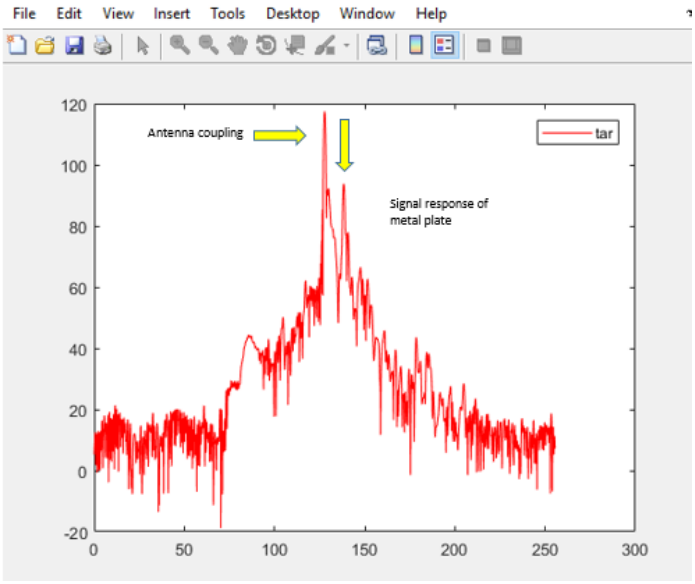

Fig. 3.10. Signal response of the metal plate

3.7 Summary

A Software-Defined Radar (SDR) module, SDR-RF 2400AD, is used as a 24GHz Radar. It can connect to a 77GHz up/down converter to form a 77GHz Radar. No matter SDR-RF 2400AD is used as 24GHz Radar or 77GHz Radar, on the software interface, set parameters as following: bandwidth = 2GHz, operating mode = FMCW, sweep time = 1ms, and samples per sweep = 512. Using RCS calibration method to check if the Radar works properly before doing real measurements. Additionally, RCS calibration can provide reference data that is needed to determine the RCS value of an object. Reflectivity calibration gets the reference data that is needed to find the radar reflectivity of an object.

4. RADAR CHARACTERISTICS OF ROADSIDE OBJECTS

4.1 Introduction

This Chapter describes the discovery of the 24GHz and 77GHz Radar property of common road edge and road boundary objects. The Transportation Active Safety Institute (TASI) at Indiana University-Purdue University Indianapolis (IUPUI) has done a pre-study of the roadside boundaries and objects. 24,762 Google street view images that randomly sampled in the U.S. were used in the study. According to the study result, the top five roadside objects are grass (54.65%), curb (16.02%), metal guardrail (8.7%), concrete divider (4.17%) and traffic cone (0.28%). This research will focus on measuring Radar property of grass, metal guardrail and concrete divider. Note that curb and concrete divider are made of the same material. Therefore, Radar property of curb can be interpreted from the Radar property of concrete divider. Moreover, it is hard to measure curb directly, since curb is fixed at very low position (about 6 inches against the ground). The environment (ground, vegetation, etc.) around the curb will strongly affect curbs measurement result.

The Radar property can be described in two parameters. One is radar reflectivity, and the other is RCS. Reflectivity is a property of the object's material but will be affected by the surface condition. Typically, if the surface smoothness level is closed to the radar wavelength, then it will not affect the radar reflectivity value much. The other parameter of radar property is RCS. RCS describes not only the object's material property but also the shape property of the object. In another word, the result of RCS measurement is an aggregative indicator. When an object has an irregular shape and occupies a fraction of the field of view of the radar, reflectivity is hard to measure, and RCS is the parameter to use.

The radar reflectivity of the metal guardrail is already known since it is made of galvanized steel. As mentioned in Chapter 2, the reflectivity of all metals can be approximated as 0 dB. Since metal guardrail occupies a fraction of the field of view of the radar, the radar property should also be described by its RCS. Since metal guardrails shape is complex, it needs to be measured from different possible radar viewing angles. Therefore, RCS of the metal guardrail is a function of radar viewing angle.

The grass is a very special object. It varies in type, height, shape, color, etc., in different locations and seasons. It is difficult to measure and describe the Radar reflectivity of grassland since each grass blade is small and different grass blades are in different orientations and may be different colors. The color of the grass usually implies the water content of the grass and water content affects the electrical conductivity that in turn affect radar reflectivity. Since the grassland is not uniform in shape and reflectivity, it is also difficult to describe grassland in RCS. In this study, we proposed to use the mean RCS of numerous grassland locations to describe the overall Radar property of grassland.

The concrete divider will focus on the reflectivity measurement. As mentioned before, reflectivity measurement requires target object has big flat surface. Moreover, the smoothness level of the surface should be close to Radars wavelength level. The concrete divider can perfectly satisfy these requirements. In addition, RCS measurement is not necessary for the concrete divider. The key reason is that the shape of the concrete divider is very simple. The majority part of the concrete divider is just a big flat surface. In this case, the shape property is not important for the concrete divider. Therefore, the result of reflectivity measurement is enough to describe concrete dividers Radar property.

The method for finding the radar characteristics of metal guardrail, concrete divider, and grass are described in following subsections.

4.2 Metal Guardrail RCS Measurement

The purpose of this task is to define the 24GHz and 77GHz radar characteristics of metal guardrail based on forward-looking measurement and side-looking measurement. The Metal guardrail consists of three parts: the horizontal W-beam, the I-beam posts, and spacers between the W-beam and I-beam. The spacers are behind the W-beam and mostly made of plastics or wood, and their RCS are considerably lower than the metal parts. Therefore, the effect of spacers in the radar characteristics of the metal guardrail is negligible and do not need to be considered.

Since the shape of the metal guardrail is standard all over the US, the age of the metal guardrail is a potential factor that could affect the RCS of the metal guardrail. Therefore, two guardrails (Fig. 4.1) of quite different ages (3 months old and over 20 years old) were used to find the RCS of the metal guardrail.

Fig. 4.1. Old (left) and new (right) metal guardrail

During vehicle motion, the radar can see the W-beam and I-beam from various angles. For further description, the viewing angles are defined as follows:

- Forward-looking: as Fig. 4.2 shown, Radar looks forward. Therefore, Radar beam and the extension direction of metal guardrail form an angle. This angle is defined as forwarding angle. When Radar beam is parallel with a metal

guardrail, the forwarding angle is 0-degree. When Radar beam is perpendicular with a metal guardrail, the forwarding angle is 90-degree.

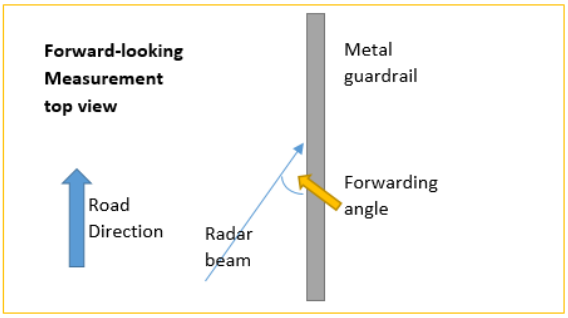

Fig. 4.2. Forward-looking measurement

- Side-looking: as the blue arrow is shown in Fig. 4.3, the 0-degree of side-looking angle is defined when the Radar beam is perpendicular to the front surface of the metal guardrail. When Radar beam. Similarly, 90-degree of side-looking angle means Radar beam is perpendicular to the top surface of metal guardrail (orange arrow).

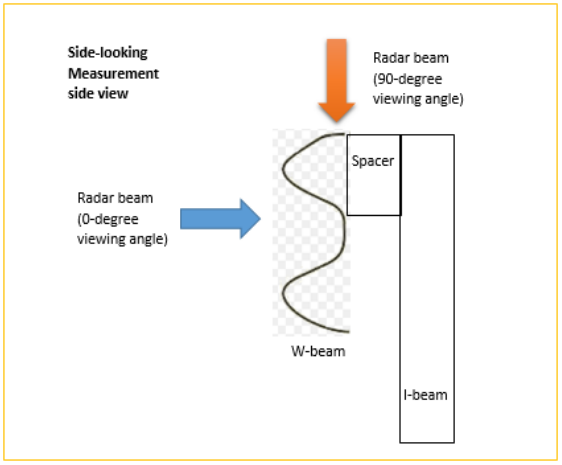

Fig. 4.3. Side-looking measurement

4.2.1 W-beam Forward-Looking Measurement

Measurement Method

1. Do the RCS calibration (Chapter 3) to check if Radar works property or not.

2. Save the data of signal response of trihedral corner reflector. It will be used to calibrate the signal response of W-beam.

3. Place W-beam horizontally on two supporting stands (Fig. 4.4 left image) at 55cm above the ground. Set the radar 55cm above the ground and 3m away from the geometric center of the W-beam. Aim the Radar center beam perpendicular to W-beam (defined as 90-degree) and record data for 2 seconds.

4. Rotate W-beam counterclockwise about the red dash line. Each time rotate 5 degrees (right image of Fig. 4.4 shows the W-beams placement after 6 of 5 degree or 30-degree rotations from 90-degree reference). The original plan is rotating 18 times (change measurement angle from 90-degree to 0-degree). However, the response signal cannot be detected after 9 rotations (from 90-degree to 45-degree). Therefore, the measurement has to stop at 45-degree. The measured RCS results are shown in Table. 4.1.2.1.2-1. and Fig. 4.1.2.1.2-1.

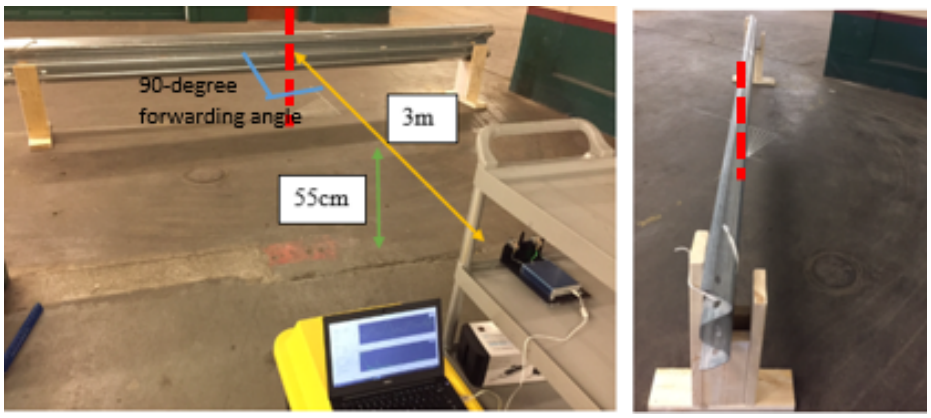

Fig. 4.4. W-beam forward-looking measurement

Measurement Result

Table 4.1.
W-beam forward-looking measurement RCS results

Degree	RCS (dBsm)
90	7.1392
85	8.4361
80	6.4926
75	2.6698
70	-0.20219
65	-5.1326
60	-8.0857
55	-11.1592
50	-14.5538
45	-15.9037

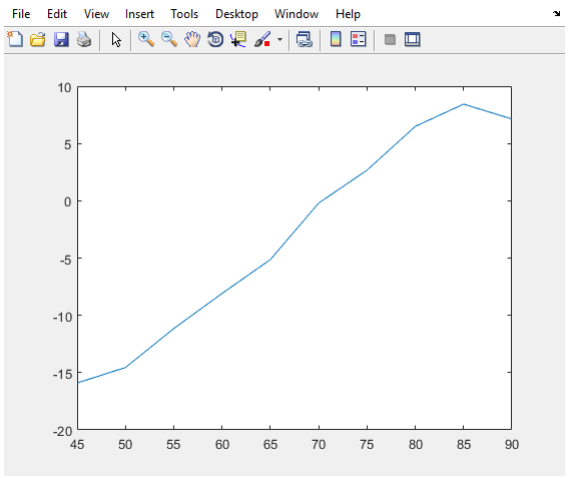

Fig. 4.5. W-beam forward-looking measurement RCS result plot

Result Discussion

Fig. 4.5 shows that the RCS value drops down quickly as the measurement angle deviates further away from 90-degree. The key reason leads to this phenomenon is that Radar can only see the area, which is perpendicular to the Radar beams. As shown in Fig. 4.6, if the W-beam is not perpendicular to the radar center beam (signal 1), then signal 1 (center beam) will be reflected to the right side and will not be returned back to the radar. In this case, signal 2 (side beam) is perpendicular to the W-beam, so signal 2 will be reflected back to the radar. Therefore, in this case, radar is looking at position B instead of position A. Note that the center beam of Radar is much stronger than the side beam. Therefore, the 90-degree measurement result is stronger than other degrees measurement result, and the measurement result keeps decreasing as forwarding angle decreasing. Moreover, if the antenna beam width is very narrow, for example, the radar beam cannot reach points between A and B, then the guardrail cannot be detected by the radar. As shown in Fig. 4.7, during the

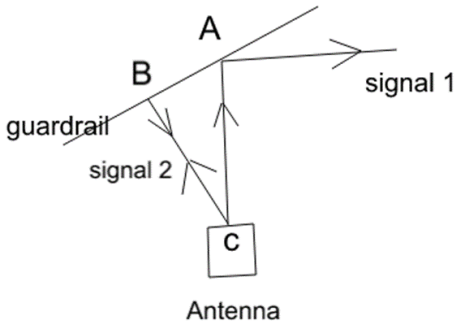

Fig. 4.6. Area of W-beam looked by radar

rotation of the W-beam about the red dash line, the radar center beam does not keep reaching the middle area of the metal guardrail! At position 1 (90-degree), Radar beam reaches the middle area. At position 2, the radar beam reaches a small area on the left side of the middle area. At position 3, the radar beam reaches a small area on the right side of the middle area. The angular bisectors of angle ACB, ACB,

ACB are perpendicular to the metal guardrail! In this case, antenna beam width and beam pattern will directly affect the measurement result. Therefore, RCS of W-beam measured at horizontally varying angles cannot be used to describe W-beams property! RCS of W-beam measured at a horizontally fixed angle (especially at 90 degrees) may be used to describe W-beams property!

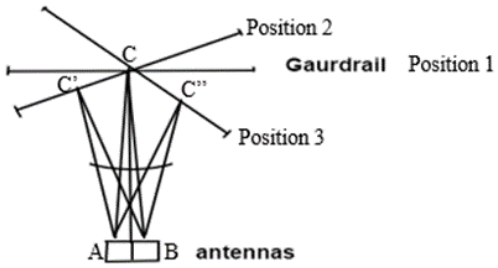

Fig. 4.7. W-beam at different positions

4.2.2 W-beam Side-Looking Measurement

Measurement Method

1. Put the Radar on a tripod (Fig. 4.8 shows the vertical polarization (left) and horizontal polarization (right) measurement of a 24GHz Radar. Fig. 4.9 shows the vertical polarization (left) and horizontal polarization (right) measurement of a 77GHz Radar). The radar is 55 cm above the ground.

2. Do the RCS calibration to check if Radar works property. Choose 3m as the distance between Radar and reflector (Chapter 3).

3. Record the trihedral corner reflectors power response, which will be used to calibrate W-beams power response.

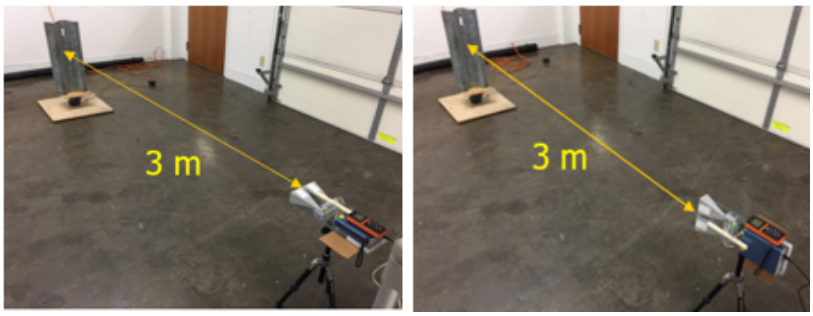

Fig. 4.8. Vertical polarization (left) and horizontal polarization (right) measurement at 24GHz Radar

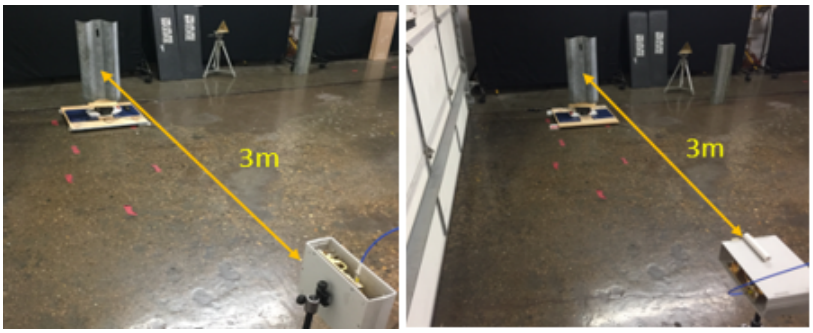

Fig. 4.9. Vertical polarization (left) and horizontal polarization (right) measurement at 77GHz Radar

4. After aiming angle calibration, replace the trihedral reflector by a W-beam and a rotating table. Let the W-beam stand in the middle of the rotating table. Use a level to ensure the W-beam be perpendicular to the ground.

5. Start the rotator, and adjust the speed, so that the W-beam can rotate at least 90 degrees within the 30s.

6. Start recording the data of W-beams signal response from 0-degree (Figure 4.10 left image) faces to Radar to 90-degree faces to Radar (Figure 4.10 right image). Click record button about 2s earlier, so that can guarantee 0-degree data to be recorded.)

Fig. 4.10. W-beam at 0-degree (left) and 90-degree (right)

7. Plot the recorded raw data and calculate the RCS value of the W-beam for each angle (0 to 90 degrees). Figure 4.11 is the raw data color map of W-beams vertical polarization measurement at a 24GHz Radar. The x-axis is the number of Radar scan. It has linear relationship with recording time (e.g. x=8000 is corresponding to 8000/500 = 16s). Note that this plot does not show full 30s data. The plot after x=9000 is not plotted since the rest of the data is just repeating the previous data. The y-axis is the distance (1.5 to 5 meters) from the radar to the measuring object. The data from 0 to 1.5 meters is not plotted since the data in that range is more related to antenna coupling. The dark red in the figure means the signal response is very strong. The lighter color means the weaker signal response (Dark blue is the background color. It means signal response is close to zero). In addition, since the target (W-beam) is rotating over time in a constant speed, angle and time has a linear relationship. Therefore, the x-axis (scan times) also has a linear relationship with the angle. In another word, this figure actually shows how the signal response change at a different angle of W-beam. In order to convert x-axis from scan times to angle, the user has to help MATLAB program to figure out where the 0-degree and 90-degree are. First, the 0-degree measurement is at 2-second (x=1000) (the straight thin black line has pointed there). There are three pieces of evidence to prove it. First, the recording started right before the 0-degree facing to the

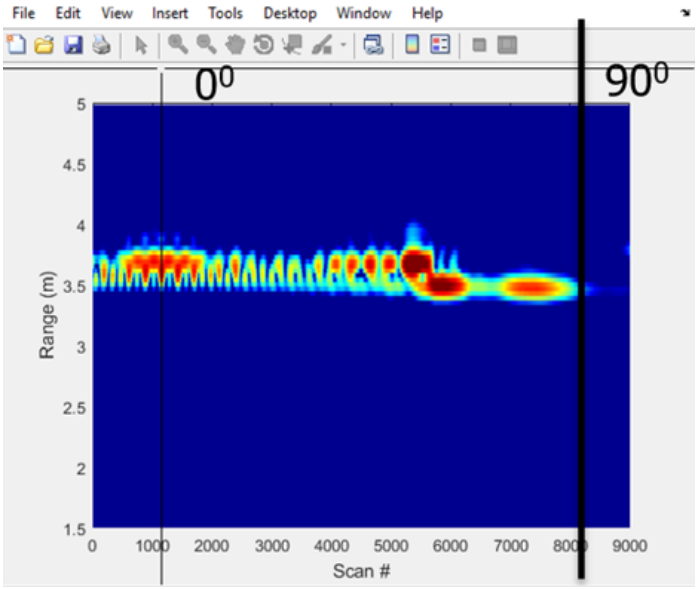

Fig. 4.11. Color map of W-beam rotation data

radar. Therefore, the 0-degree position should appear at an early time. Second, W-beam is perfectly symmetric. Therefore, the power response before the 0-degree and after the 0-degree should be symmetric as well. This figure shows that signal response from x=0 to x=1000 (0s to 2s) is the same as the signal response form x=1000 to x=2000 (2s to 4s). Lastly, at 0-degree, the middle flat surface of W-beam directly faces to Radar. In another word, the radar will receive a strong power response at this position, and the figure shows there is a local maximum power response (dark red) at x=1000. Next, the 90-degree is at x=8000 (16s) (pointed by the straight thick black line). The reason is that the signal response almost disappeared after 16- second. It is noticed that radar will not see the front side of W-beam after 90-degree. In another word, after 90-degree, part of the backside of W-beam faces to radar (Fig. 4.12). In addition, when W-beam rotates over 90-degree, most of the radar wave will be reflected to the left side, and will not be received by the radar. This is why the signal response suddenly disappears after 90-degree (16-second).

Fig. 4.12. W-beam at around 100-degree

With the knowledge of $P_r^{reference}$ (power response from trihedral corner reflector), $\sigma_{reference}$ (RCS of trihedral corner reflector), and P_r^{target} (Power response from W-beam at each angle), the RCS plot of W-beam can be calculated using calibration equation 2.6 (Fig. 4.13). The x-axis is the angle (degree). The y-axis is RCS value (dBsm). The W-beam RCS measurement at is done.

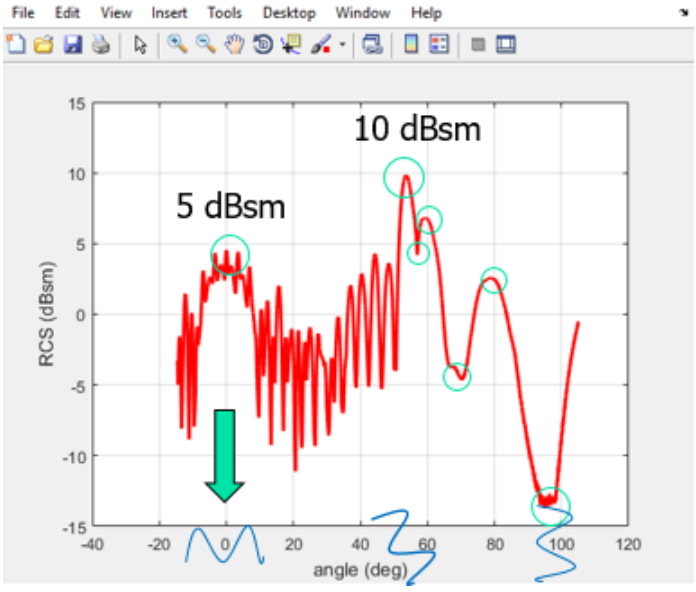

Fig. 4.13. RCS plot of a W-beam at various angles

Measurement Result

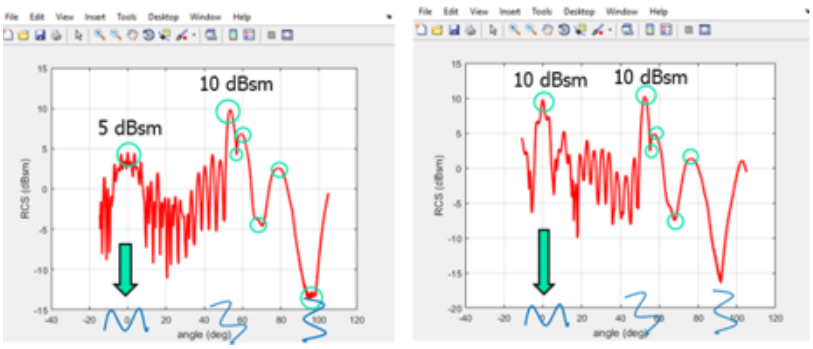

Fig. 4.14. 24GHz radar vertical polarization RCS (left) and horizontal polarization RCS (right) of a W-beam

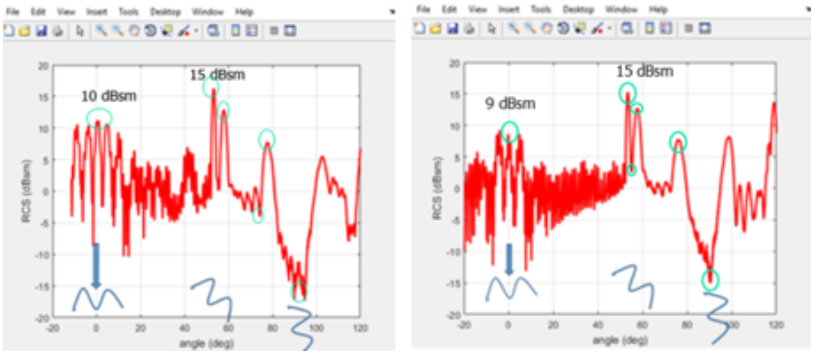

Fig. 4.15. 77GHz radar vertical polarization RCS (left) and horizontal polarization RCS (right) of a W-beam

Result Discussion

1. Effect of W-beam Age

   Fig. 4.16 shows how W-beams RCS changes from 0-degree to 90-degree. The left plot is measured by using a very old W-beam at least 20 years old. The right plot is measured by using a brand new W-beam.

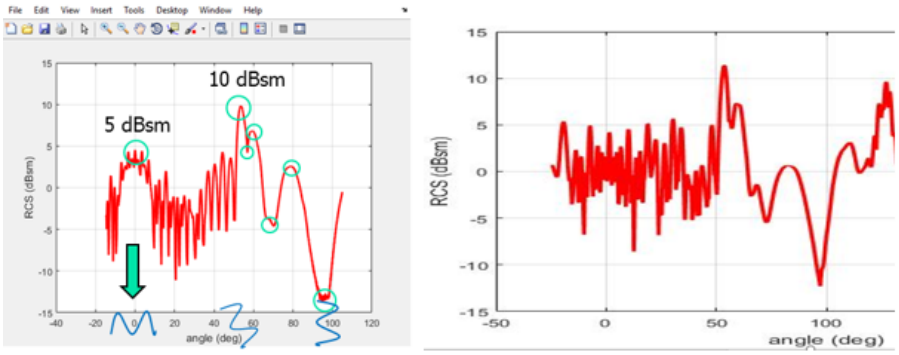

Fig. 4.16. Old (left) and new (right) W-beams RCS plots

By comparing these two results, they are almost the same. At 0-degree, both of their RCS are around 5dBsm. Between 0 to 50 degrees, both of them show unstable RCS response. From 50 to 90 degree, the shape and value of two plots are highly matched, especially their maximum response appear at the same angle (52-degree), and the values are so close (the old one is about 10 dBsm, the new one is about 11 dBsm). Therefore, the conclusion is that the age of W-beam does not affect W-beams RCS (as long as it is not rusted).

2. Maximum RCS Response

   The maximum RCS appeared is at around 52-degrees. It is because the W-beam is a better corner reflector at 52-degree (Fig. 4.17).

Fig. 4.17. W-beam at 52-degree

3. 24GHz Vertical and Horizontal Radar Polarization Results Comparison

   - As shown in Fig. 4.14 and Table 4.2, 24GHz horizontal and vertical polarization measurement have similar results. The biggest difference is at 0-degree.
   - Horizontal polarization: RCS at 0-degree is 10 ± 2 dBsm.
   - Vertical polarization: RCS at 0-degree is 5 ± 2 dBsm.
   - Between 0 to 50 degrees, the RCS response for both horizontal and vertical polarization oscillate between -10 to +5 dBsm.
   - From 50 to 90 degrees, the RCS of both horizontal and vertical polarization are smooth, and includes three peaks at about 55-degree (10 ± 2 dBsm, maximum peak), 60-degree (between 5 to 10 dBsm, local peak) and 75-degree (between 0 to 5 dBsm, local peak). Three valleys at about 58 degree (between 5 to 10 dBsm), 65 degree (-5 ± 2 dBsm) and 90 degree (-between -10 to -15 dBsm).

Table 4.2.
Comparison of Vertical and Horizontal 24GHz radar polarization results.

	0-degree	0 to 50 degree	Between 50 to 90 degree
Vertical Polarization	Local peak ($5 \pm 2dBsm$)	Oscillate between -10 to +5 dBsm	Smooth plot; 3 peaks (1 maximum peak and 2 local peaks); 3 valleys
Horizontal Polarization	Maximum Peak ($10 \pm 2dBsm$)	Oscillate between -10 to +5 dBsm	Smooth plot; 3 peaks (1 maximum peak and 2 local peaks); 3 valleys

4. 77GHz Vertical and Horizontal Radar Polarization Results Comparison

   - As shown in Fig. 4.15 and Table 4.3, 77 GHz RCS of W-beam at the vertical and horizontal polarization are similar.

- At 0 degree, both of their RCS are closed to 10(±2) dBsm.
- Between 0 to 50 degrees, the RCS response for both horizontal and vertical polarization are oscillated between -10 to +5 dBsm.
- From 50 to 90 degrees, the RCS for both horizontal and vertical polarization should be smooth, and includes three peaks at about 55-degree ($15 \pm 2dBsm$, maximum peak), 60-degree (between 10 to 15 dBsm, local peak) and 75-degree (between 5 to 10 dBsm, local peak). Three valleys at about 58-degree (between 0 to 5 dBsm), 65-degree (0 ± 2 dBsm) and 90-degree $-15 \pm 5dBsm$).

Table 4.3.
Comparison of Vertical and Horizontal 77GHz radar polarization results.

	0-degree	0 to 50 degree	Between 50 to 90 degree
Vertical Polarization	Local peak ($10 \pm 2dBsm$)	Oscillate between -10 to +5 dBsm	Smooth plot; 3 peaks (1 maximum peak and 2 local peaks); 3 valleys
Horizontal Polarization	Maximum Peak ($10 \pm 2dBsm$)	Oscillate between -10 to +5 dBsm	Smooth plot; 3 peaks (1 maximum peak and 2 local peaks); 3 valleys

5. Comparison of 24GHz and 77GHz Vertical Radar Polarization

   The left images of Fig. 4.14 and Fig. 4.15 show that RCS plots of vertical polarization at 77GHz Radar and 24 GHz Radar have the similar shape. RCS plots between 0 to 50 degrees also have similar values. Both of them oscillate between -10 to 5 dBsm. However, RCS plot at 77GHz is about 5 dBsm higher than RCS plot at 24 GHz at 0-degree and from 50 to 90 degrees. More details of comparisons are shown in Table 4.4.

Table 4.4.
24GHz and 77GHz vertical Radar polarization results comparison.

	0-degree	0 to 50 degree	Between 50 to 90 degree
24GHz	Local peak $(5 \pm 2dBsm)$	Oscillate between -10 to +5 dBsm	Smooth plot; 3 peaks (1 maximum peak and 2 local peaks); 3 valleys
77GHz	Maximum Peak $(10 \pm 2dBsm)$	Oscillate between -10 to +5 dBsm	Smooth plot; 3 peaks (1 maximum peak and 2 local peaks); 3 valleys

6. Comparison of 24GHz RCS and 77GHz RCS at Horizontal Polarization

   Right images of Fig. 4.14 and Fig. 4.15 show that the 77GHz and 24GHz horizontal polarization RCS plots have similar shape except at 0-degree. Although their RCS values are the same at 0-degree, their meanings are different. At 0-degree, 24GHz Radar receives a global maximum response, but 77GHz Radar just receives a local maximum response. Between 5 to 50 degrees, both of them are oscillating between -10 to +5 dBsm. From 50 to 90 degrees, their shapes are the same, but 77GHz Radar gives 5 dBsm higher RCS response than 24 GHz.

Table 4.5.
24GHz and 77GHz horizontal Radar polarization results comparison.

	0-degree	0 to 50 degree	Between 50 to 90 degree
24GHz	Local peak $(10 \pm 2dBsm)$	Oscillate between -10 to +5 dBsm	Smooth plot; 3 peaks (1 maximum peak and 2 local peaks); 3 valleys
77GHz	Maximum Peak $(10 \pm 2dBsm)$	Oscillate between -10 to +5 dBsm	Smooth plot; 3 peaks (1 maximum peak and 2 local peaks); valleys

Summary and RCS Recommendation of Metal Guardrail W-beam

RCS of the W-beam of the metal guardrail is not affected by their age. The vertical polarization measurement result is similar with horizontal polarization result at 77GHz Radar. However, they are slightly different at 24GHz Radar. The vertical polarization measurement result is about 5 dB lower than the horizontal measurement result at 0-degree. The recommend vertical and horizontal RCS plots at 24GHz and 77GHz Radar are shown below.

1. 24GHz Vertical Polarization RCS Recommendation

   For 24GHz radar vertical polarization measurement, the radar should be put at a distance of 3m distance away from the W-beam. The height of the radar should focus on the middle point of the W-Beam. The surrogate RCS response should have a similar shape as in Fig. 4.18, and satisfy the following requirements:

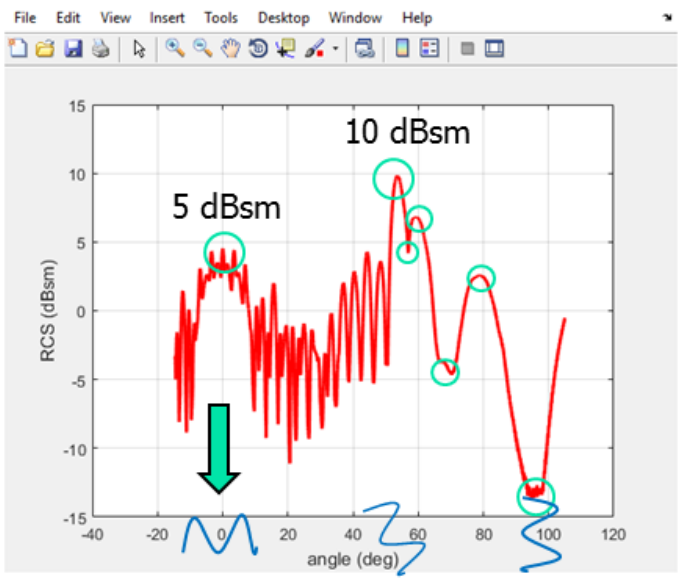

Fig. 4.18. Recommended 24GHz Radar RCS in vertical polarization for W-beam

- Be $5 \pm 2dBsm$ at 0-degree;
- Between 5dBsm to -10dBsm between 0 to 50 degrees;

- Have the maximum of 10 ± 2dBsm around 55-degree;
- Be smooth from 50 to 90 degrees;
- Include three peaks at about 55-degree, 60-degree and 75-degree;
- Include three valleys at about 58-degree, 65-degree and 90-degree.

2. 24GHz Horizontal Polarization RCS Recommendation

   For 24GHz radar horizontal polarization measurement, the radar should be put at a distance of 3m away from the W-beam. The height of the radar should focus on the middle point of the W-Beam. The surrogate RCS response should have the similar shape as in Fig. 4.19, and satisfy the following requirements:

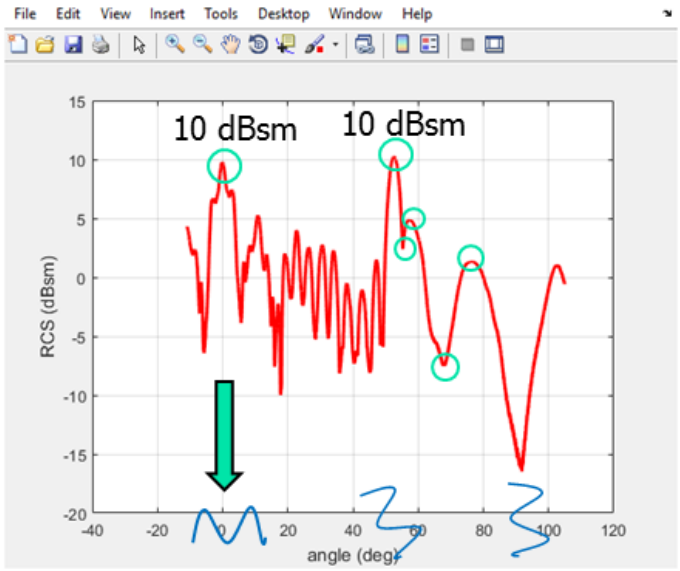

Fig. 4.19. Recommended 24GHz Radar RCS in horizontal polarization for W-beam

- Be 10 ± 2dBsm at 0-degree;
- Between 5dBsm to -10 dBsm between 0 to 50 degrees;
- Have the maximum of 10 ± 2dBsm around 55-degree;
- Be smooth from 50 to 90 degrees;

- Include three peaks at about 55-degree, 60-degree and 75-degree;
- Include three valleys at about 58-degree, 65-degree and 90-degree.

3. 77GHz Vertical Polarization RCS Recommendation

   For 77GHz radar vertical polarization measurement, the radar should be put at a distance of 3m distance away from the W-beam. The height of the radar should focus on the middle point of the W-Beam. The surrogate RCS response should have a similar shape as in Fig. 4.20, and satisfy the following requirements:

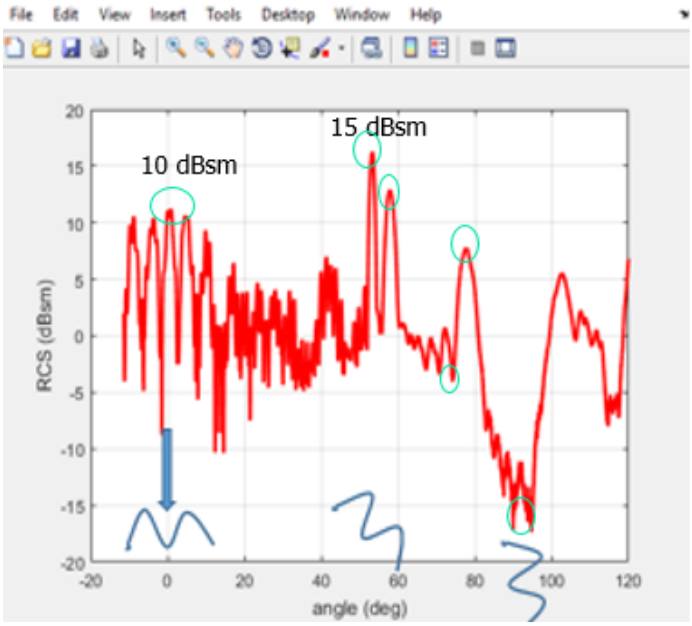

Fig. 4.20. Recommended 77GHz Radar RCS in vertical polarization for W-beam

- Be 10 ± 2dBsm at 0-degree;
- Between 5dBsm to -10dBsm between 0 to 50 degrees;
- Have the maximum of 15 ± 2dBsm around 55-degree;
- Be smooth from 50 to 90 degrees;
- Include three peaks at about 55-degree, 60-degree and 75-degree;
- Include three valleys at about 58-degree, 65-degree and 90-degree.

4. 77GHz Horizontal Polarization RCS Recommendation

   For 77GHz radar horizontal polarization measurement, the radar should be put at a distance of 3m away from the W-beam. The height of the radar should have focused on the middle point of the W-Beam. The surrogate RCS response should have a similar shape as in Fig. 4.21, and satisfy the following requirements:

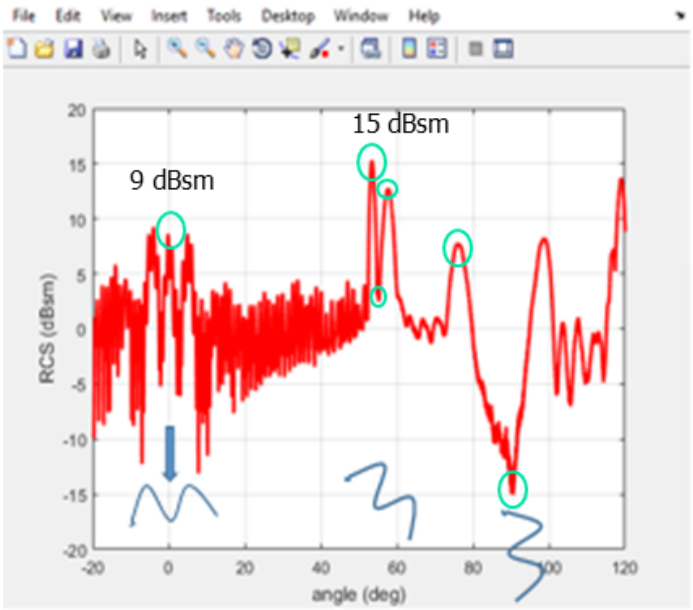

Fig. 4.21. Recommended 77GHz Radar RCS in horizontal polarization for W-beam

- Be 10 ± 2dBsm at 0-degree;
- Between 5dBsm to -10dBsm between 0 to 50 degrees;
- Have the maximum of 1 ± 2dBsm around 55-degree;
- Be smooth from 50 to 90 degrees;
- Include three peaks at about 55-degree, 60-degree and 75-degree;
- Include three valleys at about 58-degree, 65-degree and 90-degree.

4.2.3 I-beam Forward-Looking Measurement

On the real road environment, I-beam is placed behind W-beam. Therefore, half part of I-beam is not visible. Typically, the side-looking radar is not able to detect I-beam. In this case, I-beam side-looking measurement (defined at the beginning of this section) is not considered. However, the forward-looking radar is able to detect I-beam as shown in Fig. 4.1.2.3-1. Also, depending on the positions (such as A, B, C shown in Fig. 4.22) of the vehicle, Radar will look at I-beam from different angles. Therefore, the following measurements will try to figure out how the I-beam RCS changes when Radar scan the I-beam from the 0-degree surface to the 90-degree surface.

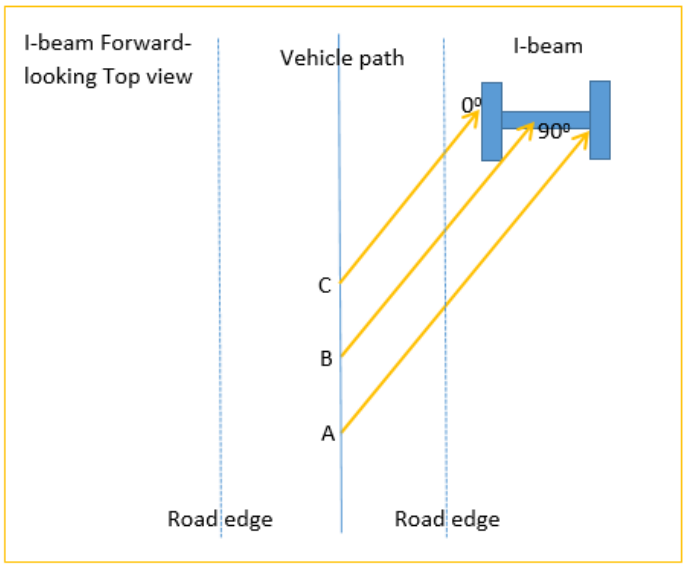

Fig. 4.22. I-beam forward-looking top view

Measurement Method

1. Put the Radar on a tripod (Fig. 4.23 shows the 24GHz RCS at the vertical polarization (left) and the horizontal polarization (right). Fig. 24 shows the

77GHz RCS at the vertical polarization (left) and the horizontal polarization (right). The radar is 55 cm above ground.

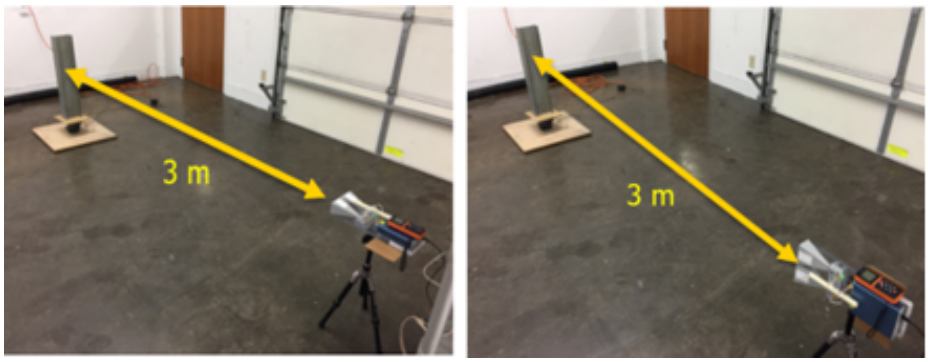

Fig. 4.23. Vertical polarization (left) and horizontal polarization (right) measurement at 24GHz Radar

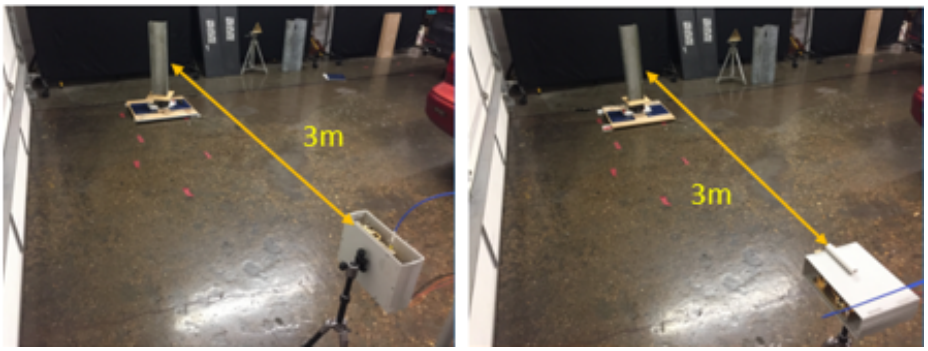

Fig. 4.24. Vertical polarization (left) and horizontal polarization (right) measurement at 77GHz Radar

2. Use RCS calibration method to check if radar works property or not. Choose 3m as the distance between Radar and reflector (Chapter 3).

3. Record the signal response of trihedral reflector that will be used to calibrate the signal response of I-beam.

4. After calibration, replace the trihedral reflector with a rotating table and let I-beam stand on the middle of the rotating table. Use a level to make sure I-beam is perpendicular to the ground.

5. Start the rotator, and adjust the speed, so that the I-beam can rotate at least 90 degrees within the 30s.

6. Start recording the data of I-beams signal response from 0-degree (Fig. 25 left image) faces to Radar to 90-degree faces to Radar (Fig. 25 right image). Click record button about 2s earlier, so that can guarantee 0-degree to be recorded.

Fig. 4.25. I-beam at 0-degree (left) and 90-degree (right)

7. Plot the recording raw data and calculate I-beam RCS value at each angle (0 to 90 degrees). Fig. 4.26 shows the continuous measurement of the I-beam. Similar to W-beams color map, the x-axis is the number of Radar scan times, which related to recording time (recording time=scan times/500). The y-axis is the distance (1.5 to 5 meters). In this figure, the 0-degree of I-beam is measured around x=2000 (4s) (pointed by a thin straight black line). The reason is that there is a wide flat surface (Fig. 4.1.2.3.1-3 left image) perfectly facing the Radar, so the Radar receives a very strong power response. When this flat surface does not perfectly face the radar, it will reflect most of the radar waves

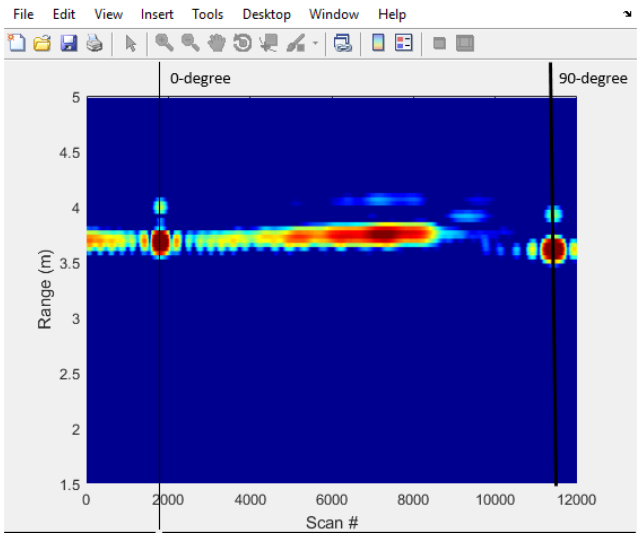

Fig. 4.26. Color map of I-beam rotation data

to left/right side. The same idea applies for 90-degree (Fig. 4.25 right image), its strong signal appears at around x=11800 (23.6s) (pointed by a thick straight black line).After raw data calibration, the RCS plot of I-beam is calculated (Fig. 4.27). The x-axis is the angle (degree). The y-axis is RCS value (dBsm). The I-beam RCS measurement is done.

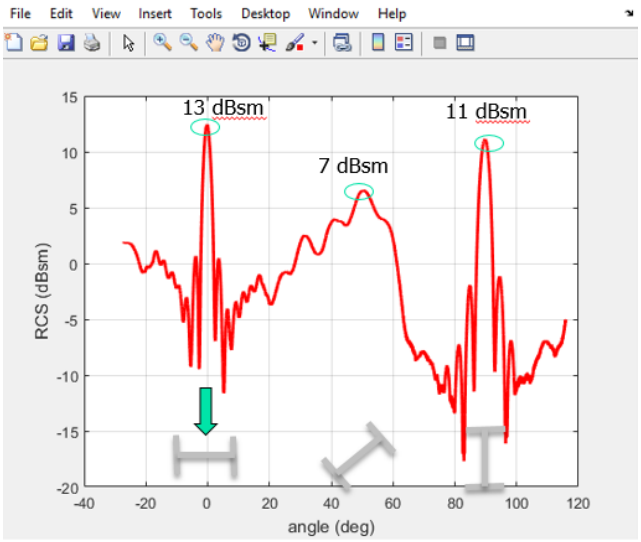

Fig. 4.27. RCS plot of an I-beam at various angles

Measurement Result

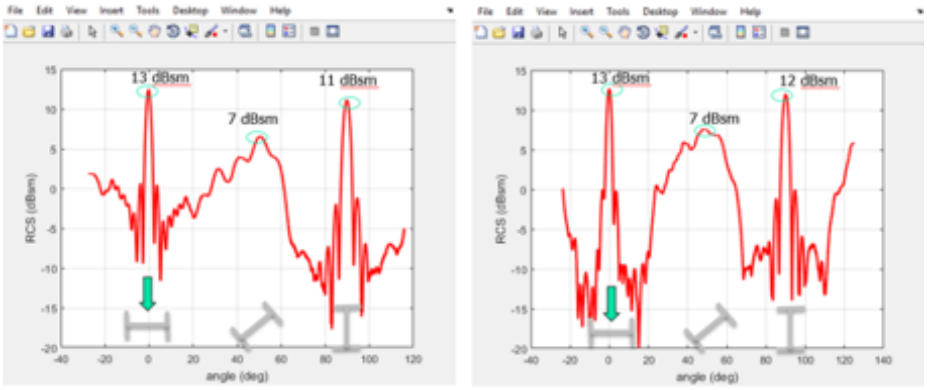

Fig. 4.28. 24GHz radar vertical polarization RCS result (left) and horizontal polarization RCS result (right).

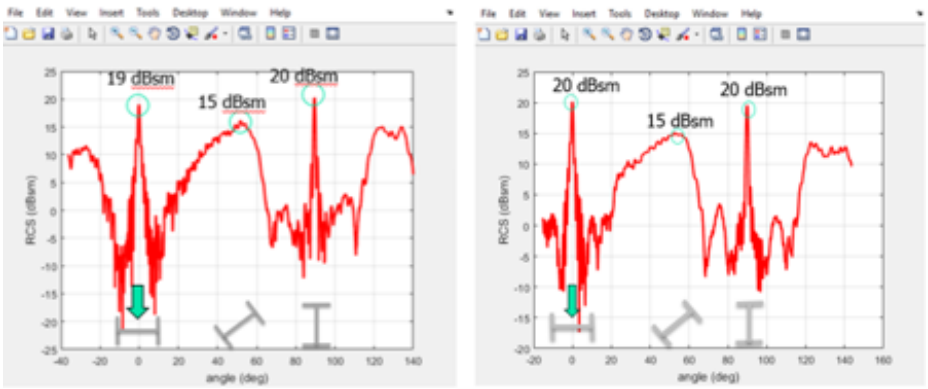

Fig. 4.29. 77GHz radar vertical polarization RCS result (left) and horizontal polarization RCS result (right).

Result Discussion

1. Maximum RCS Response

   Fig. 4.28 and Fig. 4.29 show that the two maximum RCS values are at 0-degree and 90-degree for all four types of measurements. This is because that when I-beam is placed at 0-degree or 90-degree, the flat surface of I-beam is

perpendicular to the Radar center beam. Moreover, there is a local maximum around 50-degree. Fig. 4.30 shows that a right angle corner is facing to radar at 50-degree. This corner will generate a strong signal response.

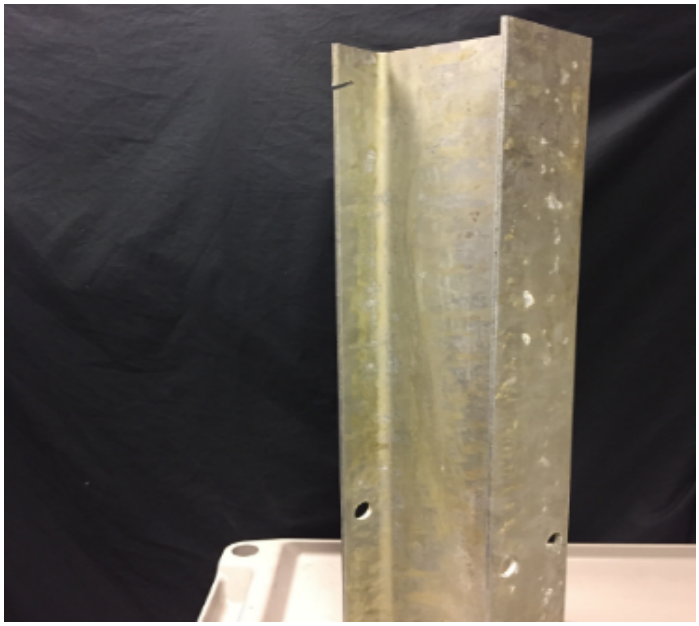

Fig. 4.30. I-beam at 50-degree

2. 24GHz Vertical and Horizontal Radar Polarization Results Comparison
   Fig. 4.28 shows that the vertical and horizontal polarization RCS results of I-beam at 24 GHz Radar are almost the same. At 0-degree and 90-degree, both of their RCS are 13 ± 2 dBsm. Around 50-degree, both of them show a local maximum which is about 7 ± 2 dBsm.

3. 77GHz Vertical and Horizontal Radar Polarization Results Comparison
   Similar to the comparison of 24GHz RCS measurement results, 77GHz RCS measurement results of vertical and horizontal polarization of I-beam are almost the same (Fig. 4.29) as well. At 0-degree and 90-degree, both of their RCS values are 20 ± 2 dBsm. Around 50-degree, both of them show a local maximum which is about 15 ± 2 dBsm.

4. 24GHz and 77GHz Vertical Radar Polarization Results Comparison
   Left images of Fig. 4.28 and Fig. 4.29 show that the shapes of 24GHz and 77GHz RCS vertical polarization plots of I-beam do not have a big difference. The main difference between them is the value. 77GHz radar measurement results are about 7 dBsm higher than 24GHz radar measurement results.

5. 24GHz and 77GHz Horizontal Radar Polarization Results Comparison
   Again, the shapes of 24GHz and 77GHz RCS horizontal polarization plots of I-beam do not have a big difference (right images of Fig. 4.28 and Fig. 4.29), but 77GHz radar measurement results are about 7 dBsm higher than 24GHz radar measurement results.

Summary and RCS Recommendation of Metal Guardrail I-beam

As proved in Section 4.2.2, RCS of metal guardrail W-beam does not affect by age. Since metal guardrail I-beam and W-beam are made of the same material, RCS of I-beam should not affect by age as well. The vertical polarization measurement result is similar with horizontal polarization result at both 24GHz Radar and 77GHz Radar. The recommend vertical and horizontal RCS plots at 24GHz and 77GHz Radar are shown below.

1. 24GHz Vertical Polarization RCS Recommendation
   This result works for vertical polarization measurement at 24GHz Radar. The Radar should be placed 3 meters away from the I-beam. The height of the Radar should be set at the middle point of the I-Beam. The surrogate RCS response does not need to be the same as the following figure (Fig. 4.31) but should have a similar shape. The need to be compared at three critical points: at 0-degree, the RCS should be 13 ± 2 dBsm; at 50-degrees, the RCS should be 7 ± 2 dBsm; and at 90-degrees, the RCS should be 11 ± 2 dBsm.

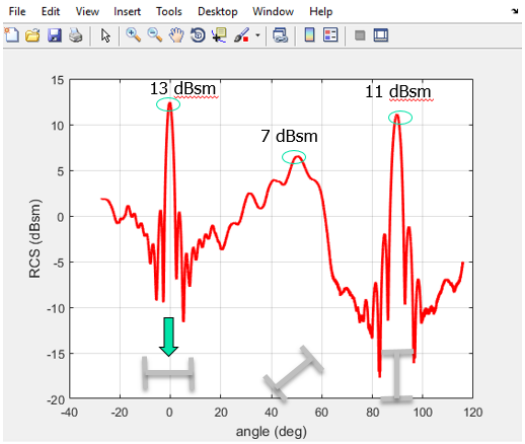

Fig. 4.31. Recommended 24GHz Radar RCS in vertical polarization for I-beam

2. 24GHz Horizontal Polarization RCS Recommendation

   This result works for horizontal polarization measurement at 24GHz. The Radar should be placed 3 meters away from the I-beam. The height of the Radar should be set at the middle point of the I-Beam. The surrogate RCS response should have a similar shape as in Fig. 4.32 and needs to satisfy the requirement at three critical points: at 0-degree and 90-degree, the RCS should be 13 ± 2 dBsm; at 50-degrees, the RCS should be 7 ± 2 dBsm.

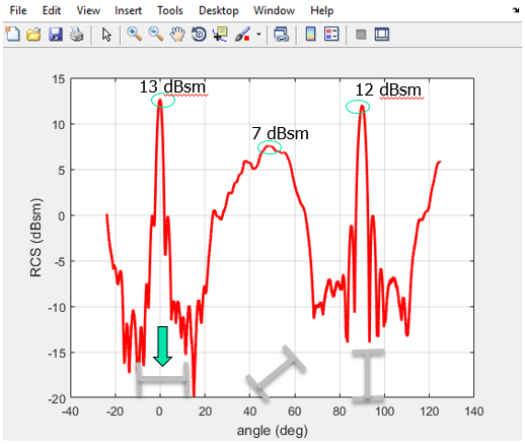

Fig. 4.32. Recommended 24GHz Radar RCS in horizontal polarization for I-beam

3. 77GHz Vertical Polarization RCS Recommendation

   This result works for vertical polarization measurement at 77GHz. The Radar should be placed 3 meters away from the I-beam. The height of the Radar should be set at the middle point of the I-Beam. The surrogate RCS response should have a similar shape as in Fig. 4.33 and needs to satisfy the requirement at three critical points: at 0-degree and 90-degree, the RCS should be 20 ± 2 dBsm; at 50-degrees, the RCS should be 15 ± 2 dBsm.

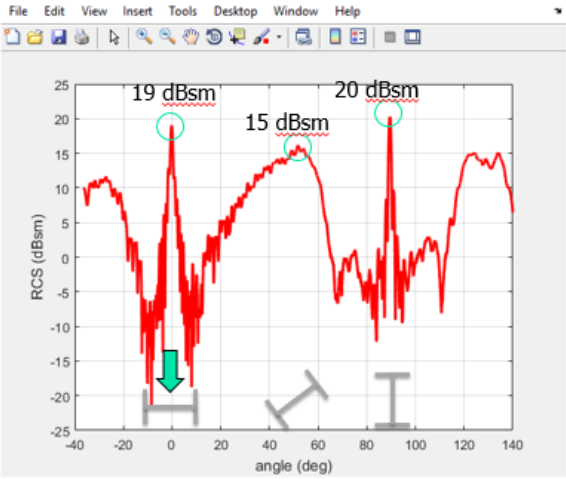

Fig. 4.33. Recommended 77GHz Radar RCS in vertical polarization for I-beam

4. 77GHz Horizontal Polarization RCS Recommendation

   This result works for horizontal polarization measurement at 77GHz. The Radar should be placed 3 meters away from the I-beam. The height of the Radar should be set at the middle point of the I-Beam. The surrogate RCS response should have a similar shape as in Fig. 4.34 and needs to satisfy the requirement at three critical points: at 0-degree and 90-degree, the RCS should be 20 ± 2 dBsm; at 50-degrees, the RCS should be 15 ± 2 dBsm.

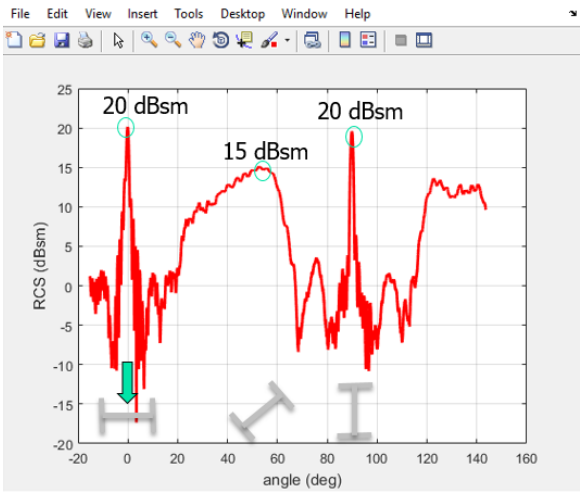

Fig. 4.34. Recommended 77GHz Radar RCS in horizontal polarization for I-beam

4.3 Grass RCS Measurement

The purpose of this subtask is to find the representative 24 GHz and 77 GHz radar characteristics of grass. RCS is used for describing the radar characteristics.

4.3.1 Sample Selection

How to select grass samples to study grass radar property is one of the most difficult parts in this research. Theoretically, the study should include all possible kinds of grass. However, in nature, grass grow randomly. Therefore, the number of kinds of grass is uncountable. One of the solutions is to make a classification for grass based on some key features of grass. Then selecting the high-ranking types of grass to be the grass samples. Four parameters are defined to classify grass: color, color evenness, height, and height evenness. 2,443 Google Street View images that show grass road edge have been studied. The result from the study shows that the most common color of grass is green and yellow mixed. In addition, only short (less than 5") and medium (6" to 10") grass can be easily seen on the road edge. Therefore, the research focus on short and medium grass. Furthermore, most grasses that grow

next to the urban road are even, but grasses that grow on the edge of the suburban road are usually uneven. In this case, even and uneven are both important. Note that the color evenness and height evenness are combined as one parameter (called evenness) since the study result shows they are highly correlated. Eventually, three grass samples are picked for the study of grass radar property.

Table 4.6 and Fig. 4.35 shows the samples of grass used in RCS measurements.

Table 4.6.
Grass samples

Object	**Height**	**Color**	**Surface Condition**	**Type**
Grass 1	Short (2-4 inch)	Green and Yellow	Somewhat even	Wild
Grass 2	Medium (8-10 inch)	Green and Yellow	Uneven	Wild
Grass 3	Short (2-4 inch)	Green	Very even	Well maintained

Fig. 4.35. Grass 1 (left), Grass 2 (middle), Grass 3 (left)

Table 4.6 shows three grass samples. Grass 1 (Fig. 4.35 left) is wild grass of mixed green and yellow colors. It is short, only about 2 to 4 inches tall. The height and color distribution looked pretty even. Grass 2 (Fig. 4.35 middle) is also wild grass. The overall color is a mix of green and yellow, but more in green side. Majority grass is about 8 to 9 inch tall. The height and color of the Grass 2 are not even. Green 3

(Fig. 4.35 right) is well-maintained grass located on IUPUI campus. Therefore, it is almost pure green and very even. The height of the grass is 2 to 4 inch.

4.3.2 Measurement Method

Since there are infinite numbers of grass shapes variations, the RCS of any specific grass location cannot represent the grass. Therefore, we measure the RCS of a grass area through a 15 feet long line and take the average as the grass RCS. Following are the process of grass RCS measurements.

1. As shown in Fig. 4.38 side view, a tripod was placed on a moving cart. 24GHz/77GHz radar was vertically/horizontally mounted on the tripod (see Fig. 4.36 and Fig. 4.37).

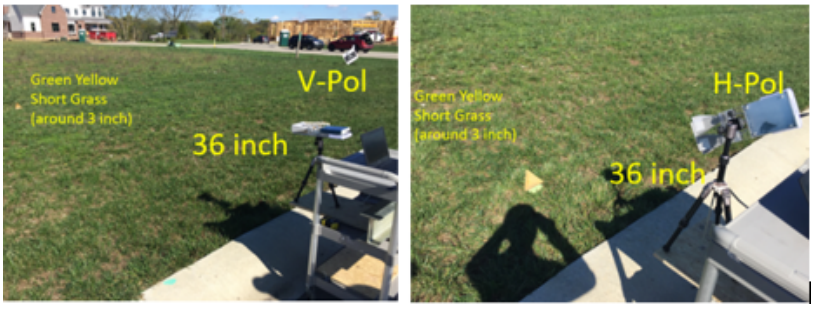

Fig. 4.36. 24GHz Vertical (left) and horizontal (right) polarization set up

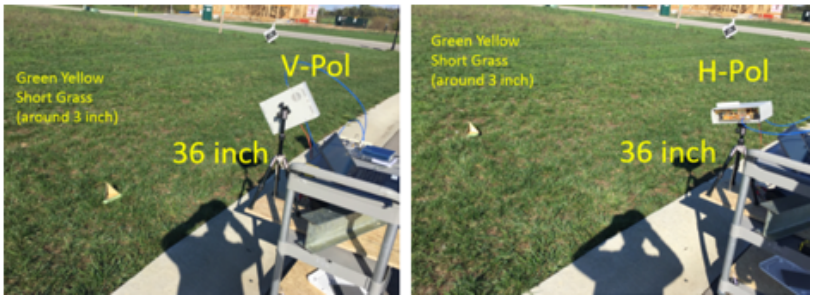

Fig. 4.37. 77GHz Vertical (left) and horizontal (right) polarization set up

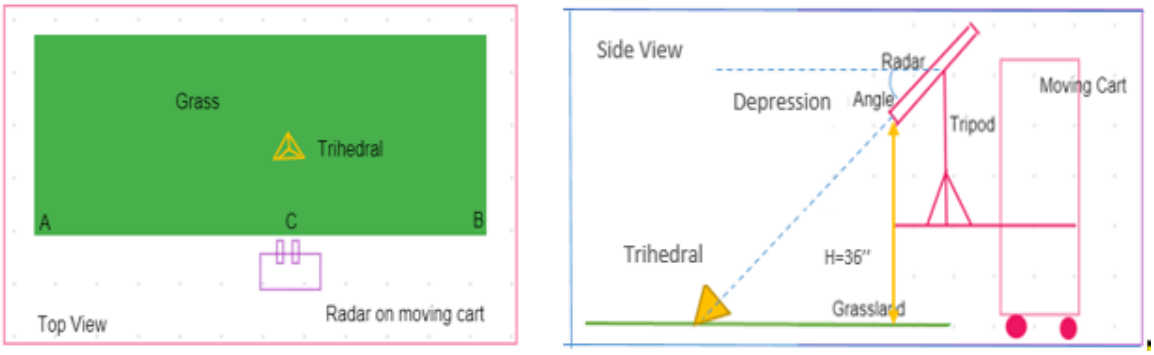

Fig. 4.38. Grass measurement top view (left) and side view (right)

2. Use a level to set the radar pitch angle (Fig. 4.38 side view). One measurement was taken every 5 degrees. The pitch angle varied from 35-degree to 10-degree referenced to the horizontal line parallel to the ground. Therefore, 6 measurements were taken for one set of measurement for each radar polarization.

3. Move the cart to position C (Fig. 4.38 top view). Position C is roughly the middle point of AB. A is the start point, and B is the end point of measurement. The length of AB is at least 15 ft. The longer, the better.

4. 36 inch is used as radar height, which is from antennas middle point to the ground (Fig. 4.38 side view). The measurement height is not necessary to be 36-inch, but this height is a reasonable height when the radar is placed on the car.

5. Adjust trihedral corner reflector. Place the trihedral corner reflector on the ground and move it until we can see the center of the trihedral reflector through the pipe that was placed on the top of the radar. Therefore, the radar center beam is aimed at the trihedral (Fig. 4.38 top view).

6. Move the cart to position A (Fig. 4.38 top view), and get ready to start the measurement.

7. Set data recording time to be 25 seconds. Start data recording and push the cart from A to B at a constant speed. The time for moving from A to B should be within 25 seconds. Therefore, the cart moving speed depends on the length of AB.

8. Plot the recording raw data and calculate the RCS value of grass over distance changing. The left image of Fig. 4.39 is the color map of raw data of grass signal response. The x-axis is the number of Radar scan times, which related to the recording time (recording time = scan times/500). Note that the full x-axis range is from 0 to 12500. The starting data (0-2500) and ending data (10000 to 12500) are cut since those data are affected by objects which are placed on grassland to indicate the starting position and ending position. The y-axis is the distance (1 to 15 meters). Note that the data from 0 to 1 meter is cute since those data are affected by antenna coupling. The signal of the trihedral corner reflector is clearly visible in the display. Click the up left corner of the trihedral area such as position A and bottom right corner such as position B to define a box that covered the signal response of trihedral corner reflector. The Matlab program will automatically find the maximum value within this box. This maximum value was the trihedral response. It would be used as the reference for calibrating the grass response and getting the RCS value of grass. After the box was defined, the rest parts were used to calculate grass maximum response, minimum response, and mean response at each distance (Fig. 4.39 right image). Therefore, it is important to make sure that the box is big enough so that no trihedral response is mixed into grass response. Otherwise, the grass response will be corrupted. In Fig. 4.39, the yellow plot, red plot, dark blue plot, and green plot are corresponding to the maximum RCS plot, mean RCS plot, medium RCS plot, and minimum RCS plot of grass at each distance. The most important plot is the mean RCS plot. It indicates the average RCS level of the grass. The straight blue line is corresponding to the location of a trihedral corner reflector. The values shown on the right top corner are the maximum,

minimum and mean grass RCS at the same distance of trihedral corner reflector. The most important part of Fig. 4.39 is the plots between the blue line and the black line. The plots before the blue line are affected by antenna coupling. The plots after the dark black line are just background noise. The plots between the blue line and black line show how the grass' RCS changes as range increases.

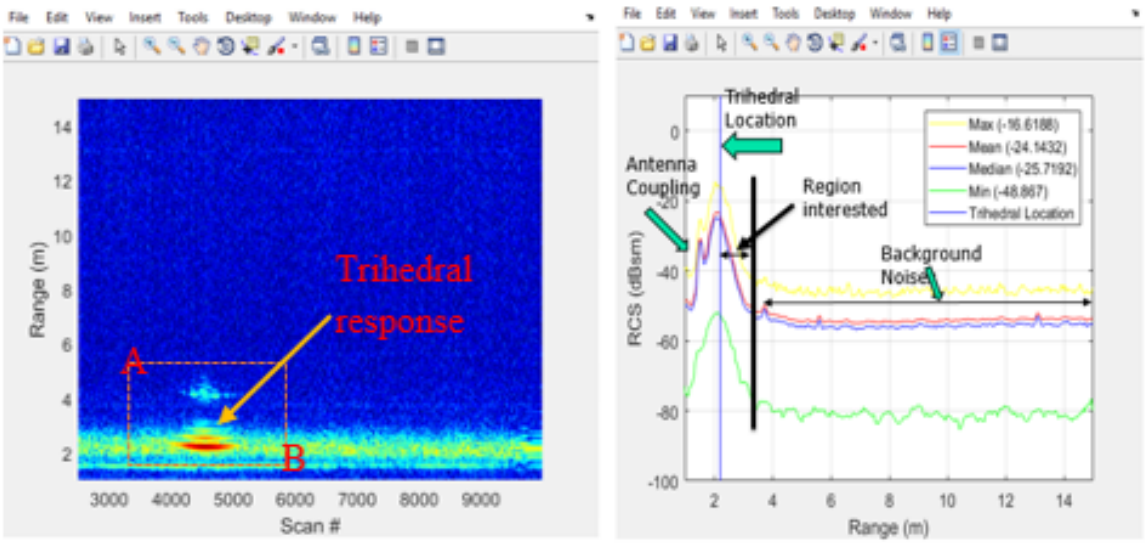

Fig. 4.39. Color map of grass raw data (left) and RCS result (right)

4.3.3 Measurement Result

Following are the measurement results under different conditions. The title of each figure indicates the measurement conditions. For example, 24GHz-V-Pol-35-degree means the result is measured under 24GHz Radar, vertical polarization, 35-degree depression angle.

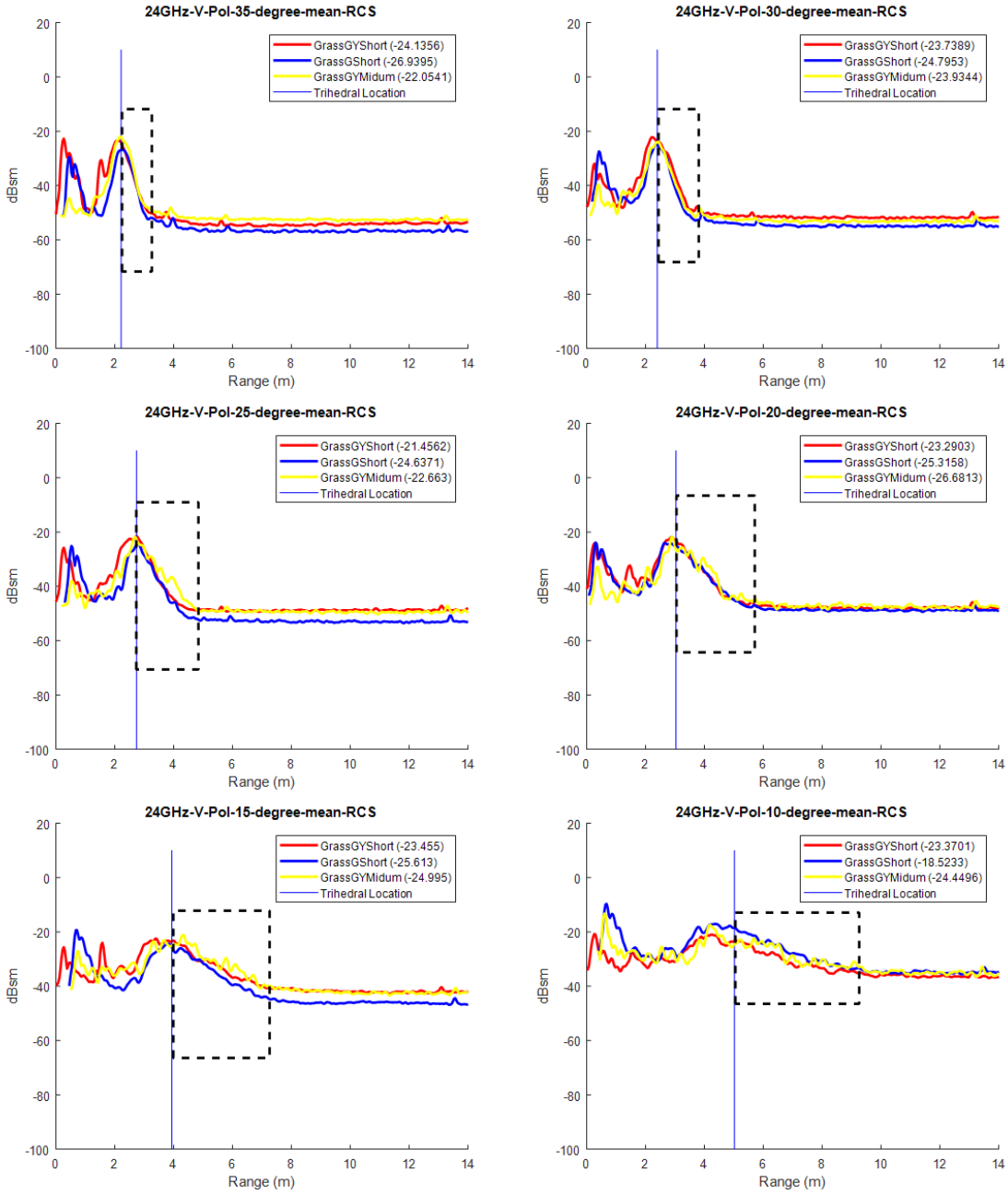

Fig. 4.40. 24GHz Radar vertical polarization measurements from 35-degree to 10-degree for 3 grass samples

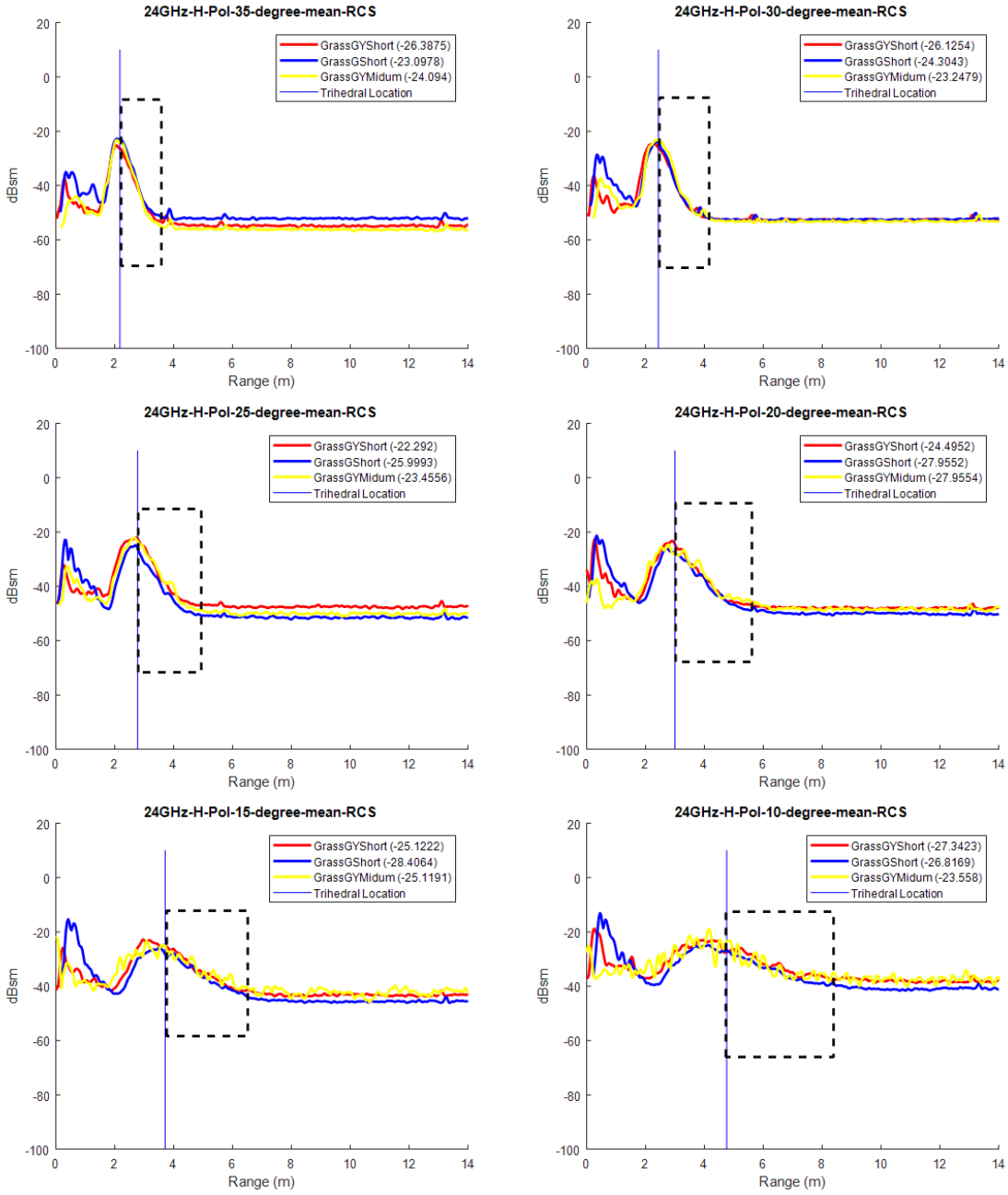

Fig. 4.41. 24GHz Radar horizontal polarization measurements from 35-degree to 10-degree for 3 grass samples

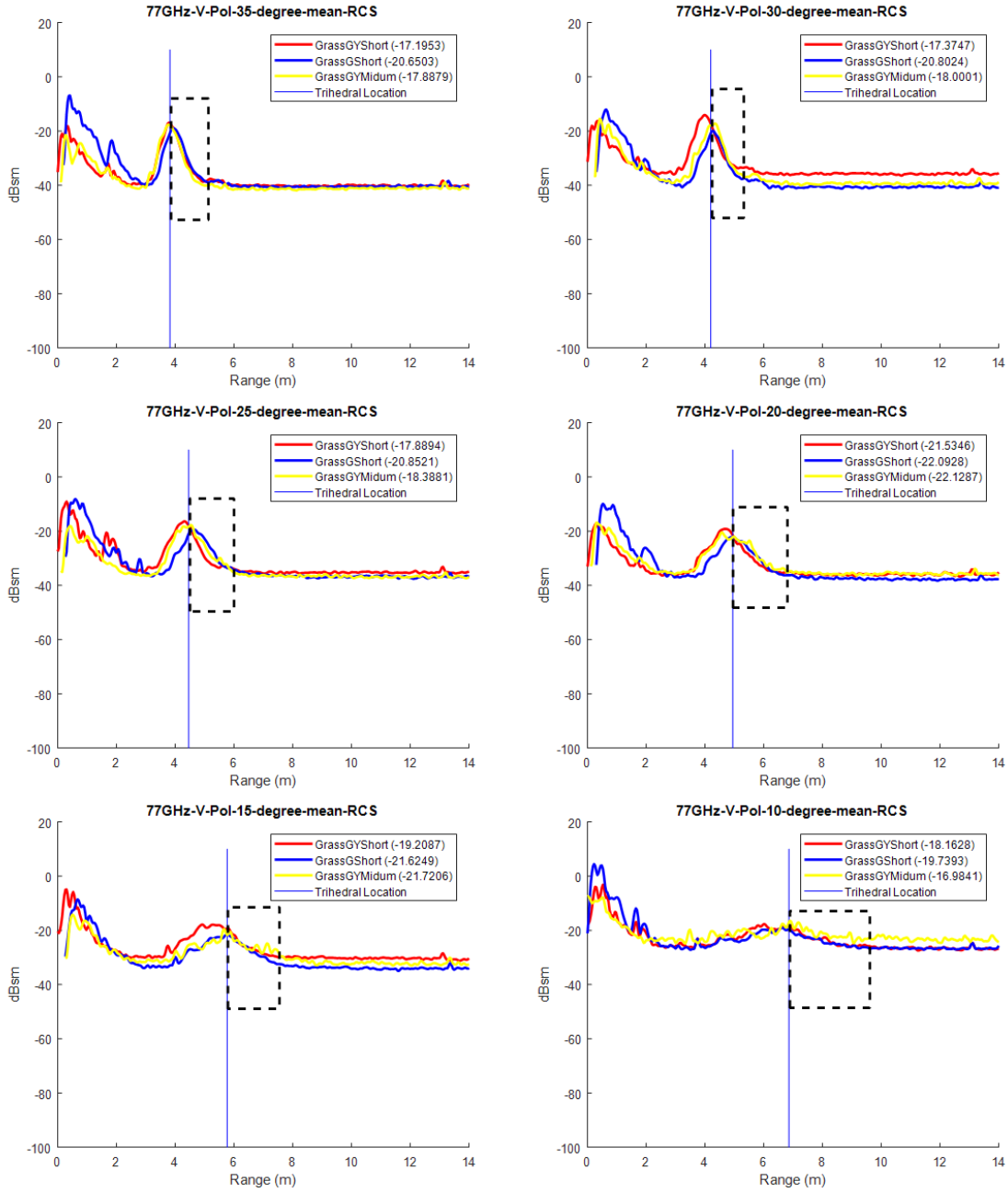

Fig. 4.42. 77GHz Radar vertical polarization measurements from 35-degree to 10-degree for 3 grass samples

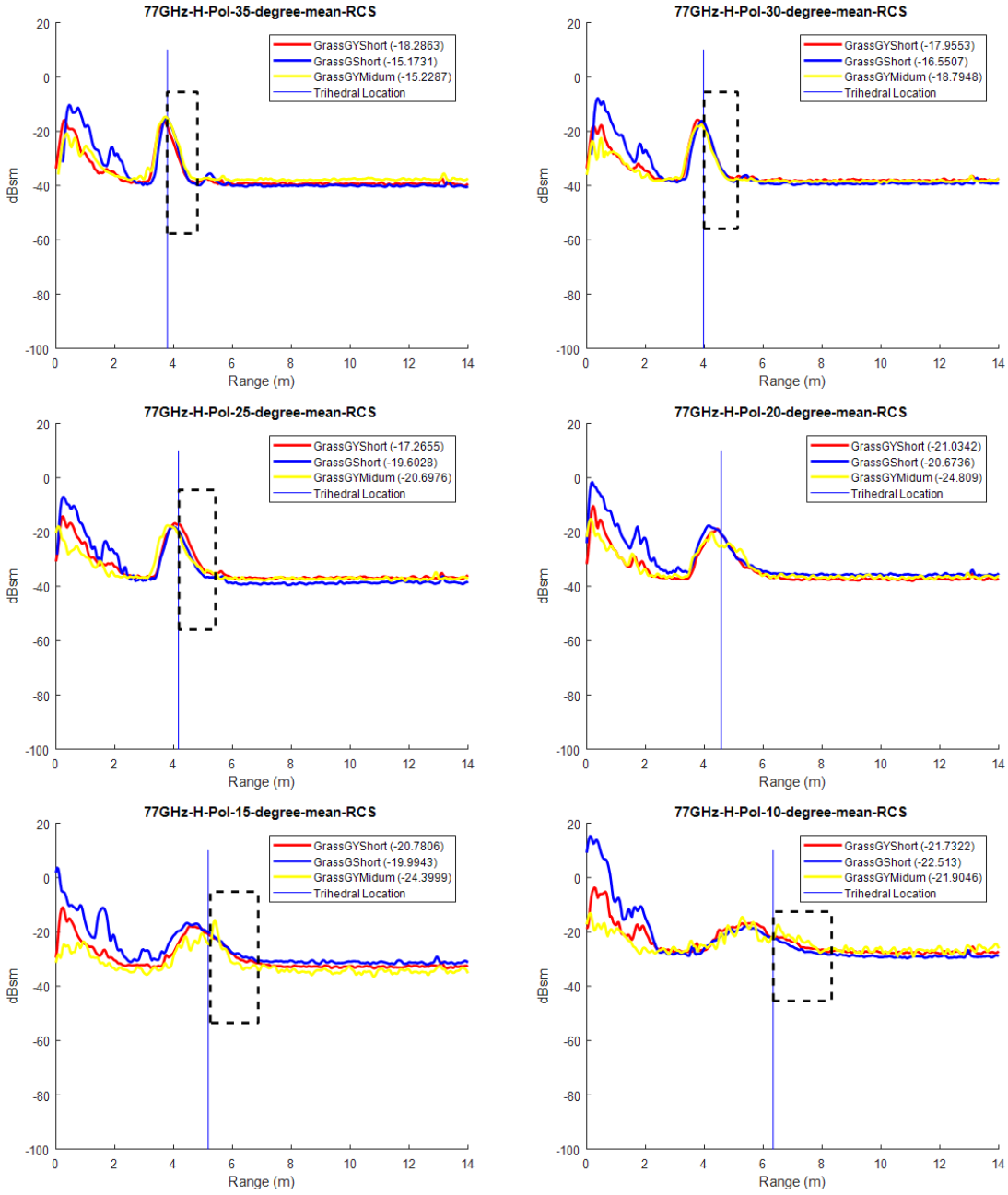

Fig. 4.43. 77GHz Radar horizontal polarization measurements from 35-degree to 10-degree for 3 grass samples

4.3.4 Discussion

1. Are the grass RCS different between different kinds of grass?

   The mean RCS plots are shown in Fig. 4.40 to Fig. 4.43 indicates that these three different samples of grass (wild vs. man maintained, short vs. medium, green yellow vs. pure green, even vs. uneven) have very similar RCS value when they are measured under the same condition (same radar type, same polarization, and same depression angle). Moreover, those figures also show that three types of grasses almost have the same RCS plot (RCS vs. Range) under any measurement condition. Therefore, grass type, height, color, and evenness will not affect grass RCS a lot.

2. Are the grass RCS different under different radar frequency (24/77 GHz)?

   As Fig. 4.40 and Fig. 4.42 show, the shape of the RCS plot generated by 24 GHz Radar vertical polarization measurement is almost the same as the shape of the RCS plot generated by 77 GHz Radar vertical polarization measurement at any depression angle. However, the magnitude of the whole RCS plot of 24GHz Radar measurement is lower than that of the 77GHz Radar measurement at any depression angle. The same conclusion will be applied for comparing the 24GHz horizontal polarization RCS plot and 77GHz horizontal polarization RCS plot (Fig. 4.41 and Fig. 4.43).

3. Are grass RCS different when using different radar polarization?

   By comparing the vertical (Fig. 4.40)and horizontal polarization (Fig. 4.41) RCS plots, it is easy to see that not only the shape of RCS plots but also the magnitudes of RCS plots are very similar for 24GHz Radar measurement at any depression angle. This is also true for comparing the 77GHz Radar vertical polarization measurement results (Fig. 4.42) and the horizontal measurement results (Fig. 4.58 to Fig. 4.43). Therefore, the grass RCS are almost the same under different radar polarization.

4.3.5 Summary and RCS Recommendation of Grass

- Type, height, color, and evenness of grass will not affect grass RCS a lot.
- 24GHz measurement results have a similar shape as the 77GHz measurement results, but the amplitudes are lower than 77GHz measurement results.
- The horizontal and vertical RCS measurement result are very similar at both 24GHz and 77 GHz Radar.

By plotting the maximum of maximum, average of mean, minimum of minimum of RCS plots of all three grass samples under the same measurement conditions, the requirements for surrogate grass under different measurement conditions can be defined. The surrogate grass RCS plot should be between the corresponding maximum plot and minimum plot; it is better to close to the mean plot. Again, the most important part of each plot is the slanting section that starts from the blue bar, since the plot before the blue line is affected by antenna coupling, and the flat tail part is just background noise. More details are showing below (the name format of each figure is frequency-polarization-depress angle)

1. Recommended 24GHz Radar Vertical Polarization RCS for Surrogate Grass (Fig. 4.44)
2. Recommended 24GHz Radar horizontal Polarization RCS for Surrogate Grass (Fig. 4.45)
3. Recommended 77GHz Radar Vertical Polarization RCS for Surrogate Grass (Fig. 4.46)
4. Recommended 77GHz Radar horizontal Polarization RCS for Surrogate Grass (Fig. 4.47)

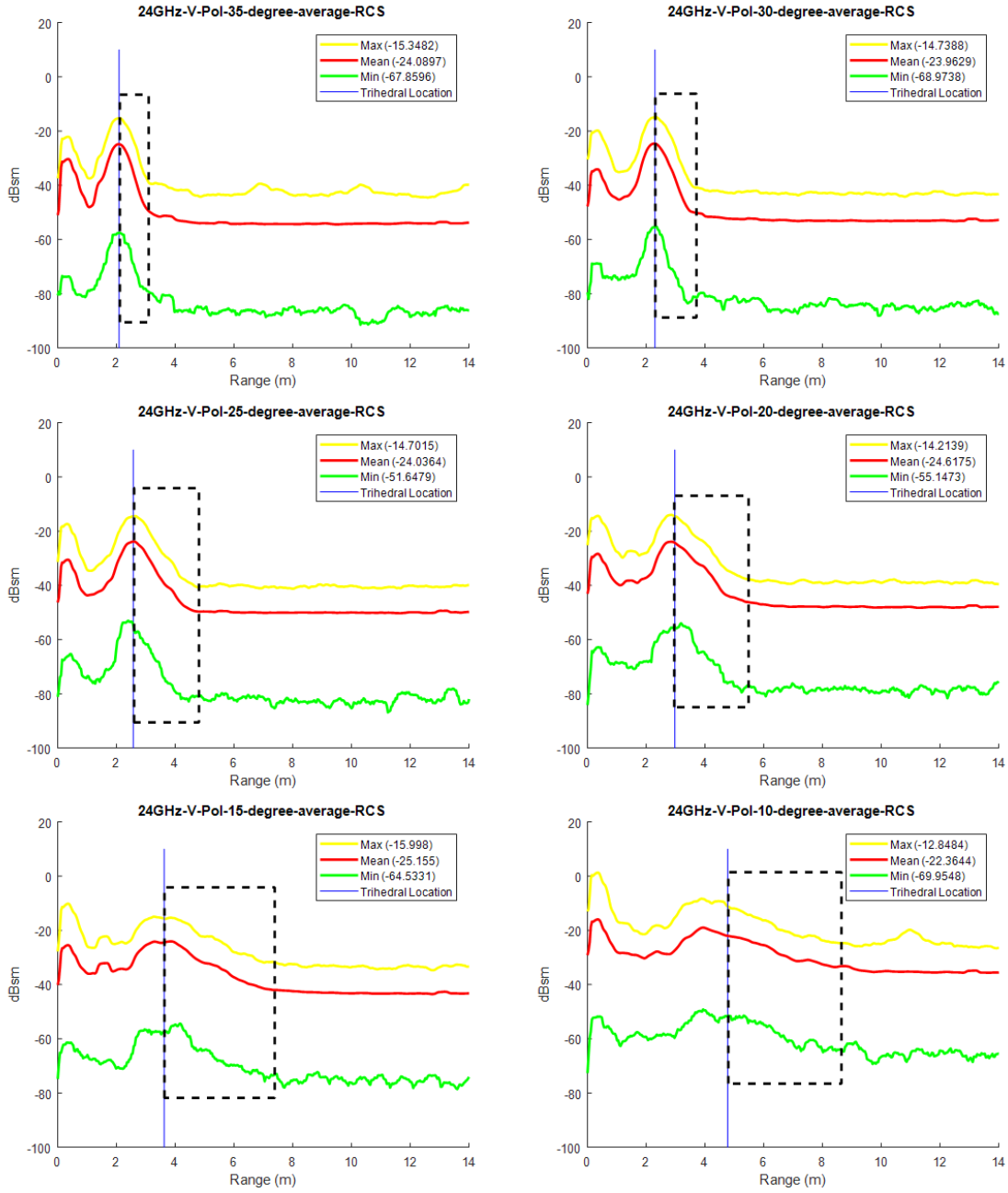

Fig. 4.44. Recommended 24GHz vertical polarization RCS for surrogate grass

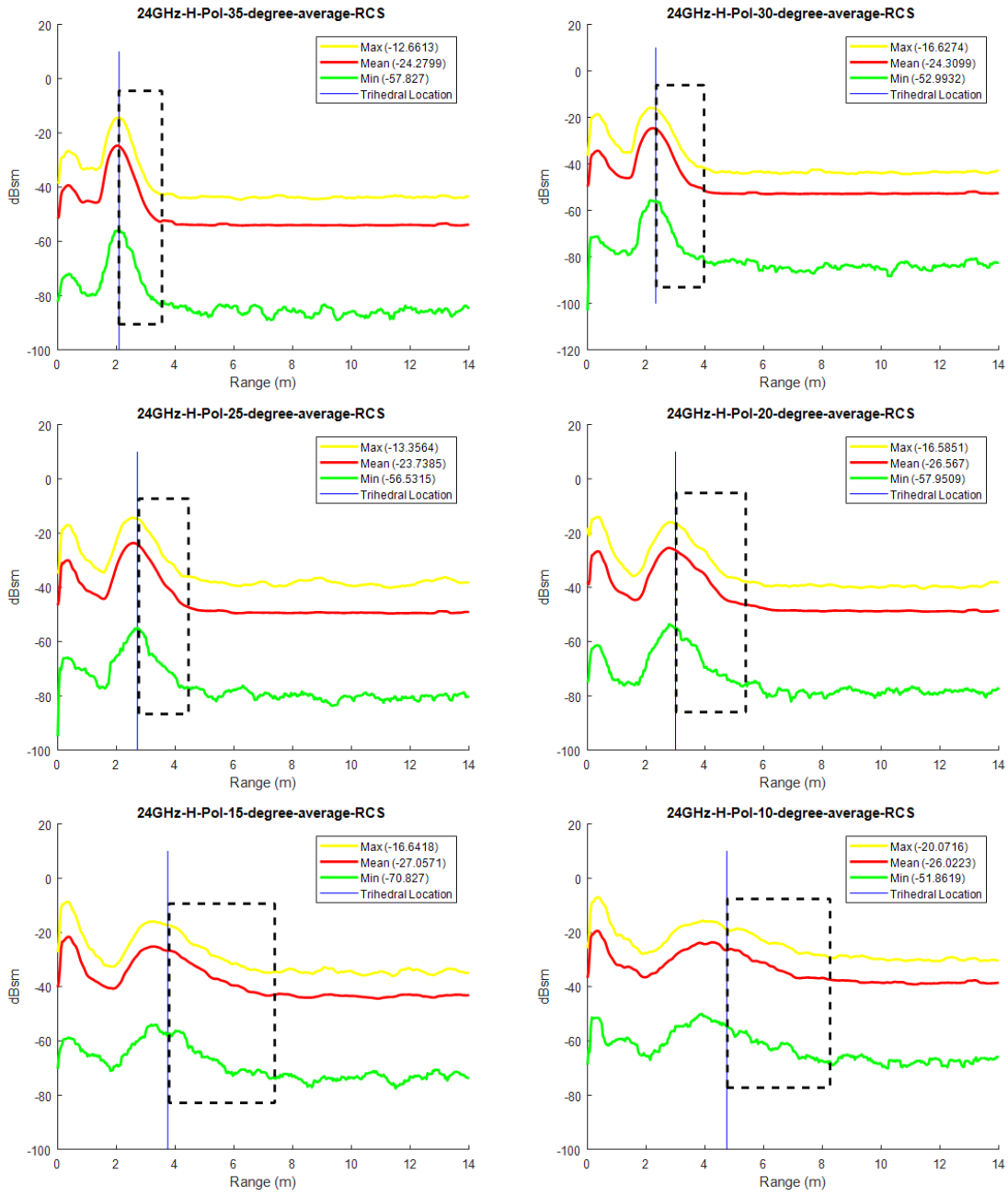

Fig. 4.45. Recommended 24GHz horizontal polarization RCS for surrogate grass

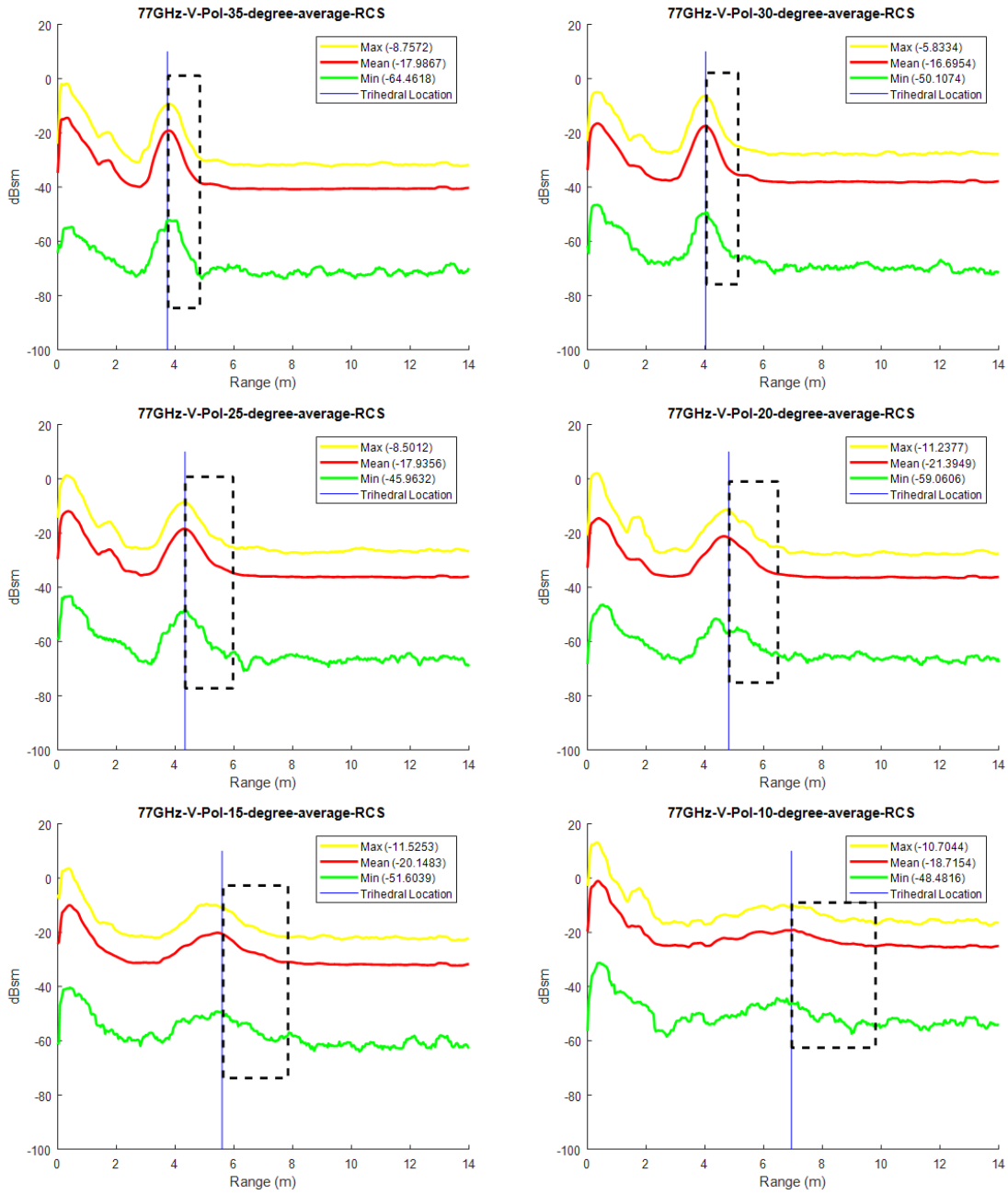

Fig. 4.46. Recommended 77GHz vertical polarization RCS for surrogate grass

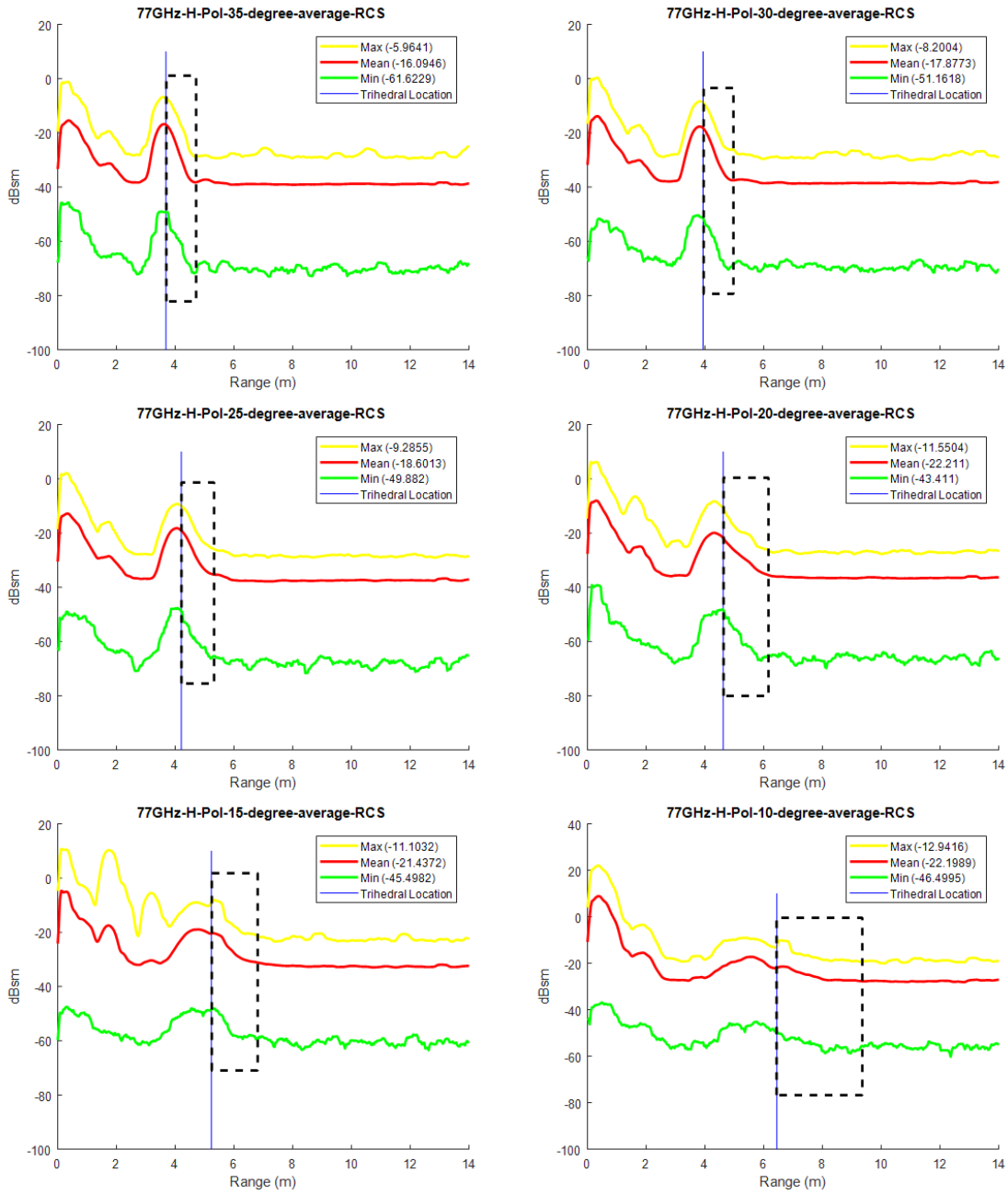

Fig. 4.47. Recommended 77GHz horizontal polarization RCS for surrogate grass

4.4 Concrete Divider Reflectivity Measurement

The purpose of this task is to find the representative 24GHz and 77GHz Radar characteristics of concrete dividers. Reflectivity is used for describing the Radar characteristics. After doing reflectivity measurement, the material property of concrete divider from radar point view will be found.

4.4.1 Sample Description

Table 4.7 describes six samples of concrete dividers. Concrete divider 2 (Fig. 4.49) is standard New Jersey Shape. Others are all standard F-shape. Only the surface of Concrete divider 1 (Fig. 4.48) is coated by some types of white coat/paint. Concrete dividers (1 to 4) have good smooth surface. There are some holes on the surface of Concrete divider 5. For Concrete divider 6, the majority part of the surface (Fig. 4.52) has been damaged. On the color side, Concrete dividers 2 and 3 have similar brownish color. Concrete divider 1 is white. Rest of the concrete dividers are in gray color. On the age side, the Concrete divider 1 looks new. Rest of them are old, but Concrete divider 2 and 3 looks newer than Concrete divider 4, 5 and 6.

Fig. 4.48. Concrete Divider 1

Fig. 4.49. Concrete Divider 2

Fig. 4.50. Concrete Divider 3

Fig. 4.51. Concrete Divider 4

Fig. 4.52. Concrete Divider 5

Fig. 4.53. Concrete Divider 6

Table 4.7.
Concrete Divider Samples

Object	Type	Color	Age	Surface Condition	Coating	Location
Concrete Divider 1	F-shape	White	Half-old	smooth	White paint coating	Indianapolis Highway I-65
Concrete Divider 2	New Jersey Shape	Brown	Old	smooth	No	Indianapolis old airport
Concrete Divider 3	F-shape	Brown	Old	smooth	No	Indianapolis old airport
Concrete Divider 4	F-shape	Gray	Very old	smooth	No	Indianapolis old airport
Concrete Divider 5	F-shape	Gray	Very old and unused	some big and deep holes	No	City wide paving, Inc.
Concrete Divider 6	F-shape	Gray	Very old and unused	worn down	No	City wide paving, Inc.

4.4.2 Concrete Divider Forward-Looking Measurement

The meaning of forward-looking is defined in the metal guardrail section (see Section 4.2). Also, based on the experience (radar can see the object only when

the surface of the object is perpendicular to radar beams) get from metal guardrail forward-looking measurement, the forward-looking measurement may not detect concrete divider very well. Only the area that is perpendicular to the Radar beams can be detected. The main purpose of the following measurement is to verify this prediction. 77GHz radar is used in the following experiment since it is usually used as a forward-looking radar.

Measurement Steps

1. Place the 77GHz Radar at 1m away from the concrete divider. Set the measurement angle to be 15-degree from the normal line of concrete divider surface (Fig. 4.54). Record 2s data for this measurement (Measurement-1). Fig. 4.55 shows the measurement result. The x-axis is time (ns). The maximum peak in each figure is antenna coupling (pointed by horizontal blue arrow). The peak pointed by the vertical blue arrow in each figure is the signal response generated by a concrete divider. In this case, the concrete signal response is about 44.9 dB.

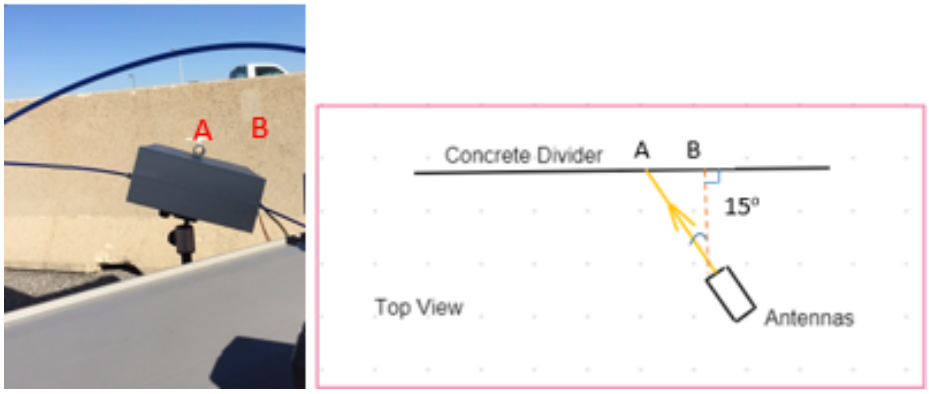

Fig. 4.54. Measurement-1 of the Forward-looking measurement setup

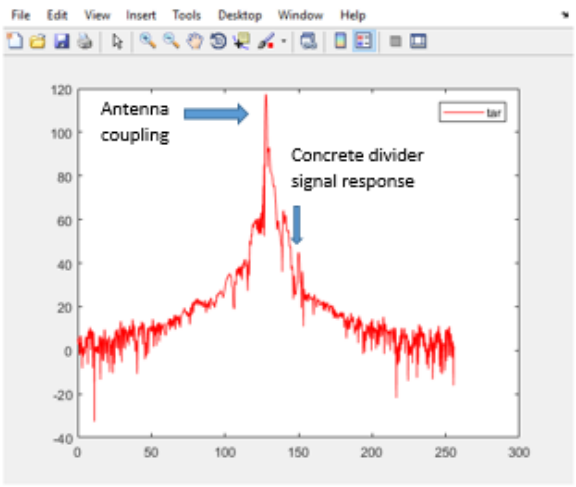

Fig. 4.55. The measurement result of Measurement-1

2. Use a radar absorber foam to cover area A (Fig. 4.56 left image). Record 2s data for this measurement (Measurement-2). In this case, the concrete signal response is about 45.2 dB (Fig. 4.56 right image).

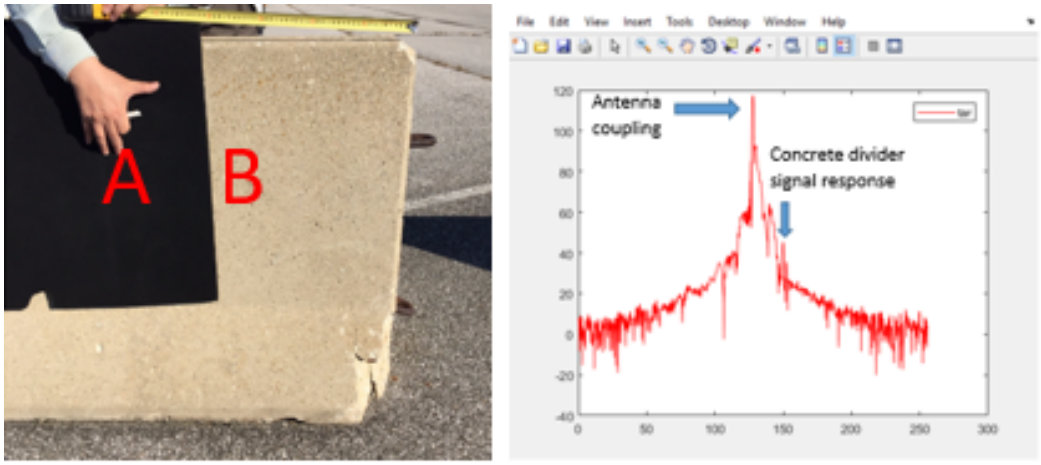

Fig. 4.56. Measurement-2 setup (right) and result (right)

3. Move the absorber foam forward, so that area B can be covered as well (Fig. 4.57 left image). Record 2s data for this measurement (Measurement-3). In

this case, the concrete signal response is about 34.2 dB (Fig. 4.57 right image).

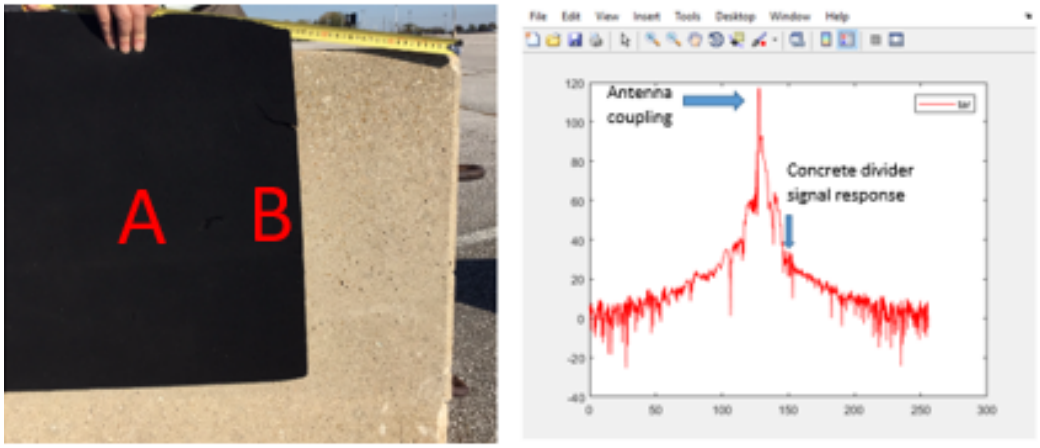

Fig. 4.57. Measurement-3 setup (right) and result (right)

Summary of Measurement Result

Table 4.8.
Forward-looking measurement results

Measurement ID	Area A	Area B	Power Response (dB)
Measurement-1	Not cover	Not cover	44.9
Measurement-2	Cover	Not cover	45.2
Measurement-3	Cover	Cover	34.2

Result Discussion

As Table 4.8 shown, the concrete signal response is about 44.9 dB in Measurement-1, and the concrete signal response is about 45.2 dB in Measurement-2. The difference

between these two results is only 0.3 dB. In another word, when area A was covered by absorber foam, the radar power response of concrete divider does not reduce. Therefore, the radar response did not come from area A. In brief, although radar center beam is looking at area A, there is no response from there.

However, if comparing the Measurement-1/Measurement-2 with Measurement-3, then it is easy to see that the signal response from concrete divider drop down about 10 dB after area B is covered by radar absorber foam. The signal response of the concrete divider in Measurement-3 (the left image of Fig. 4.57) almost disappeared. Therefore, it proves that the radar response of concrete divider comes from area B where is perpendicular to the radar side beam.

Fig. 4.58 shows that when the antennas center beam is not perpendicular to concrete divider surface, the center beam will not bounce back. Instead, the side beam, which is perpendicular to the concrete divider is measuring the concrete divider. One point must be taken care of, every antenna has its own maximum beam width (the angle between the center beam and the side beam). If the measurement angle is greater than the maximum beam width, then no side beam can be perpendicular to the concrete divider surface. In this case, the radar cannot detect the concrete divider!

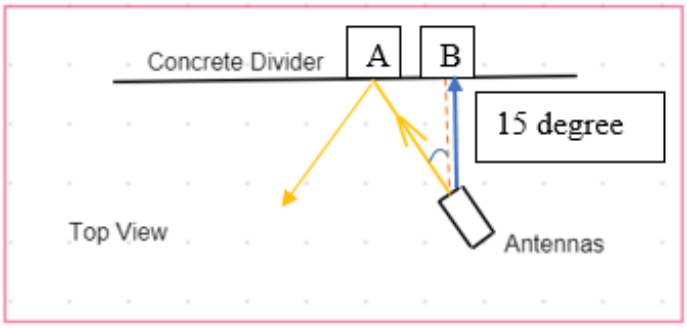

Fig. 4.58. Concrete divider forward-looking measurement analyzation

4.4.3 Concrete Divider Side-Looking Measurement

Concrete divider side-looking measurement only needs to consider one case: radar center beam perpendicular to the surface of the concrete divider (Fig. 4.59). This case also is the requirement of radar reflectivity measurement. There is another reason why this research only consider the perpendicular case. The main area of the concrete divider is just a flat surface. Therefore, only the perpendicular case can get the strongest signal response. The measurement details are described below.

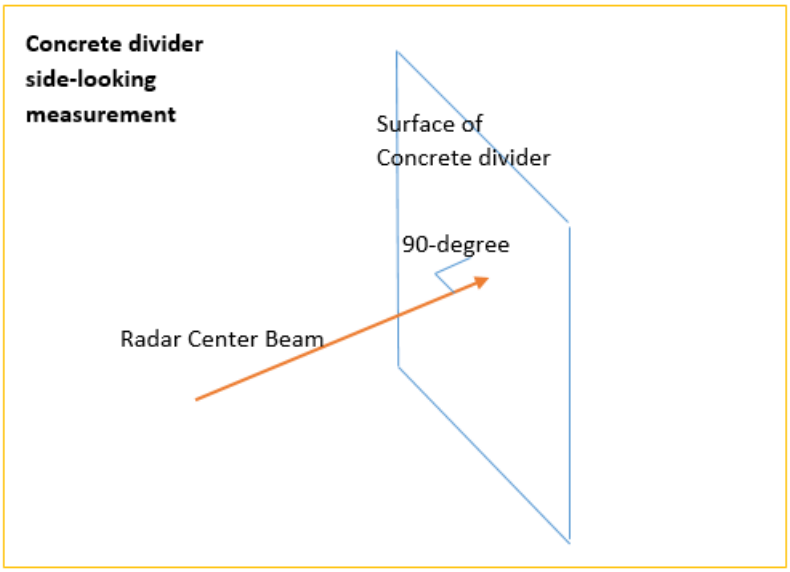

Fig. 4.59. Concrete divider side-looking measurement

Measurement Method

1. Do the reflectivity calibration (Fig. 4.60) by putting a big metal plate on the concrete divider. Usually, the metal plate is 24ft x 24ft. The distance between Radar and metal plate is 1m. Make sure the Radar center beam is perpendicular to the surface of a metal plate. More details about Radar reflectivity calibration are described in Chapter 3.

Fig. 4.60. Reflectivity calibration using an aluminum plate

2. After collecting the reference (metal plate) data, remove the metal plate from the concrete divider surface. Then, record 2s data of concrete divider.

Fig. 4.61. Concrete divider measurement using 24GHz (left) and 77GHz (right) Radar

3. Plot the 2s recording data. Fig. 4.62 shows the concrete divider measurement result and metal plate measurement result. Again, the y-axis of each figure is the magnitude of signal response (dB). The x-axis relates to time (ns). The maximum peak is antenna coupling and the peak pointed by vertical arrows

is the signal response of concrete divider/metal plate. The targets Radar reflectivity equals the difference between the signal response (dB) of the target (concrete divider) and the signal response (dB) of reference (metal plate). In this example, the calculated Radar reflectivity of the concrete divider is -7.3211 dB (Fig. 4.63).

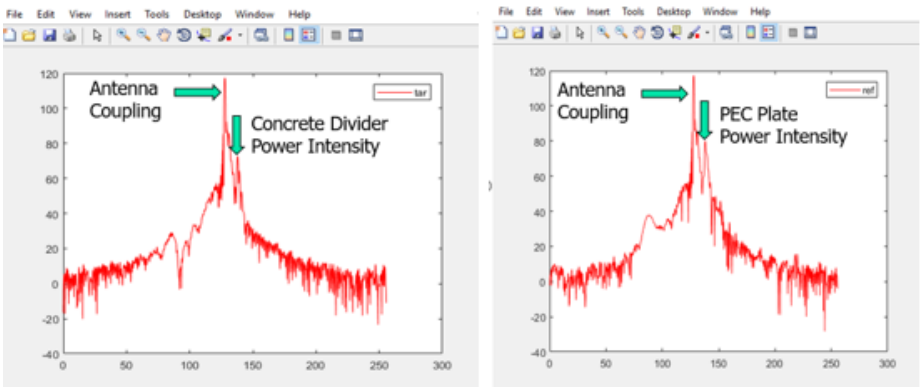

Fig. 4.62. Concrete divider measurement result (left) and aluminum plate measurement result (right)

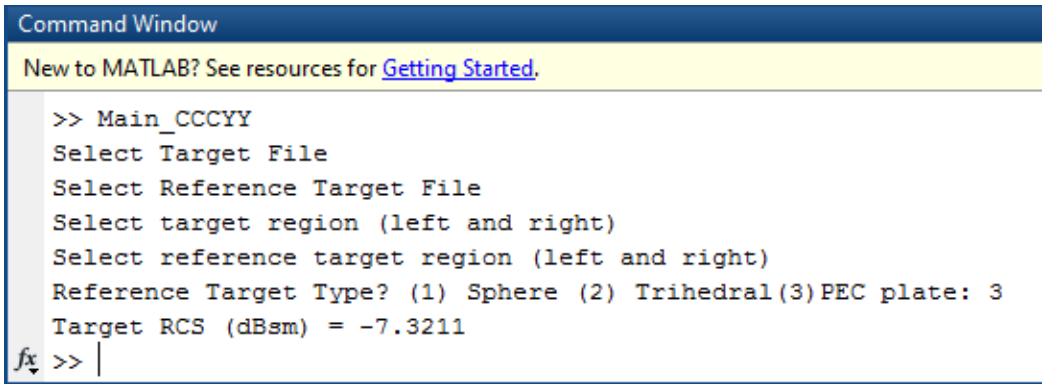

Fig. 4.63. 24 GHz radar reflectivity of concrete divider 2

Measurement Result

1. 24GHz Measurement Results

Sample ID	Measurement point	Measured surface	Reflectivity (dB)	Sample average	Sample variance
1	1	Smooth	-7.6011	-7.3970s	0.0917
	2	Smooth	-7.049		
	3	Smooth	-7.541		
2	1	Smooth	-7.3211	-7.2774	0.0461
	2	Smooth	-7.4668		
	3	Smooth	-7.0443		
3	1	Smooth	-7.4582	-7.3313	0.4029
	2	Smooth	-6.4887		
	3	Smooth	-8.0257		
	4	Smooth	-7.3525		
4	1	Smooth	-7.6843	-7.5565	0.1071
	2	Smooth	-7.8006		
	3	Smooth	-7.1846		
5	1	Some holes	-6.4647	-6.8076	0.2352
	2	Smooth	-7.1505		
6	1	Damaged	-8.2871	-8.6755	0.3672
	2	Damaged	-9.3234		
	3	Damaged	-9.2012		
	4	Damaged	-8.6787		
	5	Smooth	-7.887		

Fig. 4.64. Summary of the 24 GHz reflectivity of all concrete divider samples.

2. 77GHz Measurement Results

Sample ID	Measurement point	Measured surface	Reflectivity (dB)	Sample average	Sample variance
2	1	Smooth	-8.5	-9.0	0.15
	2	Smooth	-9.3		
	3	Smooth	-9.1		
3	1	Smooth	-7.4	-7.7	0.09
	2	Smooth	-7.8		
	3	Smooth	-8.0		
4	1	Smooth	-7.2	-11.1	44.11
	2	Broken	-18.7		
	3	Rough	-7.3		

Fig. 4.65. Summary of the 77 GHz reflectivity of all concrete divider samples.

Result Discussion

1. Effect of Color, Shape and Surface Coating

   Based on the measurement results shown in Fig. 64, the average reflectivity of Concrete dividers 2 to 4 are almost the same (-7.2774, -7.3313, -7.5565). Note that concrete dividers 2 and 3 have a similar color, and both of them have a good surface. The only difference between them is the shape. Concrete divider 1 is New Jersey shape and concrete divider 2 is F-shape. Since the measurements only focus on the flat faces, the shape does not affect the reflectivity. Moreover, concrete dividers 2 and 3 have different color compared to concrete divider 1 and 4 (1 is white; 2, 3 is brown; 4 is gray). Therefore, the color should not affect the reflectivity of concrete divider either. In addition, Concrete divider 1 is the only one that has been coated by some kind of white painting, but it does not show different reflectivity either.

2. Effect of Concrete Age

   The concrete dividers used in previous measurements are various ages but all old. They did show similar reflectivity. It is necessary to find a new concrete divider to determine the age effect to reflectivity. Unfortunately, it is very difficult to find a new concrete divider. However, since both curb and concrete divider are made of Portland concrete, and it happened that there is a brand new curb under construction. Therefore, the reflectivity for that new concrete curb (Fig. 4.66) is measured. The results are in Table 4.9. It shows that the reflectivity range of concrete curb is between -7 dB to -8 dB; and the average reflectivity is -7.3655 dB. This result is the same as the old concrete dividers, which have smooth surfaces. Note that reflectivity is used to describe the material property. In this case, the difference of average reflectivity between new concrete and old concrete is within 1dB. Therefore, the age of concrete does not affect the Radar reflectivity.

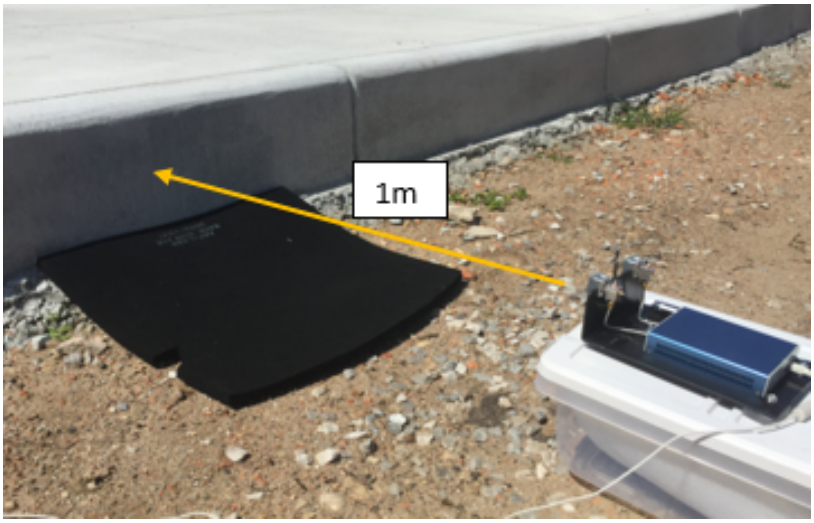

Fig. 4.66. Curb reflectivity measurement

Table 4.9.
24GHz Radar Reflectivity of a Curb

Measurement locations	**Reflectivity (dB)**
1	-7.0299
2	-8.0154
3	-7.1347
4	-7.2818
Average	-7.3655

3. Effect of Humidity

   Concrete divider 5 has a litter bit higher reflectivity (-6.8076) than other members of Group 1. It might be caused by those big and deep holes on the surface (Fig. 4.67). Those holes may have higher humidity than the surface, especially those deep holes. After the rain, water will go into these holes. Holes will take much longer time than the surface to be dry. For some deep holes, they even not able to be completely dry.

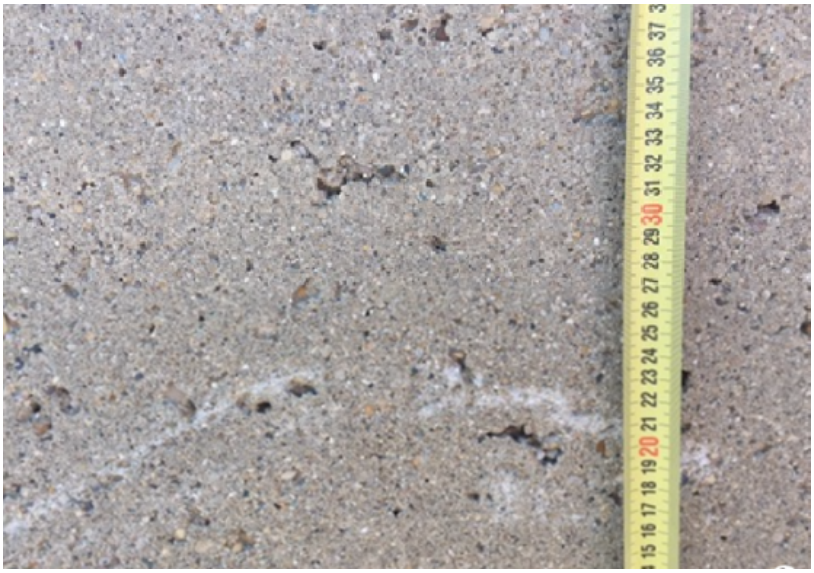

Fig. 4.67. Surface of Concrete Divider 5

A humidity experiment was designed to check how humidity affects concrete dividers reflectivity. As Fig. 4.68 shows, after spraying water on the concrete divider surface, the reflectivity quickly increase to -3.8 dB (about 4 dB higher than dry concrete divider). As concrete divider surface gets drier, the reflectivity slowly gets lower. After 30 minutes, the surface looks almost dry. However, Fig. 4.70 clearly shows that the area around holes still very wet! Therefore, even though the majority part of the concrete divider is dry, the reflectivity is still about 1 dB higher than the reflectivity when the surface is completely dry. Theoretically, this is correct. Reflectivity directly relates to the resistivity of the object. The lower resistivity, the higher reflectivity. The resistivity of concrete is quite different when it is wet and dry. During the raining, the concrete divider can be treated as a semiconductor. The resistivity is around 105 ohm-mm. However, the dry concrete divider acts as an insulator. The resistivity is around 1012 ohm-mm. Therefore, the humidity will significantly affect concrete dividers reflectivity.

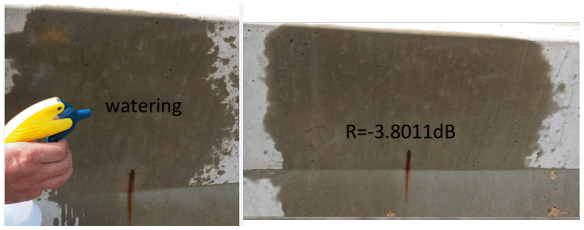

Fig. 4.68. Spray water on concrete divider surface-1

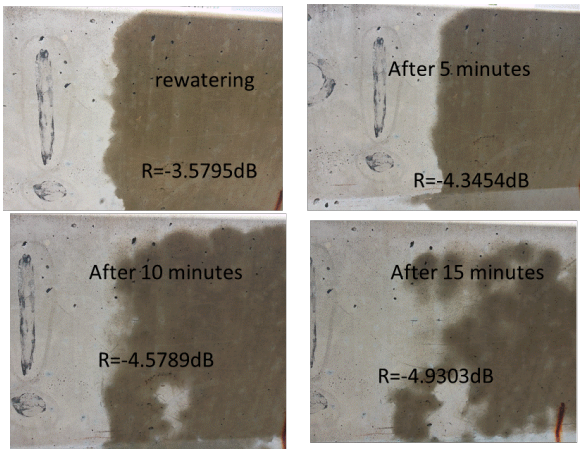

Fig. 4.69. Spray water on concrete divider surface-2

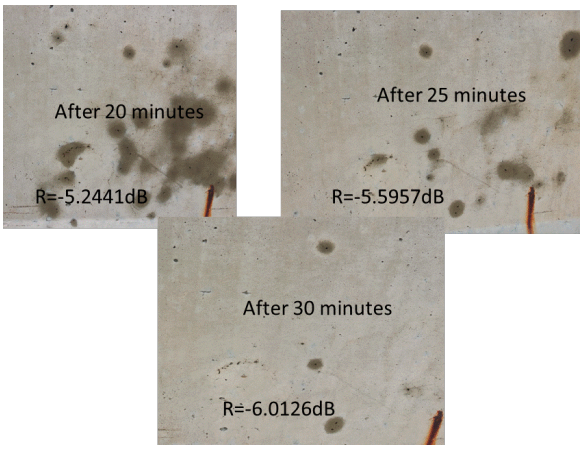

Fig. 4.70. Spray water on concrete divider surface-3

4. The average reflectivity of the concrete divider at 24GHz Radar

   Based on Fig. 4.64, six concrete dividers can be divided into 2 groups (Fig.

4.71). Group one includes concrete dividers 1 to 5 whose data are mostly measured from a smooth surface. Their reflectivity are close, and the range is between -6.5 dB to -8 dB. The average reflectivity of this group is -7.3089 dB. Group 2 only includes Concrete divider 6 whose data are mostly measured from the damaged surface. The reflectivity of Group 2 is lower than Group 1. The reflectivity range of this group is between -9.5 dB to -8 dB, and the average reflectivity is -8.6755 dB.

Group	Concrete Divider ID	Highest Reflectivity (dB)	Lowest Reflectivity (dB)	Reflectivity Range (dB)	Reflectivity Average (dB)
1	1	-7.049	-7.6011	-6.5 to -8.1	-7.3089
	2	-7.0443	-7.4668		
	3	-6.4887	-8.0257		
	4	-7.1846	-7.8006		
	5	-6.4647	-7.1505		
2	6	-7.887	-9.3234	-8 to -9.5	-8.6755

Fig. 4.71. Groups of concrete divider samples

5. 77GHz and 24GHz Smooth Surface Reflectivity Comparison

Fig. 4.65 shows that reflectivity of smooth surface of concrete divider 3 and 4 measured by 77GHz radar are very similar. All of them are about -7.31 dB. These results matched with 24 GHz Radar measurement results. In another word, if the surface of the concrete divider is smooth, then the reflectivity is similar at 24GHz Radar and 77GHz Radar, which is about -7.31 dB.

However, the 77GHz average reflectivity measured from the smooth surface of concrete divider 2 is about -9 dB. It is lower than the 24 GHz Radar measurement result (-7.3 dB). By looking closely, it is easy to see that there are some gravels visible on the surface of concrete divider 2 (Fig. 4.72). These gravels could be the reason that causes 77GHz Radar gets a lower signal response.

Fig. 4.72. Gravels visible on the surface of concrete divider sample 2

6. Smooth and Rough Surface Reflectivity Comparison

   The measured 77GHz reflectivity of the rough surface of Concrete divider 4 is -7.3 dB. Although the surface has many bumps and hole (Fig. 4.73), the measured 24GHz and 77GHz Radar reflectivity is still similar to that of a smooth concrete surface. Therefore, if the diameter of those bumps and hollows are not greater than 1 cm, then the surfaces reflectivity should not be affected.

Fig. 4.73. The rough surface of Concrete Divider 4

7. Smooth and Broken Surfaces Reflectivity Comparison

   Fig. 4.71 shows that concrete divider 6s average reflectivity (-8.6755) measured by 24GHz Radar is much lower than any other samples. It can be caused by the worn down surface. One of the possible reason is that some of the radar waves are reflected to other directions after shooting on this uneven surface (Fig. 4.74), then the receiving antenna receives less power response. Fig. 4.65 also shows that the reflectivity of the broken surface of Concrete divider 4 (Fig. 4.75) is only -18.7 dB measured by 77GHz Radar. Again, this result is much lower than other smooth surfaces reflectivity measured by 77GHz Radar. Therefore, if the surface is damaged, and the damaged surface is big, then the reflectivity will be low. The accurate relationship between broken surface and reflectivity needs more study, and that could be another research topic.

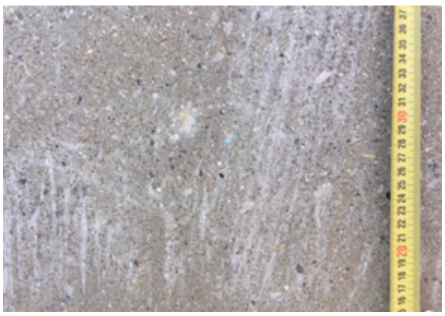

Fig. 4.74. Surface of Concrete Divider 6

Fig. 4.75. Concrete Divider 4 rough surface (left) and broken surface (right)

4.4.4 Summary and Reflectivity Recommendation of Concrete Divider

- The color, coating, and age of the concrete divider do not affect the Reflectivity,
- The surface smoothness, material (e.g., the stone on the surface) and humidity can affect the reflectivity.
- The radar only sees the reflection from the area where the surface of the divider that is perpendicular to the radar beam.
- The representative radar reflectivity for dry and smooth concrete divider is -7.3 ± 1 dB at both 24GHz and 77GHz.

4.5 Conclusion

This Chapter described the methods of measuring the Radar property of metal guardrail, grass, and concrete divider. Both W-beams and I-beams RCS values have been measured from 0-degree to 90-degree. The average mean RCS plot of grassland has been determined. The average reflectivity of concrete divider has been calculated which is around -7.3 ± 1 dB at both 24GHz and 77GHz.

5. SURROGATE ROADSIDE OBJECTS

5.1 Introduction

Chapter 4 determined the Radar specifications of metal guardrail, grass, and concrete divider. This chapter focus on finding soft and durable material to create the surrogate roadside objects. All surrogates are measured using the same method as measuring the real objects. The final products of surrogates have similar Radar properties as the real objects.

5.2 Surrogate Metal Guardrail

As mentioned in Chapter 4, RCS is used to describe the radar properties of the metal guardrail. We used two steps to create a surrogate metal guardrail. First, develop a skin with the required radar reflectivity, and then attach the skin to W-beam shaped foam.

5.2.1 Surrogate W-beam

Skin Development

A three-layer skin is developed for surrogate metal guardrail (Fig. 5.1). The first layer is a plastic film to provide the proper surface smoothness, the second layer is a layer of zinc to provide correct color and IR reflectivity, and the third layer is the aluminum film to provide radar property. Table 5.1 shows that the measurements of both 24GHz and 77 GHz reflectivity of this skin are around -0.3 dB, which is very close to required 0 dB radar reflectivity for W-beam.

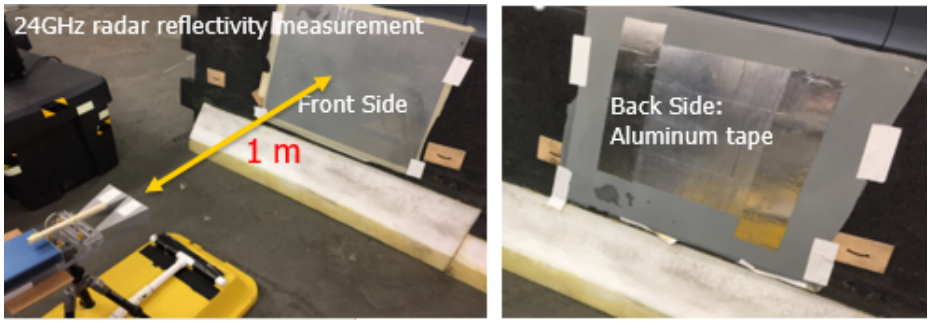

Fig. 5.1. Surrogate metal guardrail skin

Table 5.1.
Reflectivity of surrogate metal guardrail skin and galvanized steel

	Surrogate guardrail skin	**Galvanized steel**
24GHz radar reflectivity (dB)	-0.3 ± 0.5	0 ± 1
77GHz radar reflectivity (dB)	-0.3 ± 0.5	0 ± 1

RCS Comparison between Real and Surrogate of W-beam

Fig. 5.2 and Fig. 5.3 shows the RCS measurement of surrogate W-beam. The left side and right side of Fig. 5.4 shows RCS of real W-beam and surrogate W-beam of 24GHz radar under vertical polarization, respectively. The left side and right side images of Fig. 5.5 shows RCS of real W-beam and surrogate W-beam of 24GHz radar under horizontal polarization, respectively. By comparing with RCS of the real and surrogate W-beams, it is easy to see that their shapes are similar from 0-degree to 90-degree. The difference of each critical peak RCS value between the surrogate W-beam and the real W-beam is less than or equal to 2 dB. Therefore, this surrogate W-beam design can meet our 24GHz requirement.

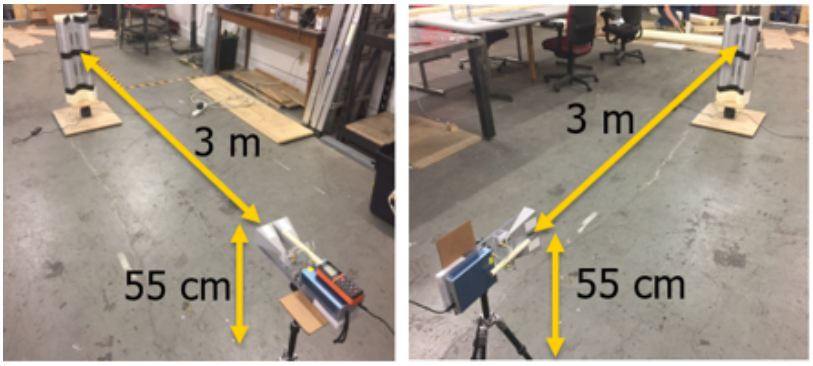

Fig. 5.2. Surrogate vertical (left) and horizontal (right) polarization measurement at 24GHz Radar

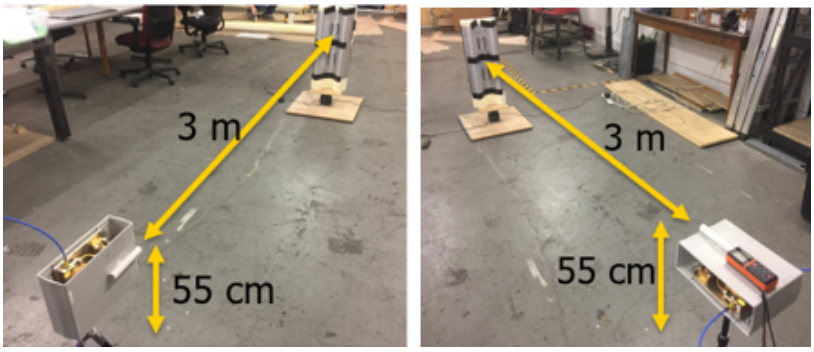

Fig. 5.3. Surrogate vertical (left) and horizontal (right) polarization measurement at 77GHz Radar

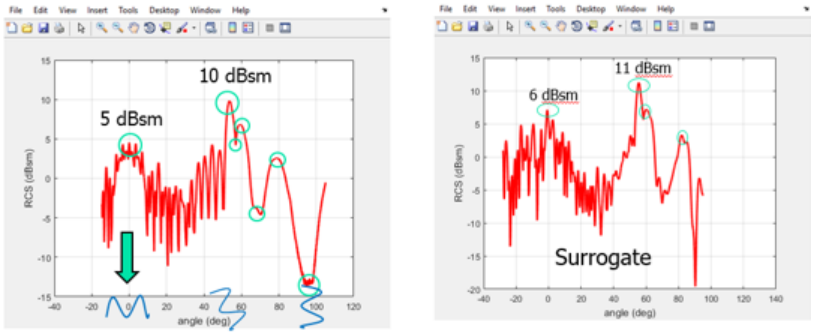

Fig. 5.4. Real W-beam RCS result (left) and surrogate W-beam RCS result (right) under vertical polarization at 24GHz Radar

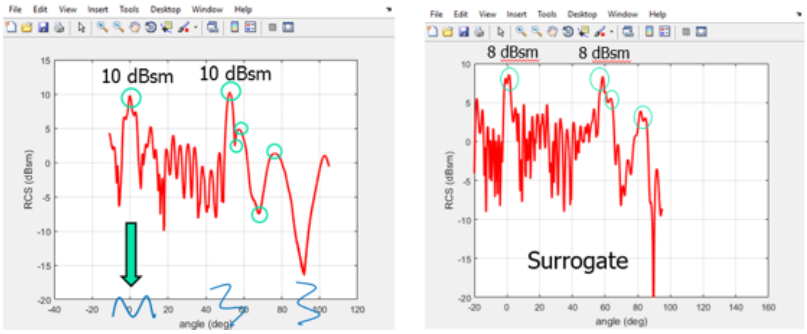

Fig. 5.5. Real W-beam RCS result (left) and surrogate W-beam RCS result (right) under horizontal polarization at 24GHz Radar

77GHz RCS measurement results of the surrogate W-beam are also similar to that of real W-beam. The left side and right side of Fig. 5.6 shows 77GHz RCS of real W-beam and surrogate W-beam under vertical polarization, respectively. The left side and right side images of Fig. 5.7 shows 77GHz RCS of real W-beam and surrogate W-beam under horizontal polarization, respectively. Their shapes and values match.

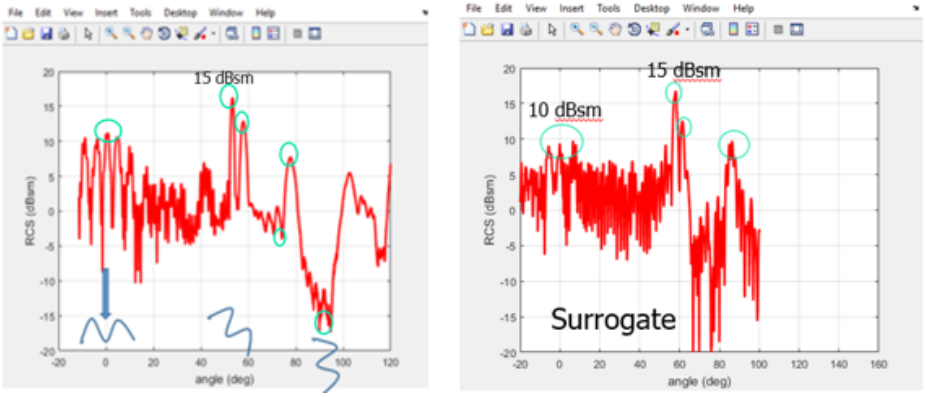

Fig. 5.6. Real W-beam RCS result (left) and surrogate W-beam RCS result (right) under vertical polarization at 77GHz Radar

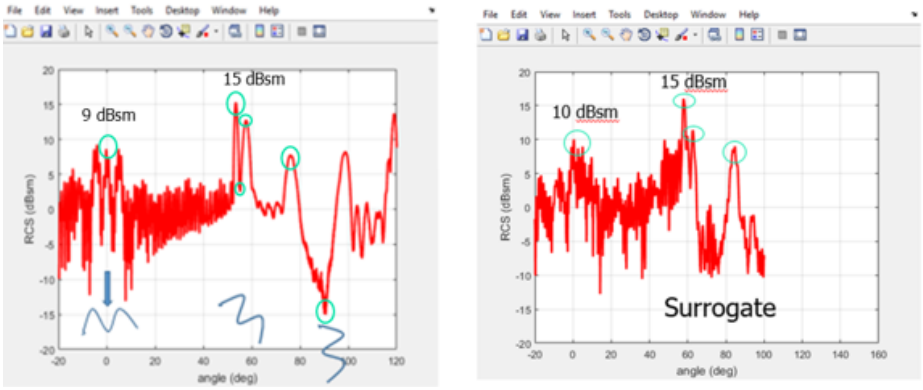

Fig. 5.7. Real W-beam RCS result (left) and surrogate W-beam RCS result (right) under horizontal polarization at 77GHz Radar

Summary

In summary, both the 24GHz and 77GHz radar reflectivity of the surrogate W-beam skin are very good (-0.3 dB compare to required 0 dB). Moreover, both the 24GHz and 77GHz RCS of the surrogate W-beam are close to that of the real W-beam. Therefore, surrogate W-beam satisfies its radar requirements.

5.2.2 Surrogate I-beam

I-beam frame

I-beam frame is made of foam in the shape of I-beam

Skin Development

Since I-beam and W-beam are made of the same material (Galvanized steel), the three-layer surrogate skin for W-beam can be used for I-beam as well.

RCS Comparison between the Real and Surrogate W-beams

Fig. 5.8 and Fig. 5.9 show set up of the 24GHz and 77GHz Radar measurement for the surrogate I-beam. The left side and right side of Fig. 5.10 show the 24GHz RCS

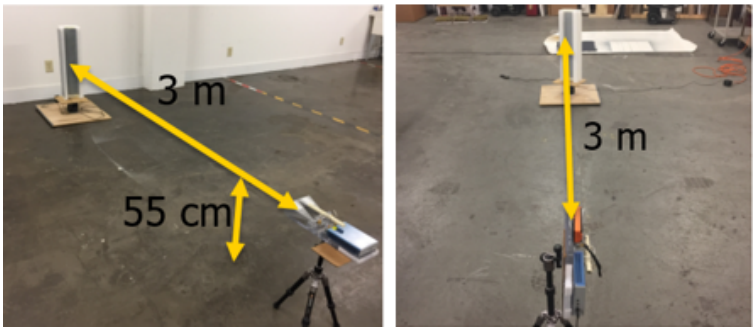

Fig. 5.8. Surrogate vertical (left) and horizontal (right) polarization measurement at 24GHz Radar

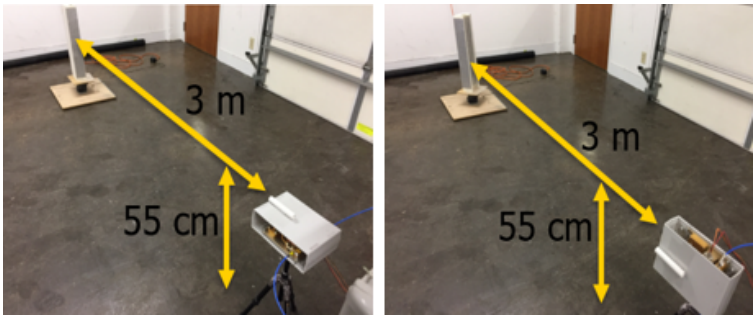

Fig. 5.9. Surrogate vertical (left) and horizontal (right) polarization measurement at 77GHz Radar

of the real I-beam and the surrogate I-beam under vertical polarization, respectively. The left side and right side images of Fig. 5.11 show 24GHz RCS of the real I-beam and the surrogate I-beam under horizontal polarization, respectively. We can see that their shapes are similar. The RCS difference of each critical peak value between the surrogate and real I-beams is less than or equal to 2 dB. Therefore, this surrogate I-beam design can meet our 24GHz radar requirement.

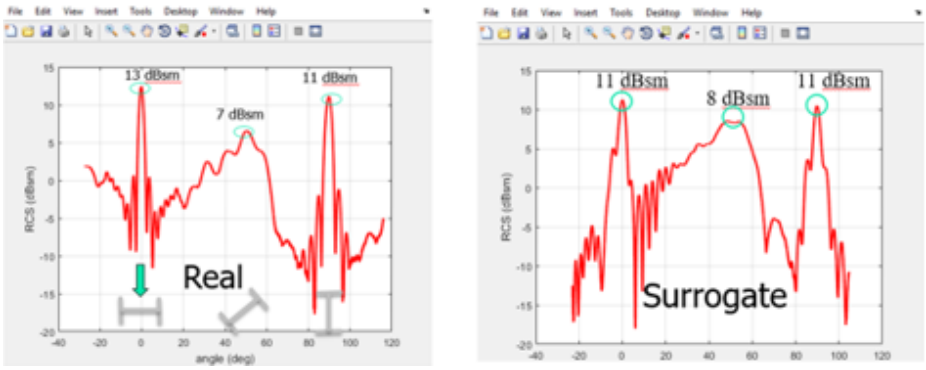

Fig. 5.10. Real I-beam RCS result (left) and surrogate I-beam RCS result (right) under vertical polarization at 24GHz Radar

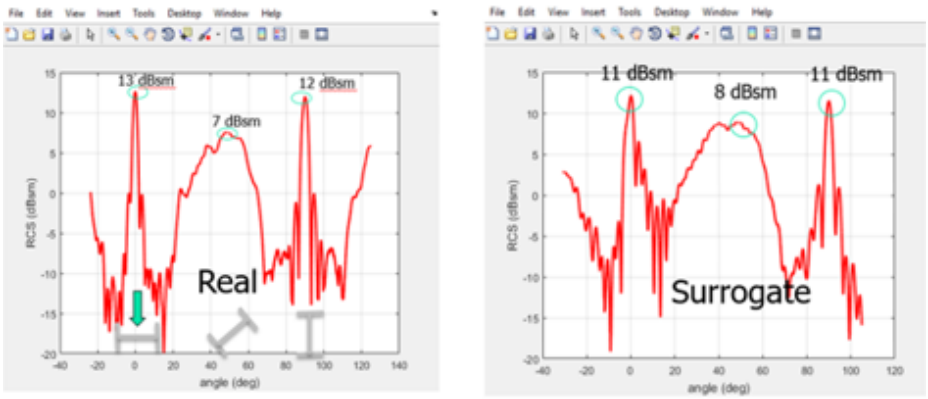

Fig. 5.11. Real I-beam RCS result (left) and surrogate I-beam RCS result (right) under horizontal polarization at 24GHz Radar

Measured 77GHz RCS of the surrogate I-beam is also similar to that of real I-beam. The left side and right side of Fig. 5.12 show 77GHz RCS of real I-beam and surrogate I-beam in vertical polarization, respectively. The left side and right side images of Fig. 5.13 show the 77GHz RCS of the real I-beam and the surrogate I-beam under horizontal polarization, respectively. Their shapes and values match with that of the real I-beam.

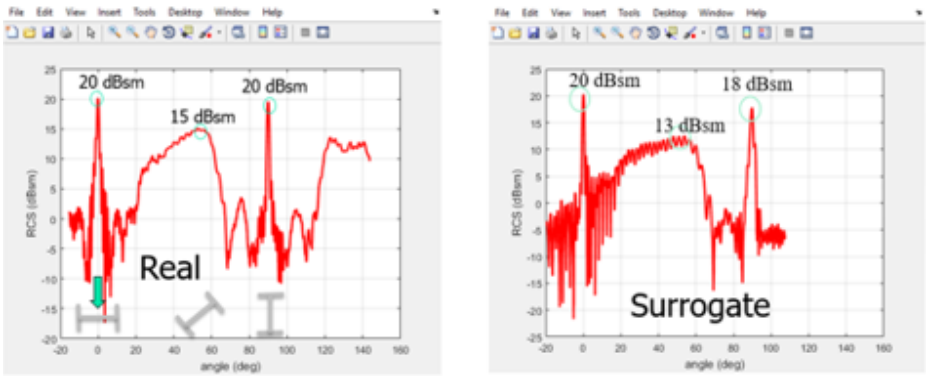

Fig. 5.12. Real I-beam RCS result (left) and surrogate I-beam RCS result (right) under vertical polarization at 77GHz Radar

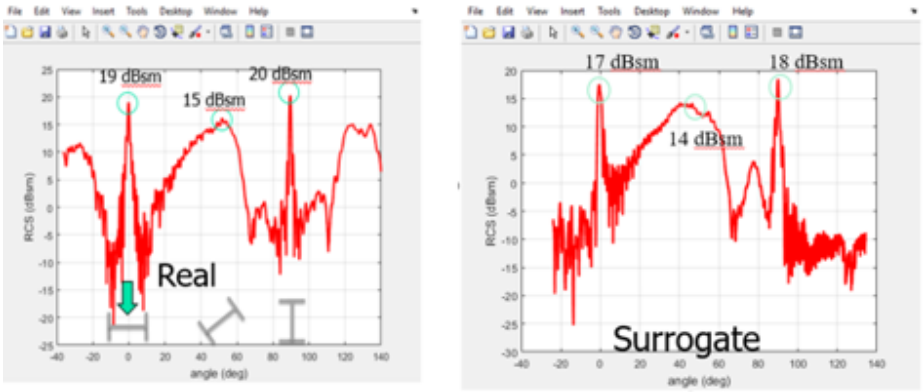

Fig. 5.13. Real I-beam RCS result (left) and surrogate I-beam RCS result (right) under horizontal polarization at 77GHz Radar

Summary

In summary, both the 24GHz and 77GHz radar reflectivity of surrogate I-beam skin are very good (-0.3 dB compare to required 0 dB). Moreover, both the 24GHz and 77GHz RCS of surrogate I-beam are close to real I-beam. Therefore, making surrogate I-beam is successful.

5.3 Surrogate Grass

It is beyond our ability financially to custom design specific surrogate grass to satisfy the color, IR and radar requirements. Therefore, the basic idea of making grass surrogate is that modifying the commercially available artificial turf.

5.3.1 Artificial Turf

Based on the grass type study, we need to find artificial turf with high blades. Two artificial turfs (Fig. 5.14 and Fig. 5.15) made of the same material are selected for this study. The key differences between these two turfs are the density and height of the blade. The details about two artificial turfs are described in Table 5.2.

Fig. 5.14. Front side and back side of the Artificial turf

Fig. 5.15. Artificial turf top close view (left) and side close view (right)

Table 5.2.
Specification of two artificial turfs

Artificial Turf	**Weight**	**Blade height**	**Color**
Sample 1	65 Qz/sqft	Uniform 2.25 inch	Green
Sample 2	70 Qz/sqft	Uniform 2.00 inch	Green

5.3.2 RCS of two different artificial turfs

It is necessary to check if two artificial turfs have different RCS or not since their density and height of blades are different. Moreover, it is interesting to check if two layers of artificial turf mimicking long grass will give different radar response. Therefore, the following three measurements are designed to check them out. All measurements are at 24GHz radar vertical polarization at 10-degree depression angle.

1. Two artificial turfs are placed together (Long blade turf up, short blade turf down as fig. 5.16 shows) on asphalt ground.

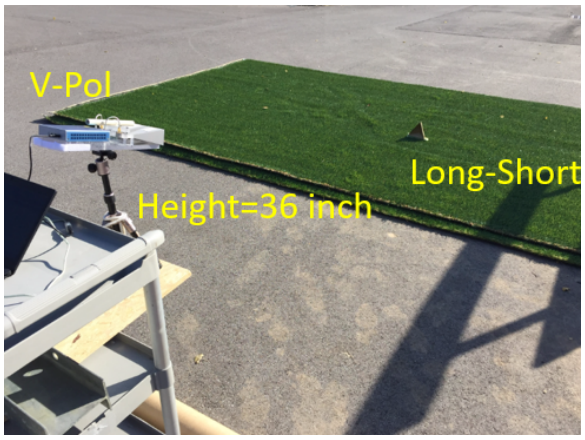

Fig. 5.16. Two artificial turfs put on together (Long blade turf up, short blade turf down)

2. Two artificial turfs are placed together (Short blade turf up, Long blade turf down) on asphalt ground.

3. Single short blade artificial turf is placed on asphalt ground.

Fig. 5.17 shows that three plots: two layers of artificial turf (long blade turf on top of the short blade turf) (black), two layers of artificial turf (short blade turf on top of long blade turf) (yellow), one layer of short blade artificial turf (blue) are almost the same. Therefore, two conclusions can be drawn here:

1. Two different artificial turf samples have similar radar property.

2. Two layers of artificial turf (one stacked on the other) have similar radar response as one single layer of artificial turf.

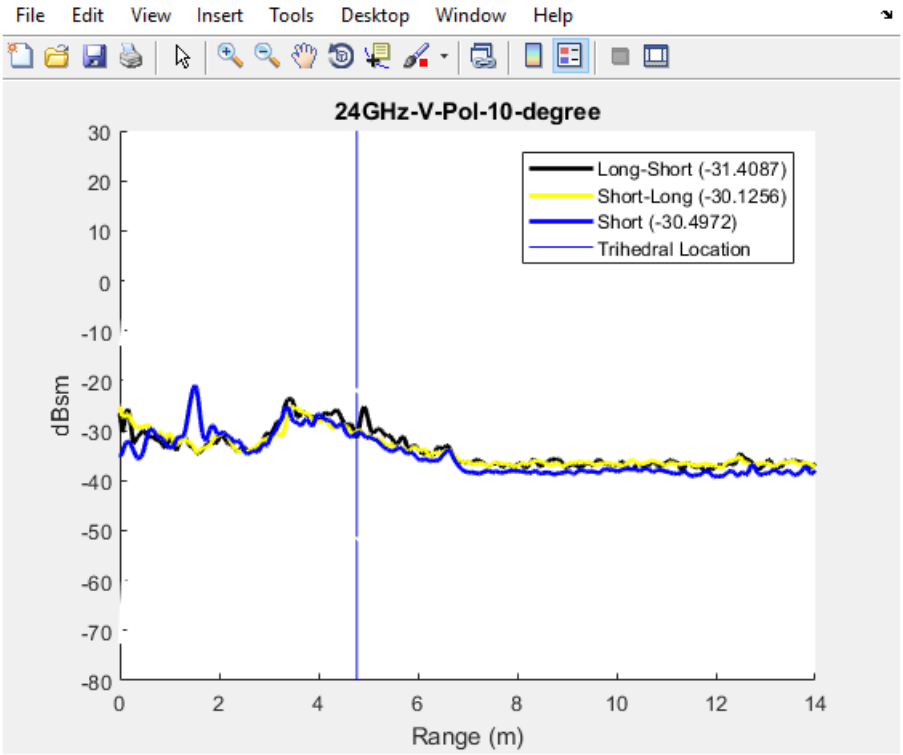

Fig. 5.17. Measurement results of three experiments

Artificial turf measurement along different sides

Since the grass blade leans in the same direction due to the rolled turf during storage, it is necessary to check if it affects the RCS when viewed in different directions. Therefore, the following measurements are conducted. As shown in Fig. 5.18, the grass blades of the artificial turf fall down uniformly on the direction indicated by the blue arrow. The artificial turfs are measured along sides 1, 2 and 3. All measurements are in 15-degree pitch angle with asphalt underneath. The measurements are under 24 GHz radar vertical polarization.

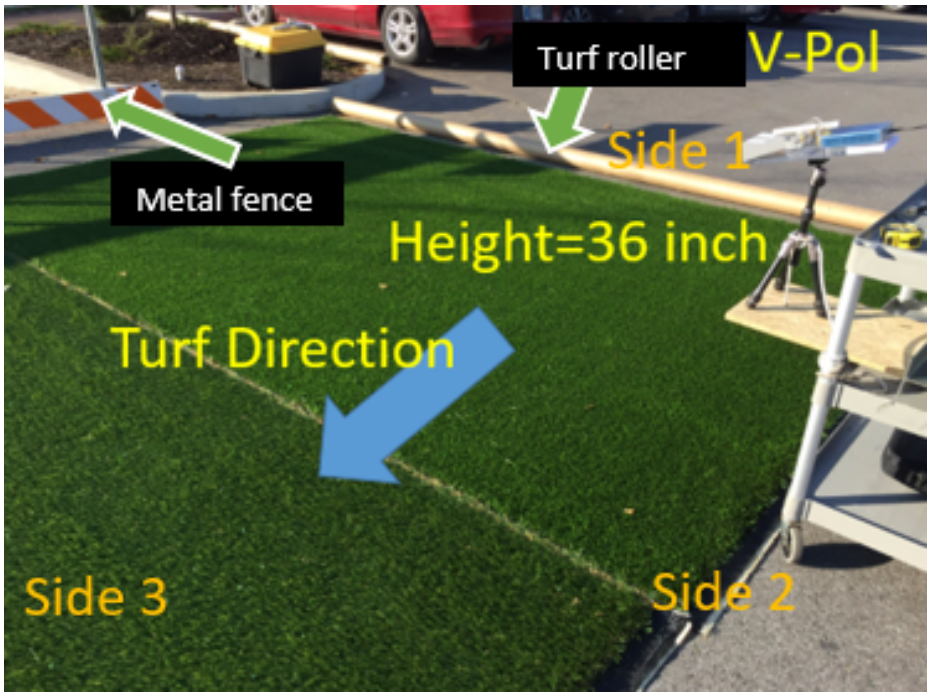

Fig. 5.18. Artificial turf measurement alone different sides

Fig. 5.19 shows that the results of a measurement taken along Side-1 (black), Side-2 (yellow) and Side-3 (blue) are very similar. Therefore, artificial turf can be measured along any side. (The metal fence caused the yellow spikes, and turf roller causes blue spikes as Fig. 5.18 shows).

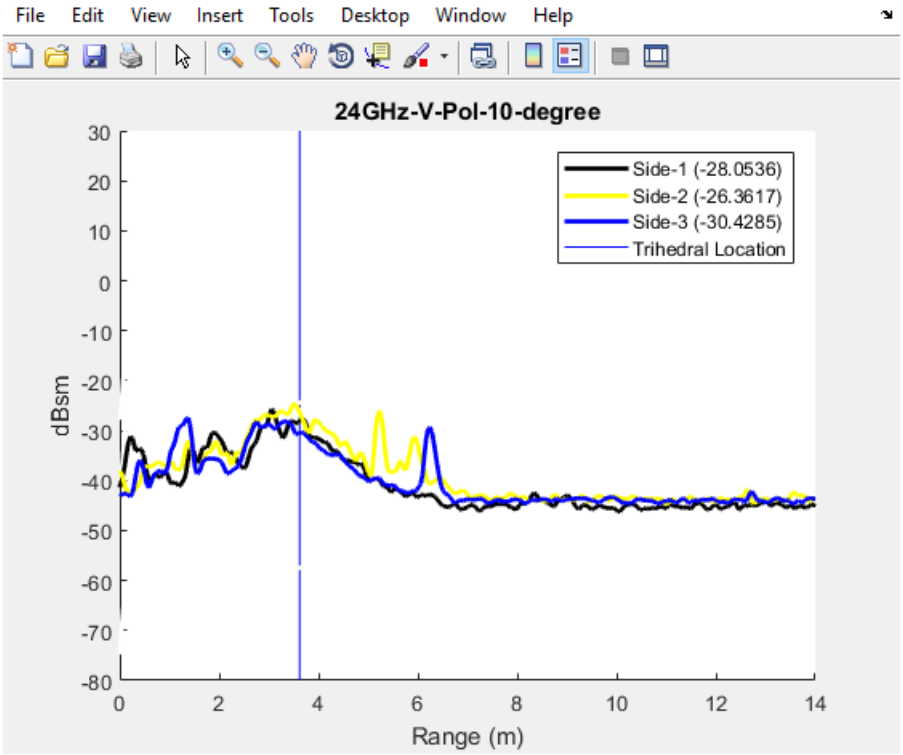

Fig. 5.19. RCS plots of measurement alone different sides

5.3.3 RCS Comparison between Grass and Artificial Turf

24GHz RCS Comparison

As shown in Fig. 5.20, artificial turf is placed on different underneath (clay, sand, asphalt, and concrete). This task not only checks if artificial turf has similar RCS plot as real grass, but also checks if the underneath material affects the RCS of the surrogate turf.

The RCS plot is shown in Fig. 5.21 can be interpreted as follows. The horizontal axis is the distance from the antenna (longer than the actual distance since it is not calibrated). The vertical axis is the RCS. The vertical blue line is the location of trihedral corner reflector where the center beam of the radar aimed. The part before

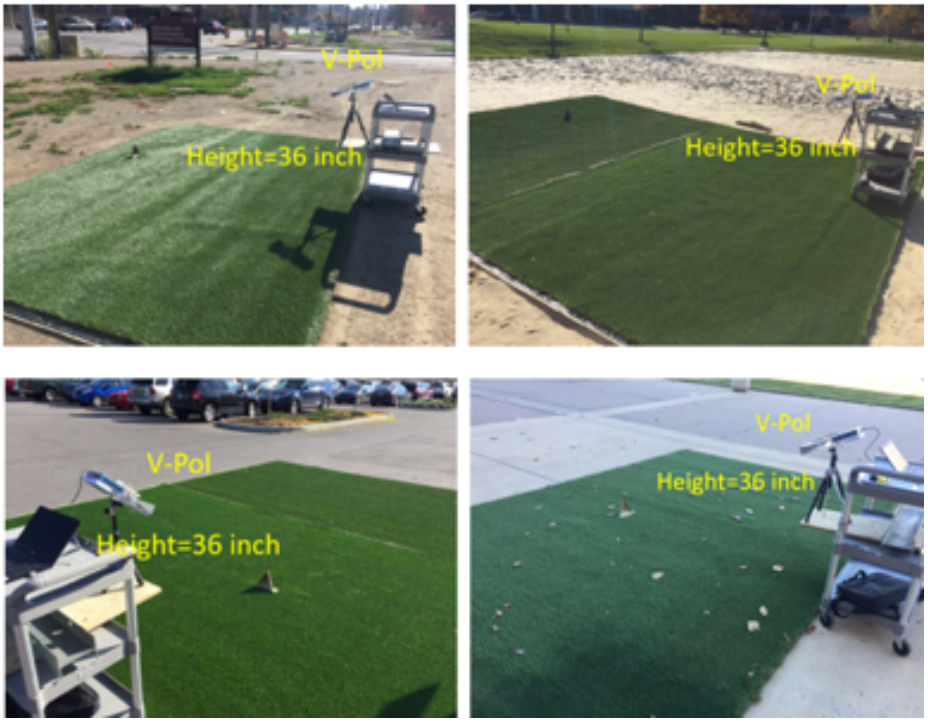

Fig. 5.20. Turf on clay (left top), on sand (right top), on asphalt (left bottom), on concrete (right bottom)

the blue line is covered by the radar center beam and downward side beam, which is not useful since it is affected by antenna coupling and near side ground reflection. The useful information is in the slant section of each plot starting from the straight blue line and ending at the beginning of the flat tail part. This section of data is covered by radar center beam and valid upward side beam. It can best describe the grass/turf property. It is noted that the real ending line of antenna coupling and near side ground reflection is not the blue line (trihedral location), and it should be in front of the blue line. However, the real ending line is hard to define, even if under the same measurement setup, the position of that line may be different. Therefore, in order to guarantee the correctness of the grass data analysis, the blue line (trihedral location) is just chosen as the dividing line. The flat tail part is actually just background measurement. Therefore, the flat tail part can be ignored.

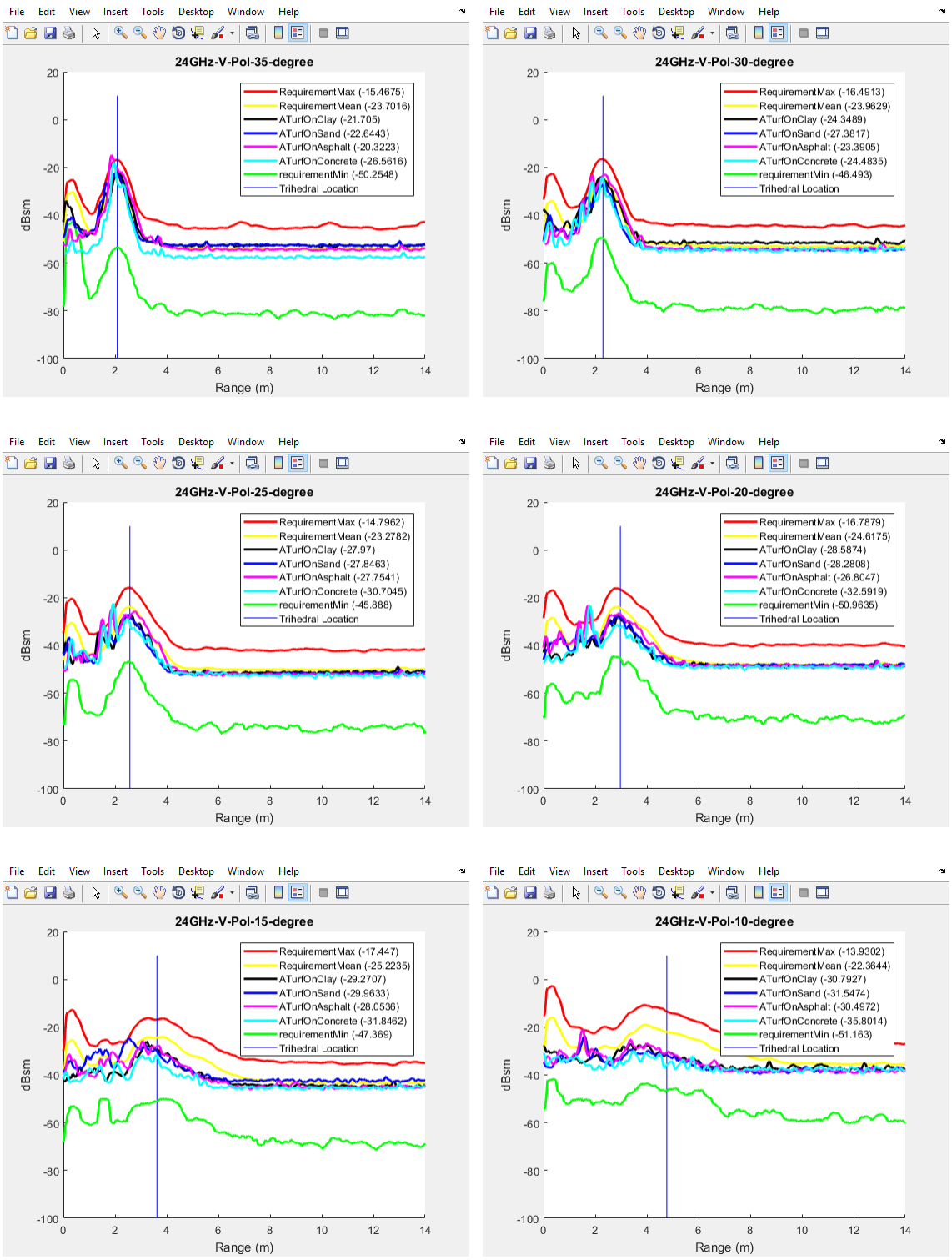

Fig. 5.21. The measurement result of Turf on clay (black) on sand (blue) on asphalt (pink) on concrete (cyan) at different pitch angle under 24 GHz vertical polarization

There are two important information shown in Fig. 5.21 for the 24 GHz radar:

1. At any depression angle, artificial turf has almost the same RCS plot when it is placed on different underneath. Only the plot of turf on concrete is a little bit lower when the pitch angle is 15-degree and 10-degree, but is still close to others. Therefore, underneath may not significantly affect artificial turf RCS. At least, the conclusion can be that the turf put on clay, sand, and asphalt will show the same radar RCS property.

2. At depression angles 35, 30, 25 and 20, the artificial turf gives the same RCS plot as real grass! However, at depression angle 15 and 10, the RCS plot of artificial turf becomes lower than the mean RCS plot of the real grass. In other words, the artificial turf has similar RCS response with real grass at high depression angle, but their RCS response becomes different if the Radars depression angle is lower than 15-degree. In reality, low depression angle is commonly used when Radar is installed on the vehicle. In this case, artificial turf could not be a good choice of grass surrogate.

77GHz RCS Comparison

In this experiment, the artificial turf was placed on asphalt ground. The results of 77GHz RCS measurement at different pitch angles under horizontal polarization is shown in Fig. 5.22.

Fig. 5.22 shows that the RCS of artificial turf (black plot) is higher than the mean RCS of the real grass plot at high pitch angles from 35 to 20. Especially at 30-degree, the RCS plot of the surrogate turf is close to the maximum RCS of the real grass (but still slightly lower than the maximum RCS). However, the RCS of the artificial turf matches with the mean RCS of the real grass at lower pitch angles (15-degree and 10-degree)!

As mentioned before, low depression angle is commonly used for forward-looking Radar setting. In this case, artificial turf can be used as grass surrogate.

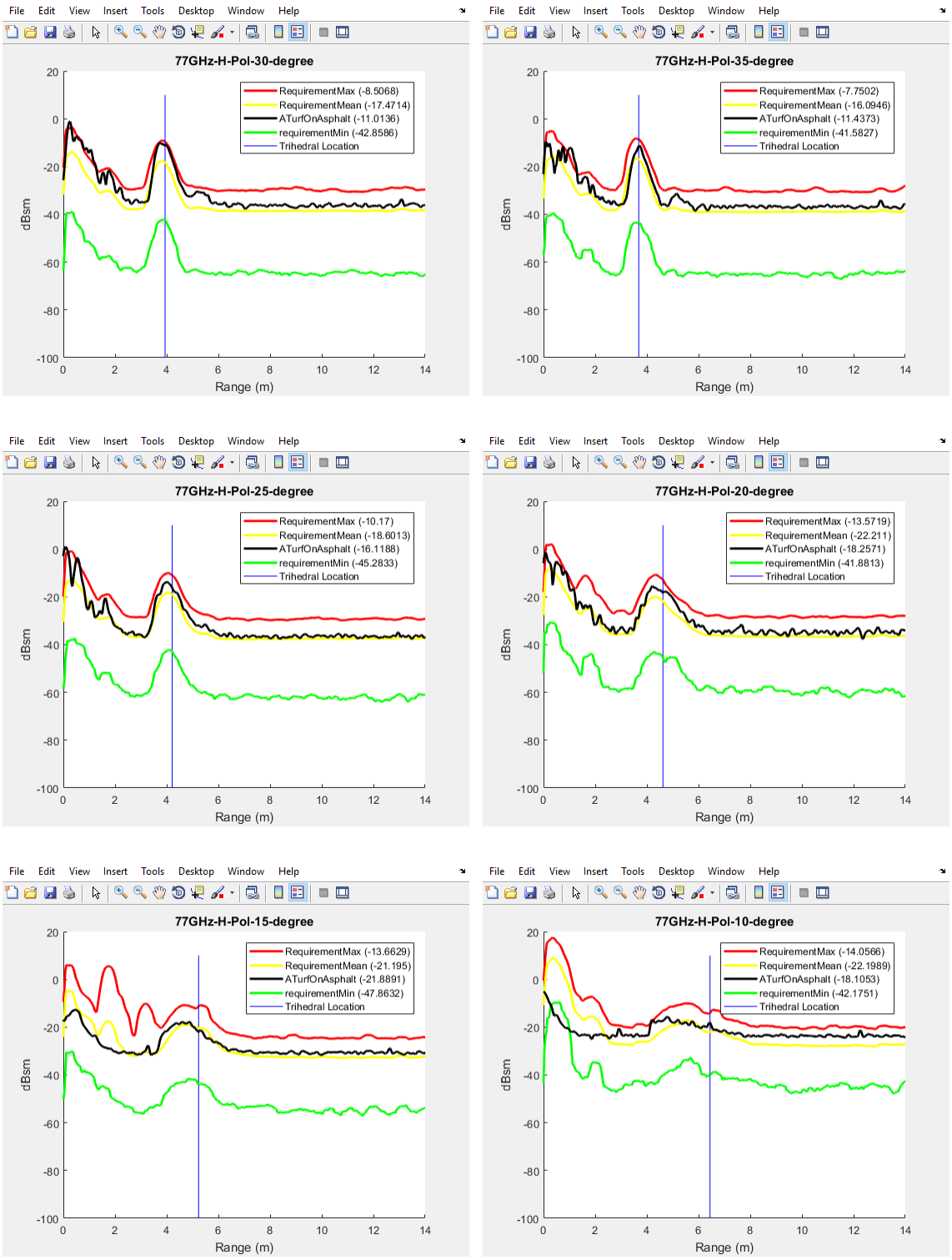

Fig. 5.22. The measurement result of Turf on Asphalt (black) at different pitch angle under 77 GHz horizontal polarization

5.3.4 Summary

A special type of artificial turf is selected as the candidate of grass surrogate. The experiments prove that density and blade height of this kind of turf will not affect its RCS much. Moreover, measuring this kind of artificial turf from different sides will get similar RCS response. In addition, this artificial turf can be used as surrogate grass when it is measured by 77GHz forwarding Radar at low depression angle (lower than 15-degree).

5.4 Surrogate Concrete Divider

Based on the study described in Chapter 4, the required 24GHz and 77GHz RCS for the concrete are both -7.3 ± 1 dB. Therefore, the goal of this task is to find or create a soft and durable material with reflectivity equals to -7.3 ± 1 dB for both 24GHz and 77GHz Radar. For light weight and durability in vehicle testing, the surrogate concrete divider is made of foam and skin.

5.4.1 Skin Development

It was a big challenge of developing the surrogate skin of concrete divider. Many different materials were tested such as conductive fabric, non-conductive fabric, non-conductive fabric with metallic paint, etc. None of them can satisfy 24GHz and 77GHz requirements at the same time. The latest and most promising skin design is also a three-layer structure. The front layer is concrete colored paint with proper IR reflectivity, the middle layer is plastic to keep the strength and back layer is conductive paint, which controls the 24GHz and 77GHz radar reflectivity.

Fig. 5.23. Final surrogate concrete divider

5.4.2 Reflectivity Comparison between Real and Surrogate Concrete Divider

Fig. 5.24 shows that the signal response (pointed by green arrow) of the surrogate concrete divider is the same as that of the real concrete divider measured by 24GHz Radar (x-axis is the time in ns, and the y-axis is the power intensity in dB). Similarly, Fig. 5.25 shows that 77GHz signal response of the surrogate concrete divider and real concrete divider are the same as well.

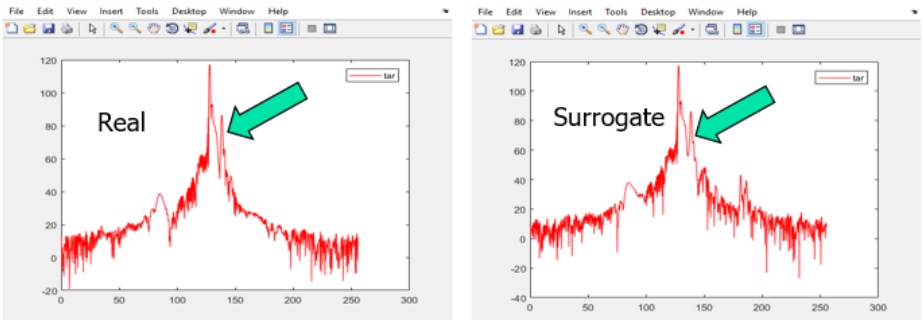

Fig. 5.24. Measurement data of real concrete divider and surrogate concrete divider at 24GHz Radar

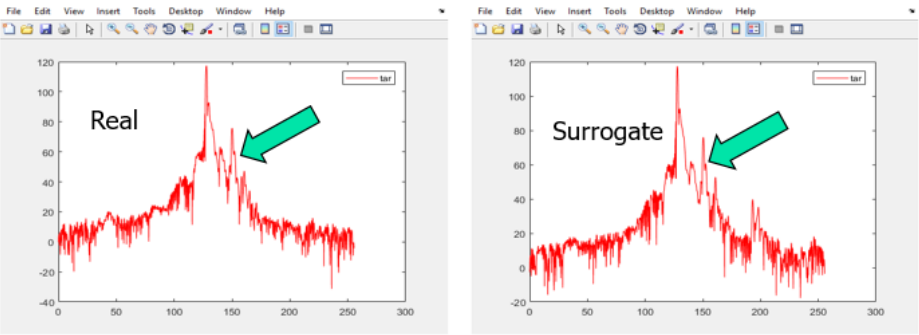

Fig. 5.25. Measurement data of real concrete divider and surrogate concrete divider at 77GHz Radar

A driving measurement was conducted to prove the similarity of the real concrete divider with concrete divider surrogate from Radar point view using 24GHz Radar. As shown in Fig. 5.26, the surrogate concrete divider was placed between real concrete dividers (5 real concrete dividers, 1 surrogate concrete divider). Fig. 5.27 shows that a 24GHz Radar was put on a pickup truck. The height of Radar against the ground was about 33 inch. The Radar depression angles changed from 0-degree to 20-degree (change 5 degrees each time). A pickup truck was 3m away from the concrete divider. It moved straightforward and scanned 6 concrete dividers (include surrogate) within the 30s.

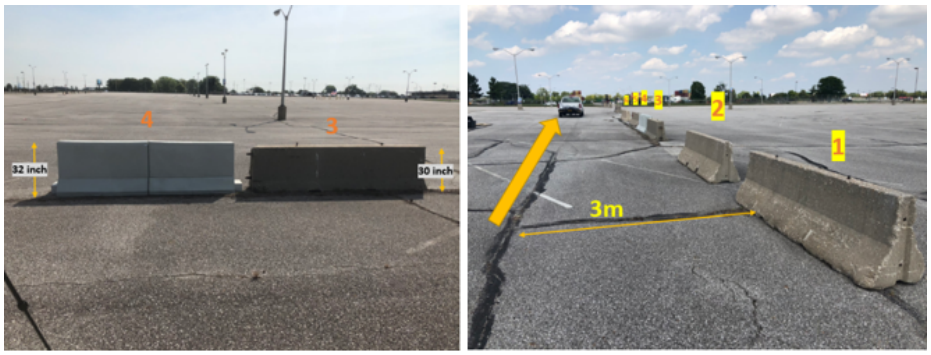

Fig. 5.26. Concrete divider surrogate is placed between real concrete dividers

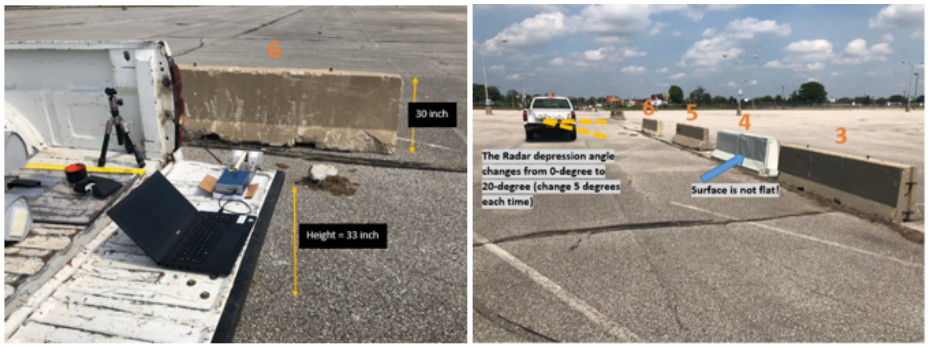

Fig. 5.27. Moving measurement setup

The top image of Fig. 5.28 is the color map of raw data. The x-axis is the number of Radar scanning times. It is corresponding to the pickup trucks driving path. The y-axis is the distance between the radar and object in meters. The color in the figure from light blue to dark red corresponds to the magnitude of signal response from 20dB to 90dB. The weak response around 7m distance are the ghost data that are generated by Fast Fourier Transform (FFT), so we can ignore it. The bottom image of Fig. 5.28 is the maximum response between 2.5m to 5m distance. This image shows the maximum response of concrete divider at each scanning position.

The magnitudes of all measured concrete divider at each depression angle have about 10dB oscillation. This is because that it is hard to guarantee the measurement distance and angle to be consistent during measurement.

When the depression angles are set as 5-degree and 10-degree (Fig. 5.29 and Fig. 5.30), all concrete dividers have a higher signal response than other depression angles. The reason is that the surface of the concrete divider is not perpendicular to the ground, and there is about 6-degree angle between the surface and the normal line to the ground. Therefore, when the depression angle is between 5-degree and 10-degree, the Radar center beam is more perpendicular to the surface of concrete divider.

When the depression angle is set as 20-degree (Fig. 5.32), the signal response of concrete dividers becomes very weak. Moreover, Radar receives a lot signal reflection

from the ground. Therefore, it is better not to set the depression angle more than 20-degrees. 5-degree to 10-degree is recommended.

According to each pair of figures (from Fig. 5.28 to Fig. 5.32), the surrogate concrete divider has a very similar signal response to that of the real concrete divider. However, it is necessary to point out that the non-flat surface of the left segment of the surrogate concrete divider makes its signal response lower. Therefore, it is important to make sure the surface is flat.

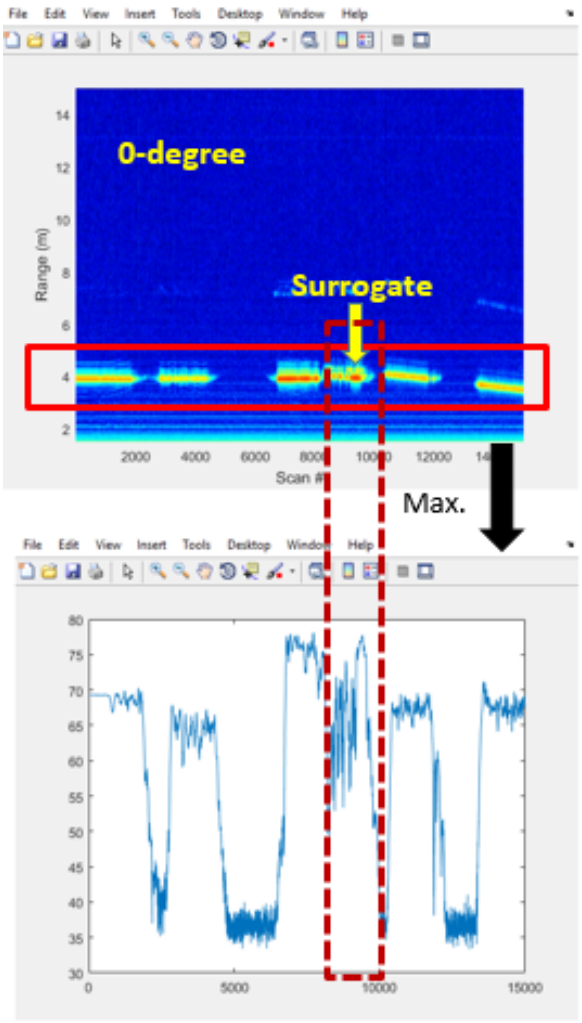

Fig. 5.28. Measurement result at 0-degee

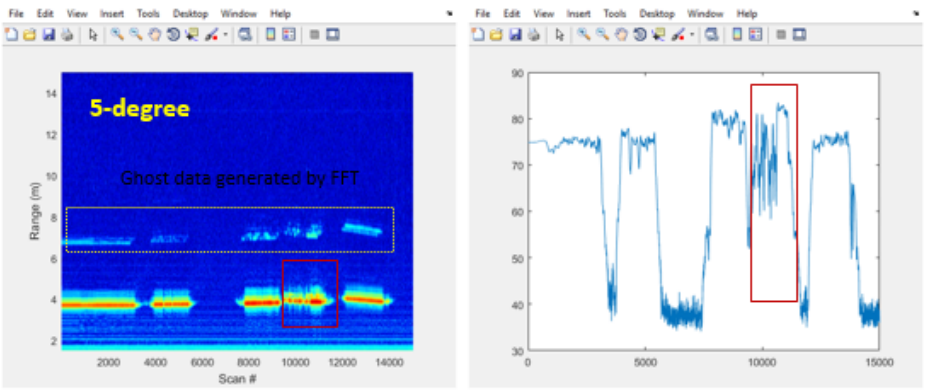

Fig. 5.29. Measurement result at 5-degee

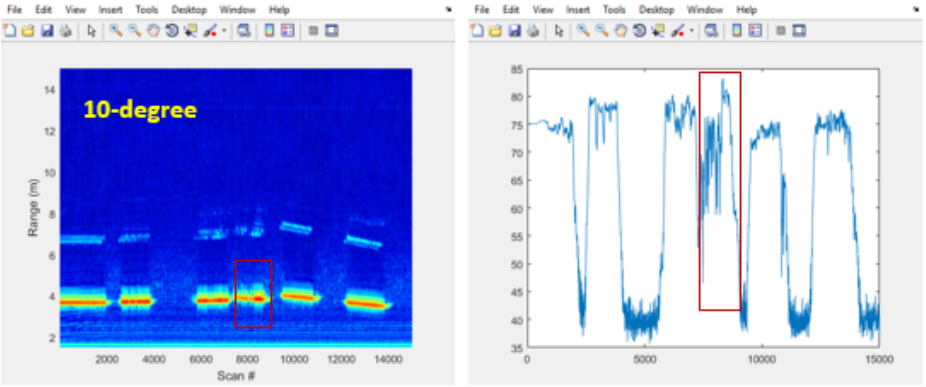

Fig. 5.30. Measurement result at 10-degee

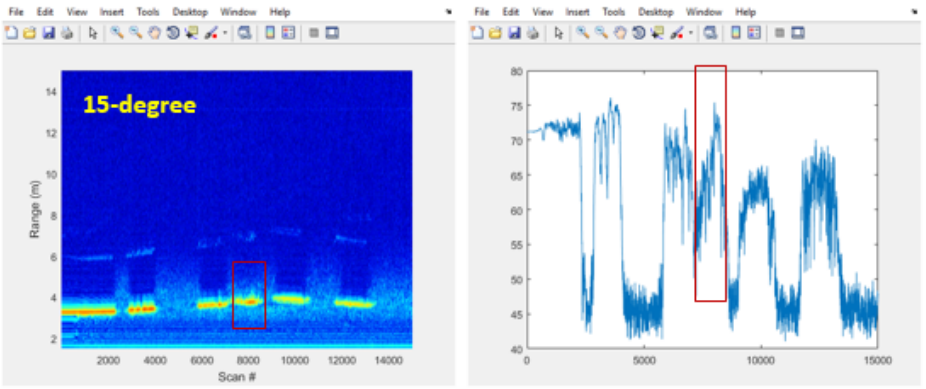

Fig. 5.31. Measurement result at 15-degee

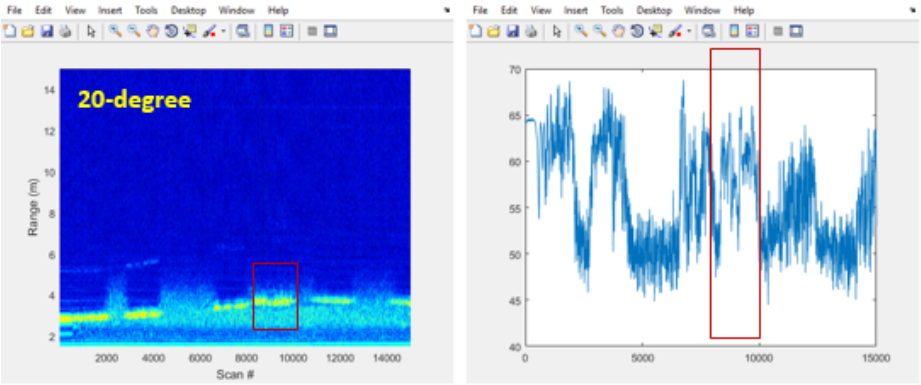

Fig. 5.32. Measurement result at 20-degee

5.4.3 Summary

The measured 24GHz Reflectivity is about -7.3 dB and measured 77GHz Reflectivity is about -7.5 dB. Therefore, the concrete divider skin design satisfies both 24GHz and 77GHz reflectivity requirement (-7.3 ± 1 dB).

5.5 Conclusion

This Chapter describes the material and methods of making surrogates for each roadside objects. For metal guardrail, the foam is used to make the body frame of W-beam and I-beam. Then a skin is attached to the frame. The 24GHz and 77GHz RCS plots of both W-beam and I-beam surrogates are similar to that of the real W-beam and I-beam. For grass, artificial turf can be used as grass surrogate when 77GHz Radar is used and the Radar depression angle set to be 15-degree or lower. For concrete divider, a special three-layer skin is developed. It can satisfy both 24GHz and 77GHz requirements.

6. CONCLUSION AND FUTURE WORK

6.1 Conclusions

This thesis described how to develop surrogate metal guardrail, grass, and concrete divider that have the same representative characteristics as real objects from automotive radar point view.

In Chapter 2, the radar theories that used in this research were summarized. 24GHz and 77GHz FMCW waveform were chosen for the study. Since radar measurements are affected by object's material property, shape property, and the smoothness of the surface, radar reflectivity measurement is used if an object has a big flat surface and the smoothness level of the surface is close to the wavelength of the radar. Otherwise, RCS measurement is used.

Chapter 3 was about preparatory work of radar measurement. This chapter gave detailed information of 24GHz and 77GHz radar. It also introduced the methods of doing RCS calibration and reflectivity calibration. The purpose of doing these calibrations was to find reference data that can be used to calibrate raw data of the target object.

Chapter 4 and Chapter 5 were the main sections of this thesis. Chapter 4 determined the radar measurement methods for metal guardrail (RCS measurement), grass (mean RCS measurement), and concrete divider (reflectivity measurement). The measurement results were discussed. According to these results, the requirement of each surrogate object was determined.

Chapter 5 focused on the generation and verification of the surrogate objects. A three-layer skin (plastic film, zinc, and aluminate film) is developed for the surrogate metal guardrail. A special type of artificial turf that can be used as grass surrogate is found. A three-layer skin (concrete colored paint, plastic, conductive paint) is

created for the surrogate concrete divider. The radar characteristics of all of these surrogates were measured. The results verified that three surrogates have similar radar properties to the real objects.

6.2 Main Contributions of This Thesis

This thesis proposed radar measurement methods for roadside objects and determined the radar properties of the three most common roadside objects, metal guardrail, grass, and concrete divider. According to those radar properties, soft, durable, and reusable materials were found/created for making surrogate roadside objects. Three developed surrogates have the same characteristics as real representative objects. These surrogates can be used to replace the real roadside objects to create a safe and consistent vehicle-testing environment for better testing and scoring the new generation of vehicle technologies.

6.3 Future Work

This research developed three types of roadside objects surrogates: metal guardrail, grass, and concrete divider. In the future, more types of roadside surrogates such as traffic cone, traffic pole, fences, can be developed using the same process described in this thesis.

REFERENCES

REFERENCES

[1] N. H. T. S. Administration, "Did you know?" last date accessed: 10/08/2018. [Online]. Available: https://www-fars.nhtsa.dot.gov/Main/index.aspx

[2] N. Euro, "Autonomous emergency braking," *Brussels, Belgium*, 2014.

[3] S. Satoh, H. Mouri, M. Shimakage, H. Kawazoe, and O. Sadano, "Lane-keep assisting system for vehicle," December 2002, US Patent 6,489,887.

[4] C.-W. Lo, S.-H. Lin, and H.-C. Wei, "Lane departure warning system," November 2013, US Patent 8,587,649.

[5] R. Gupta, A. Ranganathan, and J. Lim, "Road departure warning system," July 2015, US Patent 9,077,958.

[6] C. A. Hobbs and P. J. McDonough, "Development of the european new car assessment programme (euro ncap)," *Regulation*, vol. 44, p. 3, 1998.

[7] M. I. Skolnik, "Introduction to radar," *Radar handbook*, vol. 2, 1962.

[8] A. Ishimaru, *Electromagnetic wave propagation, radiation, and scattering: from fundamentals to applications*. John Wiley & Sons, 2017.

[9] J. Pike. Military. Last date accessed: 10/08/2018. [Online]. Available: https://www.globalsecurity.org/military/systems/aircraft/systems/radar-types.htm

[10] J. Wenger, "Automotive radar-status and perspectives," in *Compound Semiconductor Integrated Circuit Symposium, 2005. CSIC'05. IEEE*. IEEE, 2005, pp. 4–pp.

[11] M. Klotz and H. Rohling, "A 24 ghz short range radar network for automotive applications," in *2001 CIE International Conference on Radar Proceedings.* IEEE, 2001, pp. 115–119.

[12] R. H. Rasshofer and K. Naab, "77 ghz long range radar systems status, ongoing developments and future challenges," in *Radar Conference, 2005. EURAD 2005. European*. IEEE, 2005, pp. 161–164.

[13] W. D. Boyer, "Continuous wave radar," November 1964, US Patent 3,155,972.

[14] J. P. Donohoe and F. M. Ingels, "The ambiguity properties of fsk/psk signals," in *Radar Conference, 1990., Record of the IEEE 1990 International*. IEEE, 1990, pp. 268–273.

[15] A. G. Stove, "Linear fmcw radar techniques," in *IEE Proceedings F (Radar and Signal Processing)*, vol. 139, no. 5. IET, 1992, pp. 343–350.

[16] (2014, November) Polarization in radar systems. Last date accessed: 10/08/2018. [Online]. Available: https://www.nrcan.gc.ca/node/9567

[17] G. T. Ruck, D. E. Barrick, W. D. Stuart, and C. K. Krichbaum, *Radar Cross Section Handbook. Volumes 1 & 2.* Plenum Press, New York, 1970.

[18] N. C. Currie, "Radar reflectivity measurement: techniques and applications," *Norwood, MA, Artech House, 1989, 767 p. No individual items are abstracted in this volume.*, 1989.

[19] C. Wolff, "Near and far field," last date accessed: 10/08/2018. [Online]. Available: http://www.radartutorial.eu/06.antennas/an62.en.html

[20] F. D'Agostino, F. Ferrara, C. Gennarelli, G. Gennarelli, R. Guerriero, and M. Migliozzi, "On the direct non-redundant near-field-to-far-field transformation in a cylindrical scanning geometry," *IEEE Antennas and Propagation Magazine*, vol. 54, no. 1, pp. 130–138, 2012.

[21] C. A. Balanis, "Antenna theory, hoboken," *New Jersey: John Wiley & Sons, Inc*, vol. 8, pp. 21–31, 2005.